SUPPORTING INFORMATION

^{15}N-Azides as Practical and Effective Tags for Developing Long-Lived Hyperpolarized ^{15}N-Probes

Junu Bae,[1,†] Guannan Zhang,[1,†] Hyejin Park,[1] Warren S. Warren,[1,2,3,*] and Qiu Wang[1,*]

[1]Department of Chemistry, Duke University, Durham, NC 27708, USA.
[2]Department of Physics, Duke University, Durham, NC 27708, USA.
[3]Departments of Radiology and Biomedical Engineering, Duke University, Durham, NC 27708, USA.

[†] J. Bae and G. Zhang contributed equally to this work.

*Corresponding author email: warren.warren@duke.edu, qiu.wang@duke.edu

Table of Contents

1. Synthesis of $^{15}N_3$-Azides

1.1. General Experimental Information

Material Information. All commercially available reagents and solvents were used as received unless otherwise stated. Thin-layer chromatography (TLC) was performed using aluminum plates pre-coated with 0.25 mm of 230–400 mesh silica gel with a fluorescent indicator (254 nm). TLC plates were visualized by exposure to ultraviolet light and/or exposure to the solution of $KMnO_4$ and/or vanillin stain. Organic solutions were concentrated *in vacuo* using a rotary evaporator. Column chromatography was performed with silica gel (60 Å, standard grade).

Nuclear magnetic resonance spectra were recorded at ambient temperature (unless otherwise stated) on Varian iNova 400 MHz or Varian iNova 500 MHz spectrometers. NMR data are represented as follows: chemical shift, multiplicity, coupling constant, and integration. All values for proton chemical shifts (δ_H) are reported in parts per million and are referenced to the residual internal $CHCl_3$ (δ 7.26) or CHD_2OD (δ 3.31), or HDO (δ 4.79). All values for carbon-13 chemical shifts (δ_C) are reported in parts per million and are referenced to the carbon-13 resonances in $^{13}CDCl_3$ (δ 77.0) or $^{13}CD_3OD$ (δ 49.0). All values for nitrogen-15 chemical shifts (δ_N) are reported in parts per million and are referenced to an external standard of liquid $^{15}NH_3$ (δ 0.0); the reference point is calculated from the ratios of resonance frequencies following IUPAC recommendations.[1] Resonances are described as s (singlet), bs (broad singlet), d (doublet), t (triplet), q (quartet), quint (quintet), and combinations thereof. Coupling constants (*J*) are given in *Hz* and rounded to the nearest 0.1.

High resolution mass spectra were recorded by the Mass Spectrometry Facility at the Department of Chemistry at Duke University using an Agilent 6224 TOF LC/MS instrument (denoted by LC/ESI). High resolution *m*/*z* values are reported in Daltons, calculated to 4 decimal points from the molecular formula. All found values are within 5 ppm tolerance.

Infrared spectra were recorded on a ThermoScientific Nicolet 6700 FTIR equipped with a diamond ATR. Absorption maxima (ν_{max}) are described as s (strong), m (medium), w (weak), and br (broad) and are quoted in wavenumbers (cm^{-1}). Only selected peaks are reported.

1.2. Synthesis of $^{15}N_3$-Azides

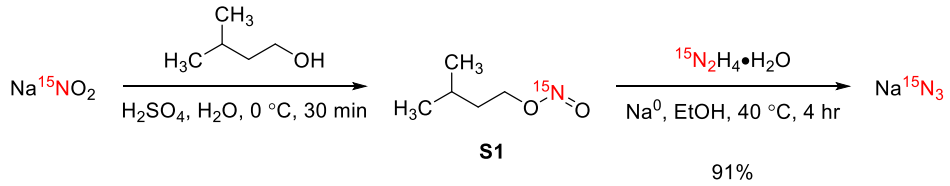

Sodium azide-$^{15}N_3$.

$Na^{15}N_3$ The following procedure was adapted from a previously reported procedure.[2] To a 2-neck 50-mL round-bottom flask, sodium metal (220 mg, 9.6 mmol, 1.25 equiv) was added portion-wise to ethanol (10 mL) over an ice-water bath. The mixture was stirred at room temperature until all solid material was completely consumed (about 1.5 hours).

Meanwhile, in a separate 25-mL pear-shaped flask, sodium nitrite-^{15}N (915 mg, 13.8 mmol, 1.8 equiv) was dissolved in 2 mL water. This solution was cooled with an ice-water bath and 3-methyl-1-butanol (1.50 mL, 13.8 mmol, 1.8 equiv) was added. Next, 4 M H_2SO_4 (1.73 mL, 6.9 mmol, 0.9 equiv) was added dropwise over 5 minutes, and the reaction was stirred vigorously over the ice-water bath for 30 minutes. Upon addition, the reaction turned blue-green and slowly became colorless. Afterwards, the bilayer mixture was transferred to a 25-mL separatory funnel and the bottom layer was removed. The top layer (neat, crude isopentyl nitrite-^{15}N **S1**) was washed with 5 mL saturated sodium chloride solution. While the top layer remained in the separatory funnel, a small amount (~100 mg) sodium sulfate was directly added to the funnel to dry the crude material, which was subsequently drawn from the separatory funnel directly using a syringe. About 1.5 mL of the light yellow, crude **S1** was collected.

To the previous sodium/ethanol mixture (once all solid material was completely consumed), hydrazine-$^{15}N_2$ monohydrate and the crude **S1** were added subsequently at room temperature. Following addition, a white solid began to precipitate. The reaction was heated at 60 °C for 4 hours, after which the reaction mixture was cooled using an ice-water bath. The reaction was filtered, and the filter cake was washed with ethanol (20 mL). The solid was dried under vacuum overnight to yield sodium azide-$^{15}N_3$ as a fine, white powder (473.7 mg, 6.96 mmol, 91%).

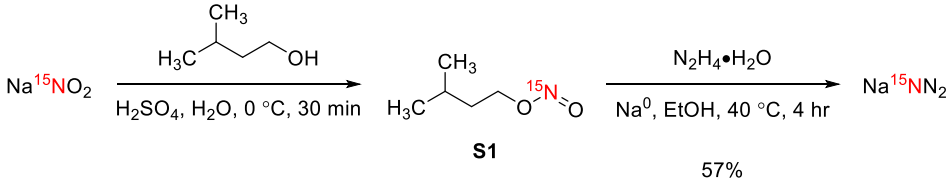

Sodium azide-$^{15}N_1$.

$Na^{15}NN_2$ Sodium azide-$^{15}N_1$ was synthesized following the same procedure as sodium azide-$^{15}N_3$ with the substitution of natural abundance-hydrazine monohydrate for hydrazine-$^{15}N_2$ monohydrate, yielding a fine, white powder (451.7 mg, 6.84 mmol, 57%).

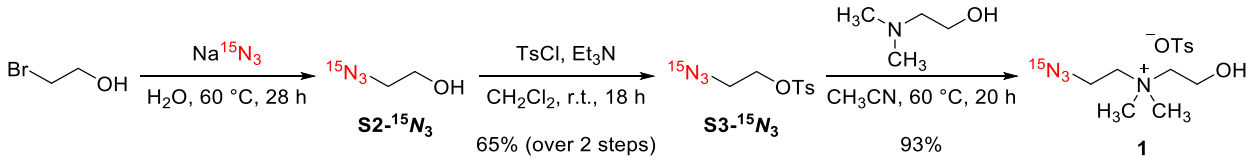

2-(Azido-$^{15}N_3$)ethan-1-ol (S2-$^{15}N_3$).

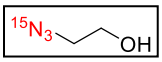

The following reagents were added in succession to a 1-dram vial: freshly distilled 2-bromoethanol (31.2 mg, 0.25 mmol, 1.0 equiv), water (250 μL), and sodium azide-$^{15}N_3$ (17.0 mg, 0.25 mmol, 1.0 equiv). The reaction was stirred at 60 °C in the dark for 28 hours, after which the reaction mixture was cooled to room temperature. Saturated sodium chloride solution (500 μL) was added, and this mixture was extracted with diethyl ether (1.5 mL × 5). The organic layers were combined, dried with sodium sulfate, and concentrated very gently *in vacuo*, such that about 200 μL of solvent remained. (Note: the azidoethanol intermediate is somewhat volatile and may have a low vapor pressure. Drying for short periods of time at medium pressure were found to give optimal results. Residual diethyl ether does not appear to significantly impact the kinetics or yield of the following step.)

2-(Azido-$^{15}N_3$)ethyl 4-methylbenzenesulfonate (S3-$^{15}N_3$).

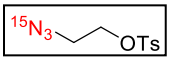

The crude material **S2-$^{15}N_3$** in a 20-mL scintillation vial was diluted with dichloromethane (1 mL) and triethylamine (70 μL, 0.50 mmol, 2.0 equiv). This mixture was cooled with an ice-water bath and tosyl chloride (57.2 mg, 0.30 mmol, 1.2 equiv) was added. The reaction was warmed to room temperature and stirred at room temperature for 18 hours, after which it was concentrated *in vacuo* and subjected to column chromatography (10% ethyl acetate–hexane) to yield **S3-$^{15}N_3$** as a light-yellow liquid (39.9 mg, 0.16 mmol, 65%).

$\mathbf{R_f}$ = 0.44 (20% ethyl acetate–hexane);

^{1}H NMR (400 MHz, $CDCl_3$): **δ** 7.76 (d, *J* = 8.3 Hz, 1H), 7.31 (d, *J* = 8.2 Hz, 1H), 4.11 (td, *J* = 5.1, 3.5 Hz, 2H), 3.45 – 3.43 (m, 2H), 2.41 (s, 3H);

^{13}C NMR (101 MHz, $CDCl_3$): **δ** 145.2, 132.4, 129.9, 127.9, 68.1, 49.5, 21.6;

FTIR (thin film, MeCN): 2918 (s), 2053 (s), 2019 (s), 1361 (s), 1175 (s), 1015 (m), 911 (s), 769 (s), 663 (s), 553 (s) cm^{-1};

HRMS-ESI (m/z): Calc'd for $C_9H_{15}N^{15}N_3O_3S^+$ ($[M+NH_4]^+$): 262.0770; found: 262.0763.

2-(Azido-$^{15}N_3$)-*N*-(2-hydroxyethyl)-*N*,*N*-dimethylethan-1-ammonium 4-methylbenzenesulfonate (1).

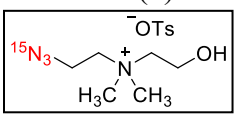

The following reagents were added in succession to a 1-dram vial: **S3-$^{15}N_3$** (37.6 mg, 0.15 mmol, 1.0 equiv), acetonitrile (150 μL), and 2-(dimethylamino)ethanol (15.4 μL, 0.15 mmol, 1.0 equiv). The reaction was stirred at 80 °C for 20 hours, after which the reaction mixture was cooled to room temperature and concentrated *in vacuo* to yield **1** as a yellow oil (47.9 mg, 0.14 mmol, 93%).

^{1}H NMR (400 MHz, CD_3OD): **δ** 7.71 (d, *J* = 8.1 Hz, 2H), 7.25 (d, *J* = 8.1 Hz, 2H), 4.00 – 3.96 (m, 2H), 3.95 – 3.90 (m, 2H), 3.65 – 3.62 (m, 2H), 3.54 – 3.52 (m, 2H), 3.20 (s, 6H), 2.38 (s, 3H);

^{13}C NMR (101 MHz, CD_3OD): **δ** 143.6, 141.8, 129.9, 126.9, 67.5 – 67.4 (m, 1C), 64.6 – 64.5 (m, 1C), 56.8, 52.8 (t, *J* = 3.7 Hz, 1C); 46.0 (m, 1C), 21.3;

FTIR (thin film, MeCN): 3368 (s, br), 2924 (m), 2034 (s), 1459 (m), 1175 (s), 1121 (s), 1033 (s), 1009 (s), 818 (m), 682 (s), 566 (s) cm^{-1};
HRMS-ESI (m/z): Calc'd for $C_6H_{15}N^{15}N_3O^+$ ([M–OTs]$^+$): 162.1151; found: 162.1147.

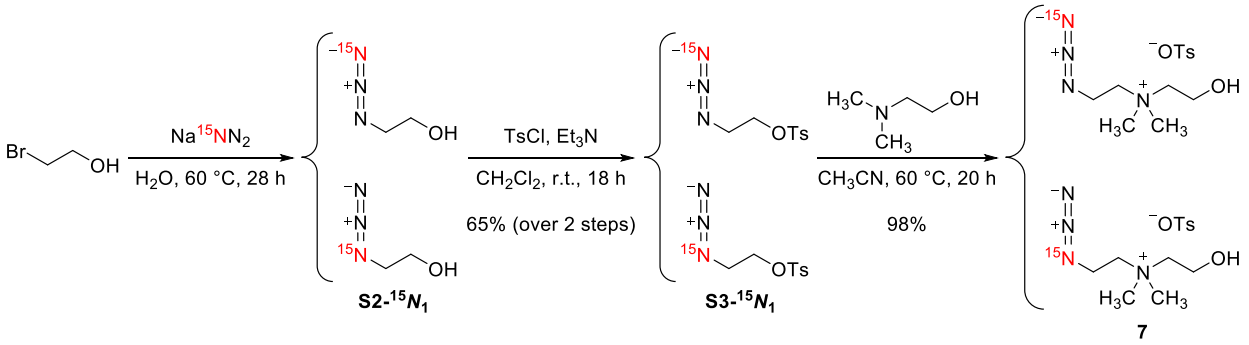

2-(Azido-1-^{15}N)ethan-1-ol & **2-(Azido-3-^{15}N)ethan-1-ol** (mixture of isotopomers, **S2-$^{15}N_1$**).

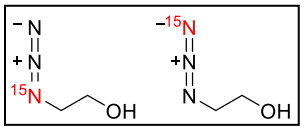

S2-$^{15}N_1$ was synthesized following the same procedure as **S2-$^{15}N_3$** with the substitution of sodium azide-$^{15}N_1$ for sodium azide-$^{15}N_3$.

2-(Azido-1-^{15}N)ethyl 4-methylbenzylsulfonate & **2-(Azido-3-^{15}N)ethyl 4-methylbenzene sulfonate** (mixture of isotopomers, **S3-$^{15}N_1$**).

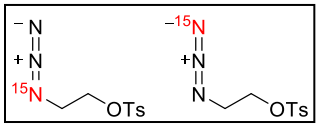

S3-$^{15}N_1$ was synthesized following the same procedure as **S3-$^{15}N_3$** with the substitution of **S2-$^{15}N_1$** for **S2-$^{15}N_3$**, yielding a light-yellow liquid (158.5 mg, 0.65 mmol, 65%).
$\mathbf{R}_f$ = 0.44 (20% ethyl acetate–hexane);
^{1}H NMR (400 MHz, $CDCl_3$): **δ** 7.82 (d, *J* = 8.2 Hz, 1H), 7.37 (d, *J* = 8.1 Hz, 1H), 4.18 – 4.14 (m, 2H), 3.50 – 3.47 (m, 2H), 2.46 (s, 3H);
^{13}C NMR (101 MHz, $CDCl_3$): **δ** 145.1, 132.2, 129.8, 127.7, 68.1, 49.3, 21.4;
FTIR (thin film, MeCN): 2975 (w), 2102 (s), 2080 (s), 1359 (s), 1172 (s), 1017 (m), 908 (s), 766 (s), 661 (s), 551 (s) cm^{-1};
HRMS-ESI (m/z): Calc'd for $C_9H_{15}N_3{}^{15}NO_3S^+$ ([M+NH_4]$^+$): 260.0830; found: 260.0827.

2-(Azido-1-^{15}N)-*N*-(2-hydroxyethyl)-*N*,*N*-dimethylethan-1-ammonium 4-methylbenzene-sulfonate & **2-(Azido-3-^{15}N)-*N*-(2-hydroxyethyl)-*N*,*N*-dimethylethan-1-ammonium 4-methylbenzenesulfonate** (mixture of isotopomers, **7**).

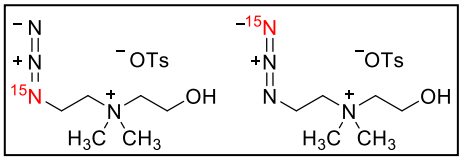

7 was synthesized following the same procedure as **1** with the substitution of **S3-$^{15}N_1$** for **S3-$^{15}N_3$**, yielding a yellow oil (69.7 mg, 0.21 mmol, 95%).
^{1}H NMR (400 MHz, CD_3OD): **δ** 7.71 (d, *J* = 8.2 Hz, 2H), 7.24 (d, *J* = 8.1 Hz, 2H), 4.00 – 3.97 (m, 2H), 3.95 – 3.91 (m, 2H), 3.66 – 3.62 (m, 2H), 3.55 – 3.52 (m, 2H), 3.20 (s, 6H), 2.38 (s, 3H);

^{13}C NMR (101 MHz, CD_3OD): **δ** 143.6, 141.7, 129.8, 126.9, 67.6 – 67.5 (m, 1C), 64.6 (m, 1C), 56.8, 52.9 – 52.8 (m, 1C); 46.0 (m, 1C), 21.3;
FTIR (thin film, MeCN): 3369 (s, br), 2974 (m), 2488 (s, br), 2073 (m), 1412 (m), 1139 (s), 970 (s), 818 (w), 686 (w), 569 (w) cm^{-1};
HRMS-ESI (m/z): Calc'd for $C_6H_{15}N_3{}^{15}NO^+$ ([M–OTs]$^+$): 160.1211; found: 160.1206.

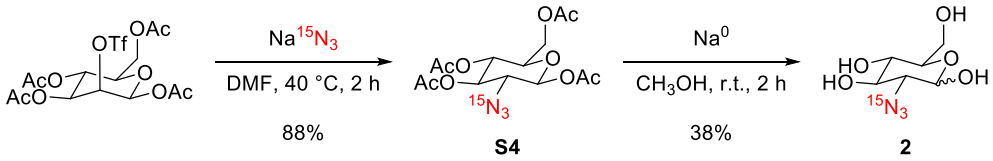

1,3,4,6-Tetra-*O*-acetyl-2-(azido-$^{15}N_3$)-2-deoxy-β-D-glucopyranose (S4).

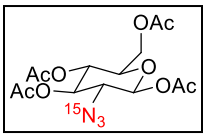

The following reagents were added in succession to a 1-dram vial: 1,3,4,6-tetra-*O*-acetyl-2-*O*-trifluoromethanesulfonyl-β-D-mannopyranose (240.2 mg, 0.50 mmol, 1.0 equiv), *N,N*-dimethylformamide (1.5 mL), and sodium azide-$^{15}N_3$ (34.0 mg, 0.50 mmol, 1.0 equiv). The reaction was stirred at 40 °C for 2 hours, after which the reaction mixture was directly subjected to column chromatography (20% ethyl acetate–hexane) to yield **S4** as a sticky, colorless oil (166.1 mg, 0.44 mmol, 88%).
$\mathbf{R}_f$ = 0.52 (25% ethyl acetate–hexane);
^{1}H NMR (400 MHz, $CDCl_3$): **δ** 5.50 (d, *J* = 8.5 Hz, 1H), 5.04 (t, *J* = 9.5 Hz, 1H), 4.96 (t, *J* = 9.5 Hz, 1H), 4.22 (dd, *J* = 12.5, 4.1 Hz, 1H), 3.99 (d, *J* = 12.5 Hz, 1H), 3.78 – 3.75 (m, 1H), 3.62 – 3.57 (m, 1H), 2.11 (s, 3H), 2.00 (s, 3H), 1.99 (s, 3H), 1.94 (s, 3H);
^{13}C NMR (101 MHz, $CDCl_3$): **δ** 170.2, 169.5, 169.3, 168.3, 92.2 (m, 1C), 72.4 (2C), 67.5 (m, 1C), 62.3 (m, 1C), 61.1, 20.6, 20.4, 20.3 (2C);
FTIR (thin film, MeCN): 2920 (m), 2045 (s), 1747 (s), 1368 (m), 1209 (s), 1072 (s), 1036 (s) cm^{-1};
HRMS-ESI (m/z): Calc'd for $C_{14}H_{23}N^{15}N_3O_9^+$ ([M+NH_4]$^+$): 394.1371; found: 394.1367.

2-(Azido-$^{15}N_3$)-2-deoxy-D-glucose (2).

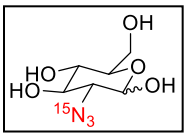

To a 20-mL scintillation vial chilled over an ice-water bath, methanol (1.0 mL) and sodium metal (11 mg, 0.48 mmol, 1.1 equiv) were added in succession. This mixture was stirred over the ice-water bath until all solids were fully dissolved (~10 minutes), after which a solution of **S4** (166 mg, 0.44 mmol, 1.0 equiv) in methanol (1.0 mL) was added. The reaction was warmed to room temperature and stirred at room temperature for 2 hours, during which the colorless solution became a light-yellow suspension. The reaction was quenched by adding acidic ion-exchange resin (450 mg of Dowex® 50WX8 resin, hydrogen form, 200-400 mesh) and stirring for 5 minutes at room temperature. This mixture was filtered and washed with additional methanol (~10 mL). The filtrate was concentrated *in vacuo* and subjected to column chromatography (0.5% methanol–ethyl acetate) to yield **2** as a sticky, yellow oil (34.9 mg, 0.17 mmol, 38%).
$\mathbf{R}_f$ = 0.42 (1.0% methanol–ethyl acetate);
^{1}H NMR (400 MHz, D_2O): [*major anomer*] **δ** 4.64 (dd, *J* = 8.1, 2.7 Hz, 1H), 3.85 – 3.76 (m, 2H), 3.44 – 3.37 (m, 3H), 3.24 – 3.18 (m, 1H);

^{13}C NMR (101 MHz, D_2O): [*major anomer*] **δ** 94.9, 75.9, 71.4, 69.7, 66.7, 60.5; [*minor anomer*] **δ** 91.0, 74.2, 71.3, 69.3, 63.4, 60.3;
FTIR (thin film, MeCN): 3296 (s, br), 2924 (m), 2039 (s), 1636 (w), 1323 (w), 1219 (m), 1018 (s), 945 (m) cm^{-1};
HRMS-ESI (m/z): Calc'd for $C_6H_{15}N^{15}N_3O_5^+$ ([M+NH_4]$^+$): 226.0948; found: 226.0944.

The spectral characterization of **S4** and **2** prepared by the above procedures were in accord with unlabeled versions reported previously.[3]

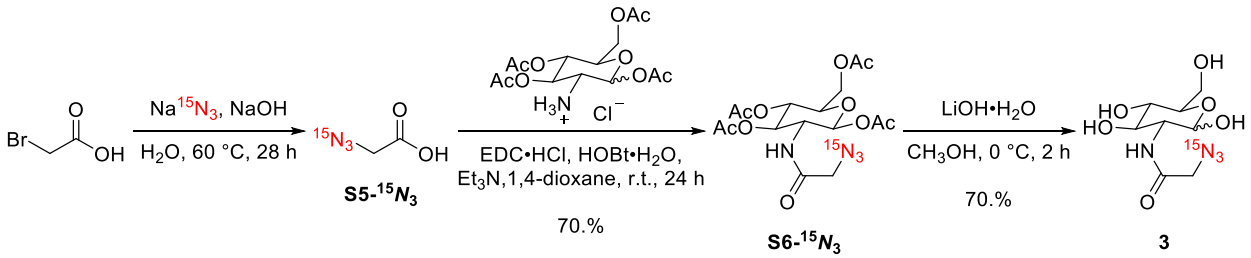

2-(Azido-$^{15}N_3$)acetic acid (S5-$^{15}N_3$).

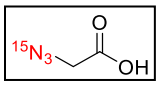

The following reagents were added in succession to a 1-dram vial: 2-bromoacetic acid (69.5 mg, 0.50 mmol, 1.0 equiv), 2 M sodium hydroxide/water (250 µL, 0.50 mmol, 1.0 equiv), sodium azide-$^{15}N_3$ (37.4 mg, 0.55 mmol, 1.1 equiv), and additional water (250 µL). The reaction was stirred at room temperature in the dark for 19 hours, after which 4 M hydrochloric acid (375 µL, 1.5 mmol, 3.0 equiv) was added and the reaction was extracted with diethyl ether (2 mL × 5). The organic layers were combined, dried with sodium sulfate, and concentrated *in vacuo* to yield **S5-$^{15}N_3$** as a clear, colorless liquid (52.8 mg, 0.51 mmol, quant.).
^{1}H NMR (400 MHz, $CDCl_3$): **δ** 8.00 (bs, 1H), 3.96 (m, 2H).

1,3,4,6-Tetra-*O*-acetyl-2-[2-(azido-$^{15}N_3$)acetylamino]-2-deoxy-β-D-glucopyranose (S6-$^{15}N_3$).

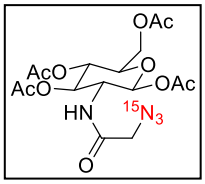

The following reagents were added in succession to a 20-mL scintillation vial: **S6-$^{15}N_3$** (52.8 mg, 0.50 mmol, 1.0 equiv), 1,4-dioxane (5 mL), 1-hydroxybenzotriazole monohydrate (91.9 mg, 0.60 mmol, 1.2 equiv), 1,3,4,6-tetra-*O*-acetyl-2-amino-2-deoxy-β-D-glucopyranose hydrochloride (230.3 mg, 0.60 mmol, 1.2 equiv), *N*-(3-Dimethylaminopropyl)-*N*′-ethylcarbodiimide hydrochloride (239.6 mg, 1.25 mmol, 2.5 equiv), and triethylamine (83.6 µL, 0.60 mmol, 1.2 equiv). The reaction was stirred at room temperature for 24 hours, after which the reaction was transferred to a separatory funnel. Water (10 mL) and ethyl acetate (15 mL) were added, and after vigorous shaking, the aqueous layer was removed. The organic layer was washed with 2 M hydrochloric acid (10 mL × 2), then saturated sodium bicarbonate solution (10 mL × 2). The organic layer was then dried with sodium sulfate and concentrated *in vacuo* to yield **S6-$^{15}N_3$** as a colorless oil (150.8 mg, 0.35 mmol, 70%).
$\mathbf{R}_f$ = 0.27 (40% ethyl acetate–hexane);
^{1}H NMR (400 MHz, $CDCl_3$): **δ** 6.97 (d, J = 9.5 Hz, 1H), 5.77 (d, J = 8.7 Hz, 1H), 5.32 (t, J = 10.0 Hz, 1H), 5.06 (t, J = 9.7 Hz, 1H), 4.28 – 4.19 (m, 2H), 4.07 (dd, J = 12.4, 2.2 Hz, 1H), 3.89 – 3.85 (m, 2H), 3.82 (d, J = 3.9 Hz, 2H), 2.05 (s, 3H), 2.02 (s, 3H), 1.99 (s, 3H), 1.99 (s, 3H);

^{13}C NMR (101 MHz, $CDCl_3$): **δ** 171.0, 170.5, 169.3, 169.2, 167.2 (t, J = 2.3 Hz, 1C), 91.9, 72.5, 72.1, 68.0, 61.7, 52.6, 52.4 – 52.3 (m, 1C), 20.7, 20.5, 20.4, 20.4;
FTIR (thin film, MeCN): 3343 (w, br), 2938 (w), 2040 (s), 1740 (s), 1676 (m), 1534 (m), 1367 (m), 1209 (s), 1032 (s), 902 (m), 570 (m) cm^{-1};
HRMS-ESI (m/z): Calc'd for $C_{16}H_{26}N_2{}^{15}N_3O_{10}^+$ ([M+NH_4]$^+$): 451.1585; found: 451.1584.

2-[2-(Azido-$^{15}N_3$)acetylamino]-2-deoxy-D-glucose (**3**).

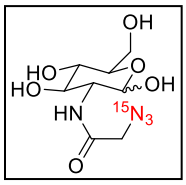

To a 20-mL scintillation vial, **S6-$^{15}N_3$** (142.9 mg, 0.33 mmol, 1.0 equiv) was dissolved in methanol (2.0 mL) and tetrahydrofuran (0.5 mL), and the solution was chilled over an ice-water bath. A solution of lithium hydroxide monohydrate (20.8 mg, 0.50 mmol, 1.5 equiv) in water (0.50 mL) was added dropwise, and the reaction was stirred over the ice-water bath for 2 hours. Subsequently, the reaction was quenched by adding acidic ion-exchange resin (300 mg of Dowex® 50WX8 resin, hydrogen form, 200-400 mesh) and stirring for an additional 15 minutes over the ice-water bath. This mixture was filtered and washed with methanol (~10 mL), and the filtrate was concentrated *in vacuo*. The crude material was then dissolved in a small amount of methanol (~0.5 mL), triturated with dichloromethane (10 mL), filtered, and washed with additional dichloromethane (10 mL) to yield **3** as a fine, white solid (61.6 mg, 0.23 mmol, 70%).
^{1}H NMR (400 MHz, CD_3OD): [*major anomer*] **δ** 5.12 (d, J = 3.5 Hz, 1H), 3.95 – 3.93 (m, 2H), 3.90 – 3.86 (m, 1H), 3.82 – 3.79 (m, 2H), 3.74 – 3.69 (m, 2H), 3.39 (t, J = 9.2 Hz, 1H);
^{13}C NMR (126 MHz, CD_3OD): [*major anomer*] **δ** 170.4, 92.4, 73.1, 72.7, 72.3, 62.7, 55.8, 52.8; [*minor anomer*] **δ** 170.8, 96.7, 78.0, 75.7, 72.1, 62.8, 58.8, 53.1;
FTIR (neat): 3303 (s, br), 2037 (s), 1652 (s), 1559 (s), 1263 (w), 1118 (s), 1022 (s), 863 (w), 565 (m) cm^{-1};
HRMS-ESI (m/z): Calc'd for $C_8H_{15}N^{15}N_3O_6^+$ ([M+H]$^+$): 266.0897; found: 266.0894.

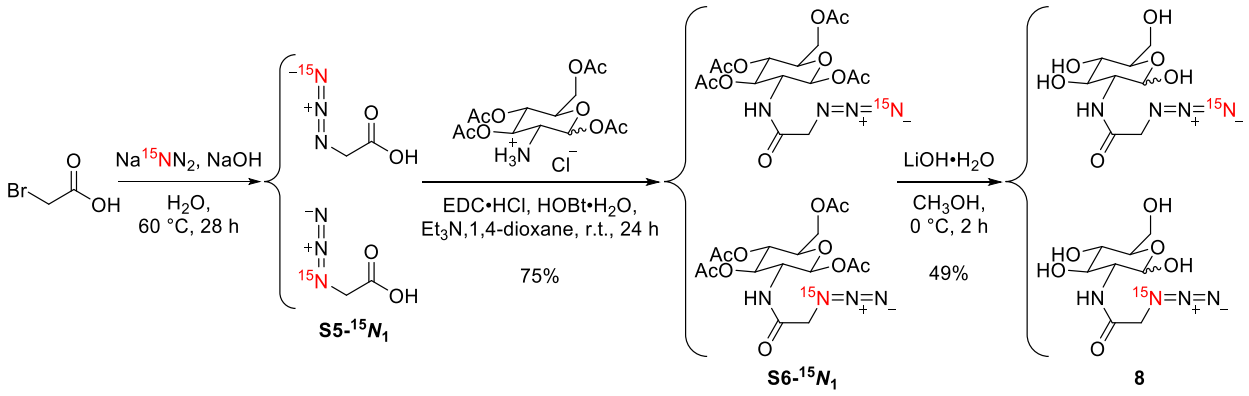

2-(Azido-1-^{15}N)acetic acid & **2-(Azido-3-^{15}N)acetic acid** (mixture of isotopomers, **S5-$^{15}N_1$**).

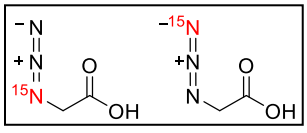

S5-$^{15}N_1$ was synthesized following the same procedure as **S5-$^{15}N_3$** with the substitution of sodium azide-$^{15}N_1$ for sodium azide-$^{15}N_3$, yielding a clear, colorless liquid.
^{1}H NMR (400 MHz, $CDCl_3$): **δ** 3.98 (s, 2H).

1,3,4,6-Tetra-*O*-acetyl-2-[2-(azido-1-^{15}N)acetylamino]-2-deoxy-β-D-glucopyranose & **1,3,4,6-Tetra-*O*-acetyl-2-[2-(azido-3-^{15}N)acetylamino]-2-deoxy-β-D-glucopyranose** (mixture of isotopomers, **S6-$^{15}N_1$**).

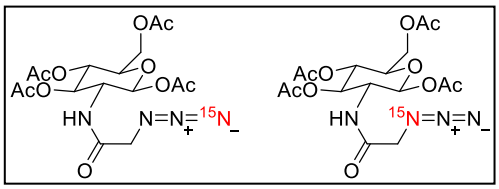

S6-$^{15}N_1$ was synthesized following the same procedure as **S6-$^{15}N_3$** with the substitution of **S5-$^{15}N_1$** for **S5-$^{15}N_3$**, yielding a colorless oil (325.4 mg, 0.75 mmol, 75%).
R_f = 0.27 (40% ethyl acetate–hexane);
^{1}H NMR (400 MHz, $CDCl_3$): **δ** 7.18 (d, *J* = 9.5 Hz, 1H), 5.79 (d, *J* = 8.7 Hz, 1H), 5.36 (t, *J* = 10.0 Hz, 1H), 5.06 (t, *J* = 9.6 Hz, 1H), 4.28 – 4.19 (m, 2H), 4.09 – 4.06 (m, 1H), 3.92 – 3.88 (m, 1H), 3.82 (s, 2H), 2.04 (s, 3H), 2.00 (s, 3H), 1.99 (s, 3H), 1.99 (s, 3H);
^{13}C NMR (101 MHz, $CDCl_3$): **δ** 170.7, 170.3, 169.1, 169.0, 167.2, 91.6, 72.2, 72.0, 68.0, 61.6, 52.4, 52.1 (m, 1C), 20.4, 20.3, 20.2, 20.2;
FTIR (thin film, MeCN): 3345 (w, br), 2975 (m), 2088 (s), 1743 (s), 1684 (m), 1534 (m), 1368 (m), 1213 (s), 1139 (s), 1037 (s), 905 (w), 570 (w) cm^{-1};
HRMS-ESI (m/z): Calc'd for $C_{16}H_{26}N_4{}^{15}NO_{10}^+$ ($[M+NH_4]^+$): 449.1645; found: 449.1643.

2-[2-(azido-$^{15}N_3$)acetylamino]-2-deoxy-D-glucose & **2-[2-(azido-$^{15}N_3$)acetylamino]-2-deoxy-D-glucose** (mixture of isotopomers, **8**).

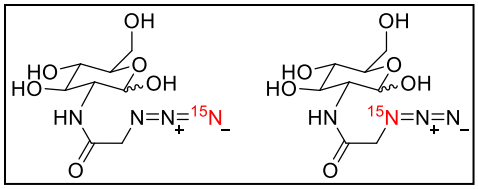

8 was synthesized following the same procedure as **3** with the substitution of **S6-$^{15}N_1$** for **S6-$^{15}N_3$**, yielding a fine, white solid (94.7 mg, 0.36 mmol, 49%).
^{1}H NMR (400 MHz, CD_3OD): [*major anomer*] **δ** 5.11 (d, *J* = 3.4 Hz, 1H), 3.94 – 3.92 (m, 2H), 3.89 – 3.86 (m, 1H), 3.82 – 3.79 (m, 2H), 3.73 – 3.68 (m, 2H), 3.38 (t, *J* = 9.2 Hz, 1H);
^{13}C NMR (126 MHz, CD_3OD): [*major anomer*] **δ** 170.4, 92.4, 73.1, 72.7, 72.3, 62.7, 55.8, 52.8; [*minor anomer*] **δ** 170.8, 96.6, 78.0, 75.7, 72.1, 62.8, 58.8, 53.1;
FTIR (thin film, MeCN): 3313 (s, br), 2472 (s), 2080 (s), 1645 (s), 1558 (m), 1457 (m), 1261 (m), 1116 (s), 1031 (s), 861 (w), 545 (m) cm^{-1};
HRMS-ESI (m/z): Calc'd for $C_8H_{15}N_3{}^{15}NO_6^+$ ($[M+H]^+$): 264.0957; found: 264.0952.

The spectral characterization of **S6** and **8** prepared by the above procedures were in accord with unlabeled versions reported previously.[4]

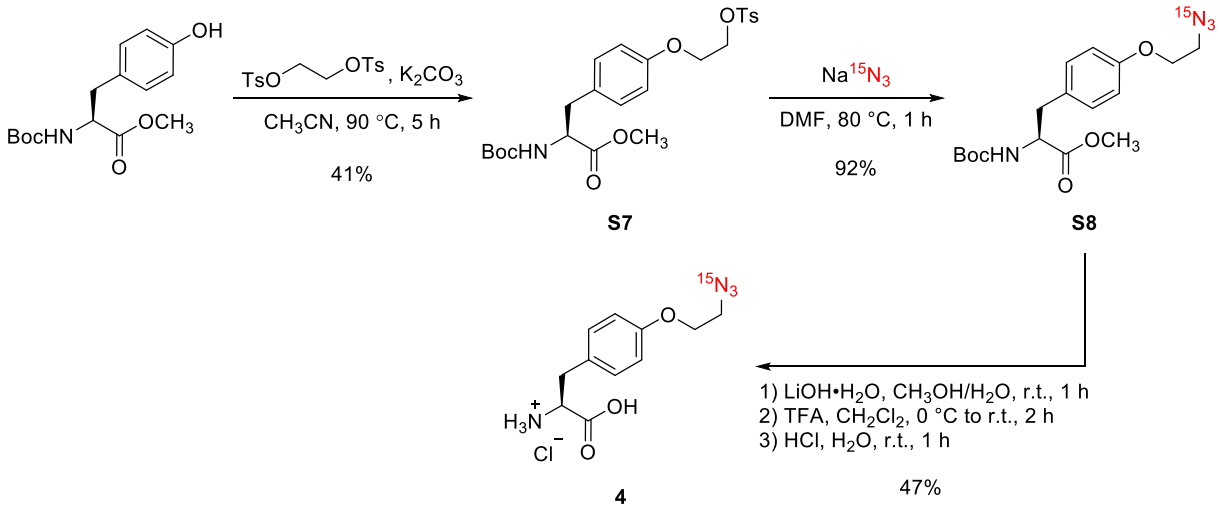

***N*-Boc-*O*-2-(tosyloxy)ethyl-L-tyrosine methyl ester (S7).**

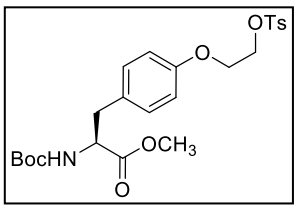

The following reagents were added in succession to a 250-mL round-bottom flask: Boc-L-tyrosine methyl ester (7.3 g, 25 mmol, 1.0 equiv), acetonitrile (50 mL), potassium carbonate (5.53 g, 40 mmol, 1.6 equiv), ethylene glycol ditosylate (15 g, 40 mmol, 1.6 equiv). The reaction was stirred at 90 °C for 5 hours, after which the reaction mixture was cooled to room temperature, concentrated *in vacuo*, and then subjected by column chromatography (5% *tert*-butyl methyl ether–45% dichloromethane–hexane) to yield **S7** as an extremely gummy, light yellow oil (5.08 g, 10.3 mmol, 41%).

R_f = 0.20 (25% ethyl acetate–hexane);

^{1}H NMR (400 MHz, $CDCl_3$): **δ** 7.80 (d, *J* = 8.3 Hz, 2H), 7.33 (d, *J* = 8.3 Hz, 2H), 6.99 (d, *J* = 8.6 Hz, 2H), 6.70 (d, *J* = 8.6 Hz, 2H), 4.96 (d, *J* = 7.8 Hz, 1H), 4.51 (dd, *J* = 13.6, 6.0 Hz, 1H), 4.35 – 4.32 (m, 2H), 4.11 – 4.09 (m, 2H) 3.69 (s, 3H), 2.99 (qd, *J* = 13.6, 6.0 Hz, 2H), 2.44 (s, 3H), 1.40 (s, 9H);

^{13}C NMR (101 MHz, $CDCl_3$): **δ** 172.2, 156.9, 154.9, 144.8, 132.7, 130.2, 129.7, 128.7, 127.8, 114.5, 79.7, 68.1, 65.3, 54.4, 52.0, 37.3, 28.1, 21.5;

FTIR (neat): 3385 (w), 2976 (m), 1709 (s), 1510 (s), 1357 (s), 1245 (m), 1171 (s), 1018 (m), 924 (s), 753 (s), 662 (s), 552 (m) cm^{-1};

HRMS-ESI (m/z): Calc'd for $C_{24}H_{31}NNaO_8S^+$ ($[M+Na]^+$): 516.1663; found: 516.1663.

***N*-Boc-*O*-2-(azido-$^{15}N_3$)ethyl-L-tyrosine methyl ester (S8).**

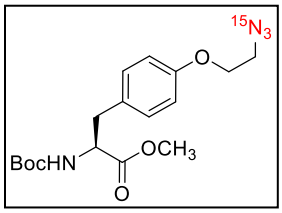

The following reagents were added in succession to a 2-dram vial: **S7** (123.4 mg, 0.25 mmol, 1.0 equiv), *N,N*-dimethylformamide (1.0 mL), and sodium azide-$^{15}N_3$ (17.0 mg, 0.25 mmol, 1.0 equiv). The reaction was stirred at 80 °C for 1 hour, after which the reaction mixture was directly subjected to column chromatography (20% ethyl acetate–hexane) to yield **S8** as a sticky, light yellow oil (84.8 mg, 0.23 mmol, 92%).

R_f = 0.32 (25% ethyl acetate–hexane);

^{1}H NMR (400 MHz, $CDCl_3$): **δ** 7.02 (d, *J* = 8.4 Hz, 2H), 6.82 (d, *J* = 8.4 Hz, 2H), 4.96 (d, *J* = 7.6 Hz, 1H), 4.52 (dd, *J* = 13.6, 6.0 Hz, 1H), 4.17 – 4.03 (m, 2H), 3.68 (s, 3H), 3.60 – 3.50 (m, 2H), 3.01 (qd, *J* = 13.6, 6.0 Hz, 2H), 1.39 (s, 9H);
^{13}C NMR (101 MHz, $CDCl_3$): **δ** 172.3, 157.2, 155.0, 130.3, 128.7, 114.6, 79.8, 66.9, 54.5, 52.2, 50.1, 37.4, 28.2;
FTIR (thin film, MeCN): 2926 (s), 2056 (s), 2020 (s), 1716 (s), 1509 (s), 1365 (m), 1245 (s), 1166 (s), 1058 (m) cm^{-1};
HRMS-ESI (m/z): Calc'd for $C_{17}H_{24}N^{15}N_3NaO_5^+$ ($[M+Na]^+$): 390.1550; found: 390.1555.

***O*-2-(Azido-$^{15}N_3$)ethyl-L-tyrosine (4).**

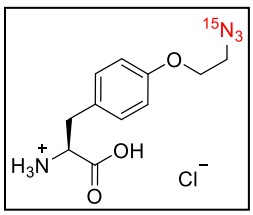

To a 2-dram vial, **S8** (79.8 mg, 0.22 mmol, 1.0 equiv) was dissolved in methanol (0.50 mL). A solution of lithium hydroxide monohydrate (13.7 mg, 0.33 mmol, 1.5 equiv) in water (0.25 mL) was added dropwise, and the colorless solution turned light yellow. The reaction was stirred at room temperature for 1 hour, after which 2 M hydrochloric acid (162 μL, 0.34 mmol, 1.5 equiv) was added dropwise, and the reaction became white and cloudy. Additional water (1 mL) was added and the mixture was extracted with ethyl acetate (3 mL × 5). The organic layers were combined, dried with sodium sulfate, and concentrated *in vacuo*. The crude material was transferred to a 25-mL round-bottom flask and dissolved in dichloromethane (2 mL). After chilling the solution in an ice-water bath, trifluoroacetic acid (166 μL, 2.2 mmol, 10 equiv) was added dropwise, then the reaction was warmed to room temperature. The reaction was stirred at room temperature for 1 hour, after which it was concentrated *in vacuo*. Diethyl ether (5 mL) was added to the crude material, causing formation of a white precipitate. This suspension was chilled in an ice-water bath for 30 minutes, after which it was filtered and washed with additional diethyl ether (~10 mL). The solid was transferred to a 1-dram vial, dissolved in water (1 mL), and then concentrated hydrochloric acid (190 μL, 2.2 mmol, 10 equiv) was added dropwise. The solution was stirred for 1 hour, after which it was frozen by placing the vial in a –80°C freezer overnight. The frozen pellet was lyophilized, yielding **4** as a fluffy, white solid (29.4 mg, 0.10 mmol, 47%).
^{1}H NMR (400 MHz, D_2O): **δ** 7.23 (d, *J* = 8.6 Hz, 1H), 6.99 (d, *J* = 8.6 Hz, 1H), 4.25 (t, *J* = 6.5 Hz, 1H), 4.21 – 4.17 (m, 2H), 3.67 – 3.63 (m, 2H), 3.25 (dd, *J* = 14.7, 5.4 Hz, 1H), 3.14 (dd, *J* = 14.7, 7.5 Hz, 1H);
^{13}C NMR (126 MHz, D_2O): **δ** 171.4, 157.2, 130.7, 126.8, 115.3, 66.9, 54.1, 49.8, 34.7;
FTIR (neat): 2874 (s, br), 2057 (s), 2016 (s), 1735 (s), 1513 (s), 1488 (m), 1251 (s), 1229 (s), 1206 (s), 838 (s), 803 (m) cm^{-1};
HRMS-ESI (m/z): Calc'd for $C_{11}H_{15}N^{15}N_3O_3^+$ ($[M–Cl]^+$): 254.1050; found: 254.1045.

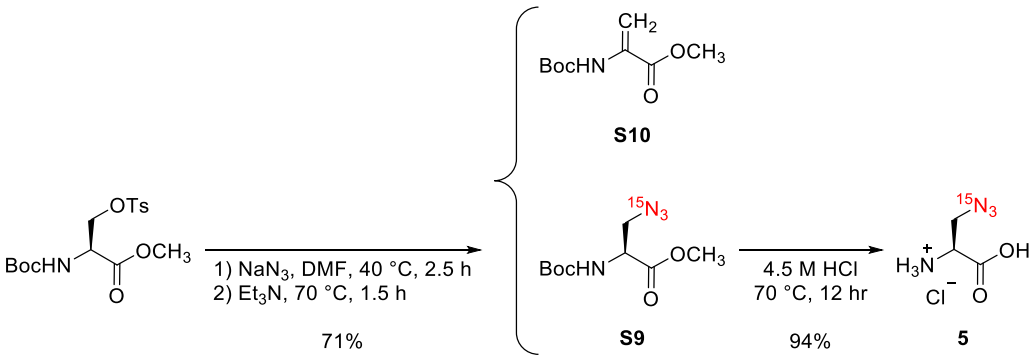

***N*-Boc-3-(azido-$^{15}N_3$)-L-alanine methyl ester (S9).**

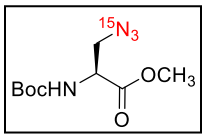

To a 1-dram vial, *N*-Boc-*O*-tosyl-L-serine methyl ester (233.4 mg, 0.625 mmol, 2.5 equiv) was suspended in *N,N*-dimethylformamide (0.65 mL) and sonicated to dissolve. Sodium azide-$^{15}N_3$ (17.0 mg, 0.25 mmol, 1.0 equiv) was added directly to the solution, and the reaction was stirred at 40 °C for 2.5 hours. Subsequently, triethylamine (52.3 µL, 0.375 mmol, 1.5 equiv) was added to the reaction, and the temperature was increased to 70 °C, where it was held for 1.5 hours. The reaction was cooled to room temperature and the reaction mixture was directly subjected to column chromatography (10% ethyl acetate–hexane) to yield **S9** as a colorless oil (44.0 mg, 0.18 mmol, 71% [based on sodium azide-$^{15}N_3$] or 28% [based on *N*-Boc-*O*-tosyl-L-serine methyl ester]) and elimination byproduct **S10** as a colorless oil (82.8 mg, 0.41 mmol, 60% [based on *N*-Boc-*O*-tosyl-L-serine methyl ester]). Note that substantial formation of **S10** has been observed with substitution reactions of *O*-tosylserine derivatives, including azidation.[5] To conserve the labeled sodium azide reagent, excess amino acid precursor was used sacrificially in our procedure.

R_f = 0.38 (20% ethyl acetate–hexane);

^{1}H NMR (400 MHz, $CDCl_3$): **δ** 5.37 – 5.36 (m, 1H), 4.49 – 4.46 (m, 1H), 3.90 (s, 3H), 3.73 – 3.72 (m, 2H), 1.46 (s, 9H);

^{13}C NMR (126 MHz, $CDCl_3$): **δ** 170.2, 155.0, 80.4, 53.4, 52.8, 52.6, 28.2;

FTIR (thin film, MeCN): 3362 (w, br), 2978 (m), 2032 (s), 1702 (s), 1504 (s), 1355 (m), 1247 (m), 1157 (s), 1046 (m), 867 (w), 779 (w) cm^{-1};

HRMS-ESI (m/z): Calc'd for $C_9H_{16}KN^{15}N_3O_4^+$ ([M+K]$^+$): 286.0715; found: 286.0715.

3-(Azido-$^{15}N_3$)-L-alanine (5).

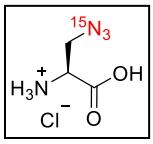

To a 25-mL round-bottom flask, **S9** (41.4 mg, 0.17 mmol, 1.0 equiv) was dissolved in 4.5 M hydrochloric acid (2.0 mL, 9.0 mmol, 53 equiv). The reaction was stirred at 70 °C for 12 hours, after which the reaction was cooled to room temperature and diluted with 1.5 mL water. The reaction mixture was transferred to a separatory funnel and washed with diethyl ether (2 mL × 3). The resulting aqueous layer was collected in a 20 mL scintillation vial and was frozen by placing the vial in a –80°C freezer overnight. The frozen pellet was lyophilized, yielding **5** as a fluffy, light brown solid (27.0 mg, 0.16 mmol, 94%).

^{1}H NMR (400 MHz, D_2O): **δ** 4.26 – 4.21 (m, 1H), 4.04 – 3.97 (m, 1H), 3.91 – 3.86 (m, 1H);

^{13}C NMR (101 MHz, D_2O): **δ** 169.4, 52.2, 49.5;

FTIR (neat): 2934 (w), 2020 (s), 1404 (s), 1353 (m), 1221 (m), 997 (w), 880 (s), 771 (w), 624 (w), 538 (w) cm^{-1};

HRMS-ESI (m/z): Calc'd for $C_3H_7N^{15}N_3O_2^+$ ([M–Cl]$^+$): 134.0475; found: 134.0473.

The spectral characterization of **S9**, **S10**, and **5** prepared by the above procedures were in accord with unlabeled versions reported previously.[5-6]

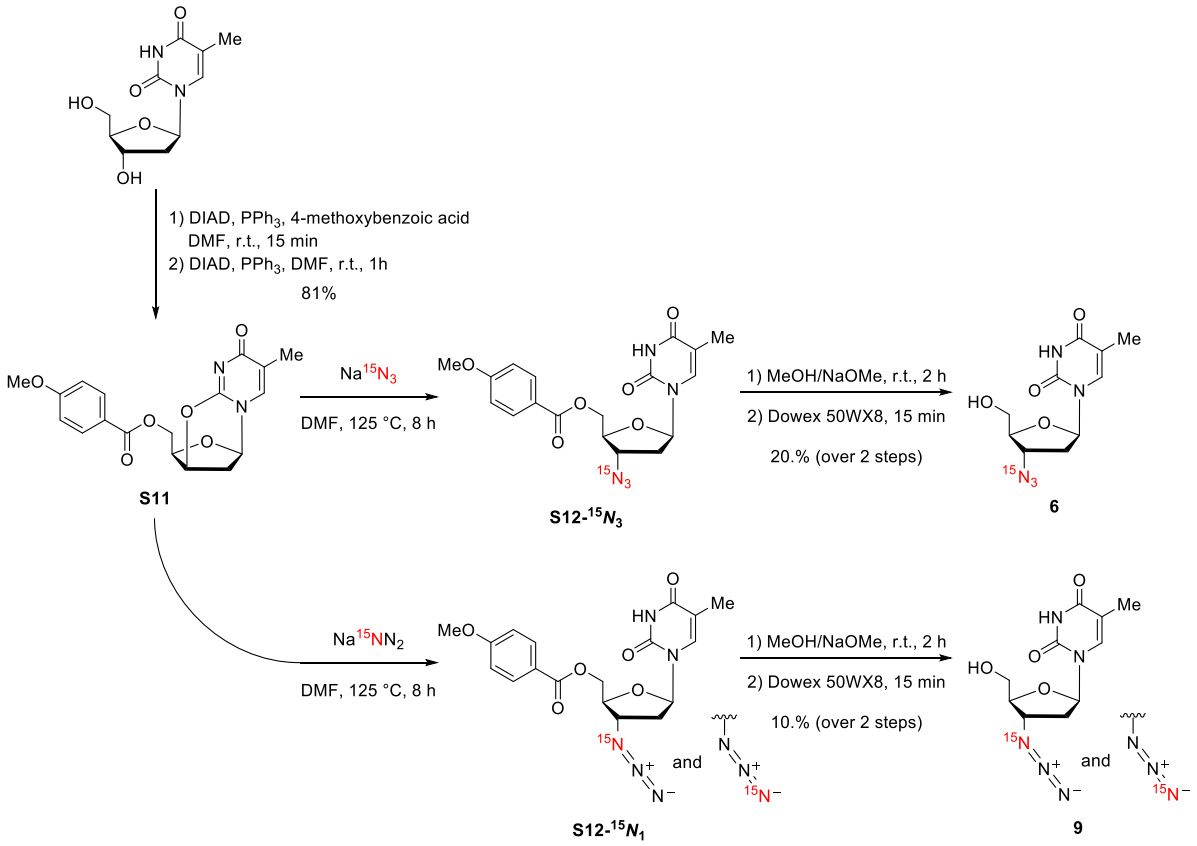

2,3'-anhydro-5'-*O*-(4-methoxybenzoyl)thymidine (**S11**).

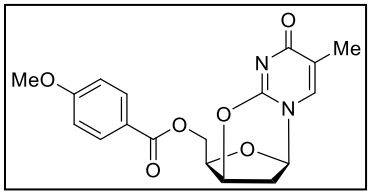

S11 was synthesized following a reported procedure[7] to afford the desired product as a white solid (0.577g, 1.61 mmol, 81%).
R_f = 0.14 (5% methanol–dichloromethane);
^{1}H NMR (500 MHz, DMSO-d_6): **δ** 7.86 (d, J = 8.9 Hz, 2H), 7.57 (s, 1H), 7.01 (d, J = 8.9 Hz, 2H), 5.89 (d, J = 3.2 Hz, 1H), 5.41 (m, 1H), 4.57 (dt, J = 5.9, 2.3 Hz, 1H), 4.48 (dd, J_{gem} = 11.8, J_{vic} = 5.2 Hz, 1H), 4.31 (dd, J_{gem} = 11.8, J_{vic} = 6.5 Hz, 1H), 3.83 (s, 3H), 2.62–2.60 (m, 1H), 2.52 (t, J = 3.2 Hz, 1H), 1.73 (s, 3H);
^{13}C NMR (126 MHz, DMSO-d_6): δ 171.3, 165.5, 163.8, 153.8, 137.1, 131.9, 121.7, 116.6, 114.5, 87.4, 82.5, 77.7, 62.8, 56.0, 33.2, 13.5;
FTIR (neat): 1706 (s), 1532 (s), 1468 (s), 1265 (s) cm^{-1};
HRMS-ESI (m/z): Calc'd for $C_{18}H_{19}N_2O_6^+$ ([M+H]$^+$): 359.1238; found: 359.1244.

3′-(Azido-$^{15}N_3$)-3′-deoxy-5′-*O*-(4-methoxybenzoyl)thymidine (**S12-$^{15}N_3$**).

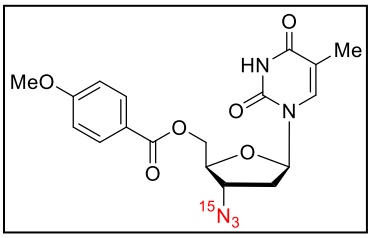

To a 25-mL round-bottom flask, **S11** (287 mg, 0.80 mmol, 1.0 equiv) and sodium azide-$^{15}N_3$ (82 mg, 1.2 mmol, 1.5 equiv) were suspended in DMF (20 mL). The reaction was heated to 125 ºC and stirred for 8 hours. The resulting orange solution was then cooled to room temperature, poured into H_2O (15 mL) and was added 0.2 M HCl (4 mL). The aqueous layer was extracted with EtOAc (10 mL × 3). The combined organic layers were washed with water (10 mL) followed by saturated sodium chloride solution (10 mL), dried with sodium sulfate, and filtered. The filtrate was concentrated *in vacuo* to yield **S12-$^{15}N_3$** as a foamy solid. The crude material was used directly for the next step without purification.

3′-(Azido-$^{15}N_3$)-3′-deoxythymidine (6).

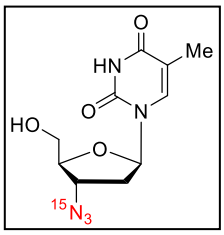

To a 25-mL round-bottom flask was added crude **S12-$^{15}N_3$** and methanol (4 mL). A solution of NaOMe in methanol (1 M, 0.92 mmol, 0.92 mL, 1.15 equiv) was added dropwise, and the resulting mixture was stirred at room temperature for 2 hours. Water (6 mL) was added to this mixture, and then the methanol was evaporated *in vacuo*. The aqueous layer was washed with diethyl ether (10 mL × 2). Acidic ion-exchange resin (~500 mg of Dowex® 50WX8 resin, hydrogen form, 200-400 mesh) was added to the aqueous later, and the mixture was stirred at room temperature for 15 minutes, resulting in a milky, off-white solution. The resin was filtered, washed with water (20 mL), and the filtrate was frozen at –80 ºC. The frozen pellet was lyophilized to afford **6** as a fluffy white solid (43 mg, 0.162 mmol, 20%).

R_f = 0.071 (5% methanol–dichloromethane);

^{1}H NMR (400 MHz, D_2O): **δ** 7.63 (s, 1H), 6.18 (pseudo-t, J = 6.3 Hz, 1H), 4.34 (m, 1H), 4.00 (m, 1H), 3.85, 3.78 (dAB, J_{gem} = 12.6 Hz, J_{vic} = 4.5 Hz, 2H), 2.48 (dt, J = 6.3, 2.6 Hz, 2H), 1.87 (s, 3H);

^{13}C NMR (101 MHz, D_2O): **δ** 166.3, 151.4, 137.4, 111.2, 84.9, 84.0, 60.8, 59.7, 36.1, 11.4

FTIR (neat): 3190 (br), 2027 (s), 1658 (s), 1271 (m) cm^{-1};

HRMS-ESI (m/z): Calc'd for $C_{10}H_{14}{}^{15}N_3O_4^+$ ([M+H]$^+$): 271.0951; found: 271.0958.

3′-(Azido-1-^{15}N)-deoxy-5′-*O*-(4-methoxybenzoyl)thymidine & 3′-(Azido-3-^{15}N)-deoxy-5′-*O*-(4-methoxybenzoyl)thymidine (mixture of isotopomers, **S12-$^{15}N_1$**).

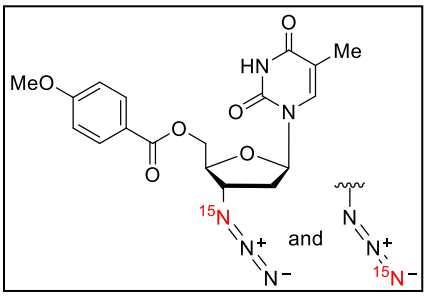

S12-$^{15}N_1$ was synthesized following the same procedure as **S12-$^{15}N_3$** with the substitution of sodium azide-$^{15}N_1$ for sodium azide-$^{15}N_3$.

3′-(Azido-1-^{15}N)-3′-deoxythymidine & 3′-(Azido-3-^{15}N)-3′-deoxythymidine (mixture of isotopomers, **9**).

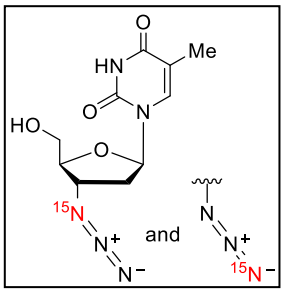

9 was synthesized following the same procedure as **6** with the substitution of **S12-$^{15}N_1$** for **S12-$^{15}N_3$**.

^{1}H NMR (500 MHz, D_2O): **δ** 7.66 (s, 1H), 6.23 (pseudo-t, J = 6.3 Hz, 1H), 4.38 (m, 1H), 4.04 (m, 1H), 3.89, 3.81 (dAB, J_{gem} = 12.6 Hz, J_{vic} = 4.5 Hz, 2H), 2.53 (dt, J = 6.3, 2.6 Hz, 2H), 1.91 (s, 3H);

2. Hyperpolarization Experiments

2.1 Sample Composition for d-DNP Experiments

Table S1. Sample composition for d-DNP experiments.

azide	glass-forming solvent mixture	$c_{initial}$(azide) for polarization / mM	c_{final}(azide) after dissolution / mM	c_{final}(Gd-DTPA) after dissolution / mM
1	50% DMSO, 50% D_2O	500	3.4	0.0078
2	50% DMSO, 50% D_2O	500	3.3	0.0074
3	50% DMSO, 50% D_2O	500	3.3	0.0074
4	50% DMSO, 50% D_2O, 10% 10 M NaOH in D_2O	220	2.1	0.011
5	50% DMSO, 40% D_2O, 10% 5 M NaOH in D_2O	500	3.6	0.0081
6	50% DMSO, 50% D_2O	500	3.7	0.0087
7	50% DMSO, 50% D_2O	500	3.7	0.0087
8	50% DMSO, 50% D_2O	500	4.2	0.0098
9	50% DMSO, 50% D_2O	500	4.4	0.010

2.2 NMR Spectroscopic Data Acquisition and Analysis

For T_1 measurements of $^{15}N_3$-azide compounds hyperpolarized by d-DNP, a series of ^{15}N NMR spectra were acquired on a 1 T NMR spectrometer (Magritek Spinsolve Nitrogen, Wellington, New Zealand) using the pulse sequence ($[\alpha$–acquire$]_{\times n}$). The small flip angle α of the excitation pulse was 10°, with pulse strength ($\gamma B_1/2\pi$) = 1.92 kHz. A total of n = 60 transients was acquired over a duration of 20 min. In each transient, a total of 8192 complex points was collected with an acquisition time of 4.1 s.

For T_1 measurements of $^{15}N_3$-azide **3** hyperpolarized by SABRE-SHEATH, the hyperpolarized sample was stored in the 1 T NMR spectrometer (Magritek Spinsolve Nitrogen, Wellington, New Zealand) without bubbling for a variable time prior data acquisition. Variation of the holding time (τ = 0, 2, 4, 6, 8, 10, 15, 20 min) yields T_1. Note that the residual *para*-H_2 in the solution does not lead to increased polarization during the holding time since 1 T is not the appropriate magnetic field for creating hyperpolarized ^{15}N magnetization. For signal detection, a 90° hard pulse was applied on the ^{15}N channel, with pulse strength ($\gamma B_1/2\pi$) = 1.92 kHz. A total of 8192 complex points was collected with an acquisition time of 4.1 s.

For the hydride spectrum of $^{15}N_3$-azide **3**, the sample (the same composition as that for the SABRE-SHEATH experiment) was activated under a H_2 atmosphere (9 bar) for 30 minutes by constant bubbling *para*-H_2 through the solution (20 sccm/min, *para*-H_2 enrichment ~ 90%). After activation, the sample was transferred to the magnetic field of 8.45 T and a hydride spectrum was acquired with *para*-H_2 bubbling but at a slower rate. The small flip angle α of the excitation pulse was 45°, with pulse strength ($\gamma B_1/2\pi$) = 10.4 kHz. A total of n = 16 transients was acquired over a duration of 3 min. In each transient, a total of 132,000 complex points was collected with an acquisition time of 4.6 s.

T_1 measurement of thermally polarized $^{15}N_3$-azide **1** was performed on a 16.4 T NMR spectrometer (Bruker, Billerica, MA) using an inversion recovery pulse sequence with a variable decay list τ = 0 s, 2 s, 5 s, 10 s, 30 s, 60 s, 90 s, 120 s, 150 s. The pulse strength ($\gamma B_1/2\pi$) of the 90° hard pulse was 8.26 kHz. Proton decoupling was applied during data acquisition.

All data analysis was conducted using Mnova 8.0.1 (Mestrelab Research S. L.) and Matlab program (MathWorks, Natick, MA). ^{15}N chemical shifts are reported on the IUPAC unified Ξ-scale using liquid ammonia as external reference.[8]

In the current procedures, the radicals were not removed in the dissolution step of d-DNP experiments before NMR detection. There was no removal of the catalyst in SABRE experiments before NMR detection. Note that the presence of either the radical or the catalyst does present a potential concern with respect to toxicity for *in vivo* applications or reducing T_1 relaxation lifetime. On the positive note, several strategies regarding on removing the radicals for DNP experiments or removing catalysts in SBARE experiments have been reported, such as by the precipitation and filtration during the dissolution process,[9] the use of functionalized SiO_2 microparticles,[10-11] and other methods.[12-16]

2.3 Determination of T_1 Relaxation

The signal integral from each scan was fitted to a first order exponential decay function $f(t) = I_0 \cdot \exp(-t/T_{1,exp}) + y_0$, with initial signal integral I_0 and relaxation time $T_{1,\mathrm{exp}}$. T_1 values (See Table 1 and 2 in the main text for T_1 lifetimes of different azide compounds) were determined by $T_1 = ({T_{1,exp}}^{-1} + \lambda)^{-1}$, where $\lambda = \ln(\cos(\alpha))/\Delta t$,[17] with α = 10° and Δt = 20 s the time interval between two scans, accounts for signal depletion due to the small flip angle pulses.

2.4 Determination of Enhancement and Polarization Level

For determination of ^{15}N signal enhancement ($\varepsilon_{15\mathrm{N}}$), the hyperpolarized ^{15}N signal acquired with an α = 10° excitation pulse at t = 0 was compared to a thermally polarized signal of neat ^{15}N labeled acetonitrile acquired with a 90° excitation pulse (98 %+, 19.1 M, B = 1 T, Cambridge Isotope Laboratories). $\varepsilon_{15\mathrm{N}}$ was calculated using Eq. S1.

$$\varepsilon_{15N} = \frac{c(acetonitrile)}{c_{final}(azide)} \cdot \frac{S(hyperpolarized\ signal\ (t=0))/\sin(\alpha)}{S(thermal\ reference)/\sin(90^o)} \qquad [Eq.(S1)]$$

Here, c(acetonitrile) = 19.1 M, c_{final}(azide) is the concentration of azide after dissolution (See Table S1).

^{15}N polarization level ($P_{15\mathrm{N}}$) was calculated from ε_{15N} using Eq. S2.

$$P_{15N} = P_{15Nthermal} \cdot \varepsilon_{15N} = (\gamma_{15N}\hbar B/2k_B T) \cdot \varepsilon_{15N} = 3.46 \cdot 10^{-7} \cdot \varepsilon_{15N} \qquad [Eq.(S2)]$$

Here $\gamma_{15\mathrm{N}}$= 2.71·10^7 rad/(s·T), $\hbar$ = 10^{-34} (m^2·kg)/s, B = 1 T, k_B = 1.38·10^{-23} (m^2·kg)/(s^2·K), T = 298.2 K.

2.5 Dependence of ^{14}N-Mediated Scalar Relaxation on the Applied Magnetic Field

Since ^{14}N (I = 1) is a quadrupolar nucleus, scalar and dipolar relaxation mechanisms both contribute to ^{15}N (I = 1/2) relaxation lifetimes within azides **7–9**. In contrast, in the absence of ^{14}N nuclei, the scalar relaxation mechanism is significantly less pronounced for azides **1–6**.[18] The contribution of the ^{14}N-mediated scalar relaxation (second kind; R_1^{sc}), which is dependent on the applied magnetic field, can be expressed as follows,[19,20]

$$R_1^{sc} = \frac{4}{3}\pi^2 I_{14N}(I_{14N}+1)\sum_i J_i^2\left(\frac{2\tau_{sc}}{1+(\omega_{15N}-\omega_{14N})^2\tau_{sc}^2}\right) \qquad [Eq.(S3)]$$

where I is the spin number of a coupled ^{14}N nucleus, J is the scalar coupling constant to the ith ^{14}N nucleus, τ_{sc} is the correlation time characteristic of the scalar interaction which represents the longitudinal relaxation time (T_1) of a coupled ^{14}N quadrupolar nucleus,[19,20] ω is the Larmor angular frequencies of scalarly coupled ^{15}N and ^{14}N nuclei. At near zero field (~ 10 G), the differences of the Larmor angular frequencies $(\omega_{15N}-\omega_{14N}) \approx 0$. As a result, $\left(\frac{2\tau_{sc}}{1+(\omega_{15N}-\omega_{14N})^2\tau_{sc}^2}\right) \approx 2\tau_{sc}$. Therefore, the scalar coupling relaxation caused by the fast-relaxing ^{14}N nucleus cannot be neglected.

During sample transfer from DNP polarizer (B = 3.35 T) to NMR spectrometer (B = 1 T), the magnetic field of the transfer path is < 10 G. As a result, polarization is lost during this process caused by scalar coupling of the ^{15}N to the fast-relaxing quadrupolar ^{14}N within azides **7–9**.[20,21] Furthermore, scalar relaxation scales with J-coupling. The different $J_{14N\text{-}15N}$ coupling among (^{15}N)(^{14}N)$_2$-azides **7–9** leads to varied ^{14}N-mediated scalar relaxation contribution, resulting in differences of the observed polarization for the compounds.

The ^{15}N T_1 lifetimes were measured at magnetic field of 1 T. The similar ^{15}N T_1 lifetimes for azides **7–9** and azides **1–6** suggest that ^{14}N-mediated scalar relaxation is not a dominant contribution to ^{15}N T_1 lifetime at magnetic field of 1 T.

2.6 Theoretical Derivation of Resonance Conditions that Create Hyperpolarized ^{15}N Magnetization

In a SABRE experiment, a polarization transfer catalyst was used to establish contact between the polarization source, *para*-H_2 and the target nuclei. As shown in Scheme S1, the catalyst has an octahedral coordination environment for iridium. The *para*-H_2 derived hydrides and an $^{15}N_3$-azide occupy the catalyst equatorial position and act as exchanging ligands. A DMSO (dimethyl sulfoxide) and an IMes ([1,3-bis(2,4,6-trimethylphenyl)-imidazoyl] occupy the catalyst axial position and act as non-exchanging ligands. In the catalyst equatorial plane, polarization is transferred from hydrides to the ^{15}N nuclei through the *J*-coupling network across the iridium center. The reversible exchange of hydrides and the substrate results in the continuous hyperpolarization buildup on the ^{15}N nuclei if fresh *para*-H_2 was continuously supplied.

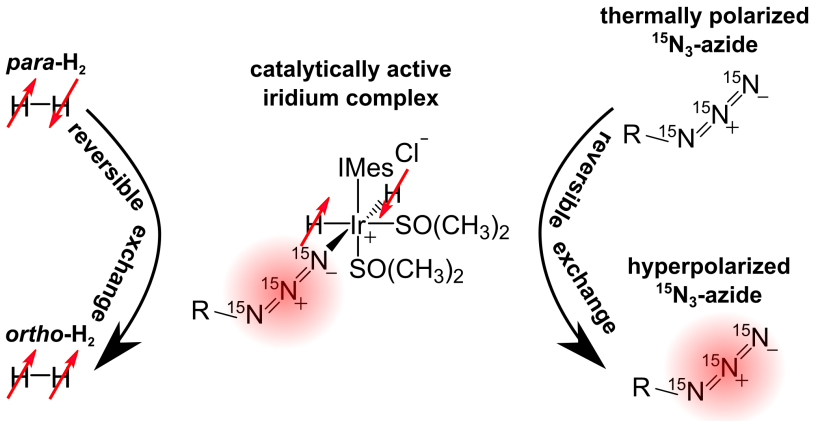

Scheme S1. Schematic representation of generation of hyperpolarized $^{15}N_3$-azide. IMes represents [1,3-bis(2,4,6-trimethylphenyl)-imidazoyl].

The polarization transfer occurs in a AA'BMX spin system, containing five NMR active nuclei (two ^1H nuclei and three ^{15}N nuclei). A simplified sketch is shown in Scheme S2.

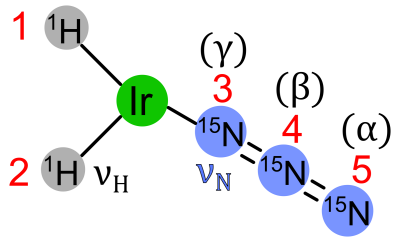

Scheme S2. Spin system for polarization transfer. In the depicted AA'BMX spin system, polarization is transferred from *para*-H_2 derived hydrides to $^{15}N_3$-azide. Note that ^{15}N (3, 4, 5) corresponds to ^{15}N (γ, β, α) in the main text. It is assumed that the polarization transfer process occurs at a magnetic field that is sufficiently low so that the frequency of both hydrides is equivalent to one frequency ν_H and that the frequency of nitrogens is equivalent to one frequency ν_N.

To understand the resonance conditions for polarization transfer driven in the spin system, the Hamiltonian was derived,

$$\widehat{H} = \nu_H\left(\widehat{I_{1z}} + \widehat{I_{2z}}\right) + \nu_N\left(\widehat{S_{3z}} + \widehat{S_{4z}} + \widehat{S_{3z}}\right) + J_{12}\widehat{I_1}\cdot\widehat{I_2} + J_{34}\widehat{S_3}\cdot\widehat{S_4} + J_{45}\widehat{S_4}\cdot\widehat{S_5} + J_{35}\widehat{S_3}\cdot\widehat{S_5}$$
$$+ J_{13}\widehat{I_1}\cdot\widehat{S_3} + J_{14}\widehat{I_1}\cdot\widehat{S_4} + J_{15}\widehat{I_1}\cdot\widehat{S_5} + J_{23}\widehat{I_2}\cdot\widehat{S_3} + J_{24}\widehat{I_2}\cdot\widehat{S_4} + J_{25}\widehat{I_2}\cdot\widehat{S_5} \quad (Eq.S4)$$

As shown in Eq. S4, the Hamiltonian contains magnetic field dependent NMR frequencies ν_H and ν_N as well as magnetic field independent *J*-coupling constants. Further analysis was performed in a matrix representation of the Hamiltonian using a singlet-triple basis for the ^{1}H (1,2) spin pair and the ^{15}N (3,4) spin pair, and the Zeeman basis for the ^{15}N (5) spin. This results in 32 possible states for the spin system:

$$S_0^H S_0^N \alpha_N, T_0^H T_0^N \alpha_N$$
$$S_0^H S_0^N \beta_N, T_0^H T_0^N \beta_N$$
$$T_+^H T_+^N \alpha_N, T_-^H T_-^N \alpha_N$$
$$T_+^H T_+^N \beta_N, T_-^H T_-^N \beta_N$$
$$T_+^H T_-^N \alpha_N, T_-^H T_+^N \alpha_N$$
$$T_+^H T_-^N \beta_N, T_-^H T_+^N \beta_N$$
$$T_+^H T_0^N \alpha_N, T_0^H T_+^N \alpha_N$$
$$T_+^H T_0^N \beta_N, T_0^H T_+^N \beta_N$$
$$T_-^H T_0^N \alpha_N, T_0^H T_-^N \alpha_N$$
$$T_-^H T_0^N \beta_N, T_0^H T_-^N \beta_N$$
$$S_0^H T_0^N \alpha_N, T_0^H S_0^N \alpha_N$$
$$S_0^H T_0^N \beta_N, T_0^H S_0^N \beta_N$$
$$S_0^H T_+^N \alpha_N, T_+^H S_0^N \alpha_N$$
$$S_0^H T_+^N \beta_N, T_+^H S_0^N \beta_N$$
$$S_0^H T_-^N \alpha_N, T_-^H S_0^N \alpha_N$$
$$S_0^H T_-^N \beta_N, T_-^H S_0^N \beta_N$$
$$(Eq.S5)$$

The complete Hamiltonian (Eq. S4) represented in the basis introduced in Eq. S5 leads to a 32×32 matrix. The Hamiltonian can drive the hyperpolarization from the hydrides' singlet state (S_0^H state) to other ^{15}N states (T_+^N, T_-^N states for the ^{15}N (3,4) spin pair or the α_N, β_N states for the ^{15}N (5) spin) so that hyperpolarized ^{15}N magnetization can be created.

Initially, the parahydrogen derived singlet on the hydride pair is populated and all other states have nearly zero population (Eq. S6):

$$p(S_0^H S_0^N \alpha_N) = p(S_0^H S_0^N \beta_N) = p(S_0^H T_0^N \alpha_N) = p(S_0^H T_0^N \beta_N) = p(S_0^H T_+^N \alpha_N) = p(S_0^H T_+^N \beta_N)$$
$$= p(S_0^H T_-^N \alpha_N) = p(S_0^H T_-^N \beta_N) = 0.25$$
$$p(other\ states) = 0 \quad (Eq.S6)$$

Hyperpolarization of ^{15}N magnetization is a process of building up a significant amount of excess population in $|\alpha_N>$, $|\beta_N>$ Zeeman states or $|T_+^N>$, $|T_-^N>$ triplet states. Therefore, we are

interested to find subsets of state combinations from the full Hamiltonian matrix that connect the hydride singlet state with the ^{15}N triplet states or Zeeman states so that hyperpolarized ^{15}N magnetization can be created on the ^{15}N (3,4) spin pair or the ^{15}N (5) spin, respectively.

A) Creating hyperpolarized ^{15}N magnetization on the ^{15}N (3,4) spin pair

Hyperpolarized ^{15}N magnetization on the ^{15}N (3,4) spin pair can be created by connecting the hydride singlet state with the ^{15}N triplet states, for example, the $|S_0^H T_+^N \alpha_N>$ state can be connected to the $|T_+^H S_0^N \alpha_N>$ state,

$$\begin{array}{c} \\ |S_0^H T_+^N \alpha_N> \\ |T_+^H S_0^N \alpha_N> \end{array} \begin{array}{c} \begin{array}{cc} |S_0^H T_+^N \alpha_N> & |T_+^H S_0^N \alpha_N> \end{array} \\ \begin{bmatrix} \frac{(J_{35}+J_{45})}{4} & \frac{(J_{13}-J_{14}-J_{23}+J_{24})}{4} \\ \frac{(J_{13}-J_{14}-J_{23}+J_{24})}{4} & \nu_{\mathrm{H}}-\nu_{\mathrm{N}}+(J_{12}-J_{34})+\frac{(J_{15}+J_{25})}{4} \end{bmatrix} \end{array} \quad \text{(Eq. S7)}$$

If the difference between the diagonal elements is made small, the connection between the states is established, allowing hyperpolarization transfer from the hydride singlet state S_0^H to the ^{15}N triplet states T_+^N. The driving force of the hyperpolarization transfer is the off-diagonal element $\frac{(J_{13}-J_{14}-J_{23}+J_{24})}{4}$. Therefore, the optimal condition for hyperpolarization transfer is obtained on resonance when the diagonal elements are equal. By setting the diagonal elements the same, Eq. S8 is derived

$$\nu_N - \nu_H = J_{12} - J_{34} + \frac{(J_{15}+J_{25}) - (J_{35}+J_{45})}{4} \qquad (Eq.S8)$$

By substituting $\nu_N - \nu_H = B(\gamma_N - \gamma_H)$, Eq. S9 is obtained

$$B = \frac{J_{12} - J_{34} + \frac{(J_{15}+J_{25}) - (J_{35}+J_{45})}{4}}{(\gamma_N - \gamma_H)} \qquad (Eq.S9)$$

Note that, according to Eq. S7, hyperpolarized ^{15}N magnetization on the ^{15}N (3,4) spin pair is obtained by depleting the T_+^N state, resulting in populated S_0^N state. Also note that other resonance conditions that deplete the ^{15}N population in the T_+^N and T_-^N states have the potential to create hyperpolarized ^{15}N magnetization. All such subsets of the state combinations from the Hamiltonian matrix were identified as listed below:

$|S_0^H T_+^N \alpha_N>$ and $|T_+^H S_0^N \alpha_N>$; $|S_0^H T_+^N \beta_N>$ and $|T_+^H S_0^N \beta_N>$; $|S_0^H T_-^N \alpha_N>$ and $|T_-^H S_0^N \alpha_N>$; $|S_0^H T_-^N \beta_N>$ and $|T_-^H S_0^N \beta_N>$ $\qquad (Eq.S10)$

After deriving the resonance conditions, we obtain the magnetic field

$$B = \pm\frac{J_{12} - J_{34} \pm \frac{(J_{15}+J_{25}) - (J_{35}+J_{45})}{4}}{\gamma_H - \gamma_N} \qquad (Eq.S11)$$

Alternatively, hyperpolarized ^{15}N magnetization can be created on the ^{15}N (3,4) spin pair by depleting the S_0^N state, resulting in the populated T_-^N or T_+^N state. For example, the combination of the $|S_0^H S_0^N \alpha_N>$, $|T_+^H T_-^N \alpha_N>$ states. Note that other resonance conditions that populate the ^{15}N population in the T_+^N and T_-^N states have the potential to create hyperpolarized ^{15}N magnetization. All such subsets of the state combinations from the Hamiltonian matrix were identified as listed below:

$|S_0^H S_0^N \alpha_N>$ and $|T_+^H T_-^N \alpha_N>$; $|S_0^H S_0^N \alpha_N>$ and $|T_-^H T_+^N \alpha_N>$; $|S_0^H S_0^N \beta_N>$ and $|T_+^H T_-^N \beta_N>$; $|S_0^H S_0^N \beta_N>$ and $|T_-^H T_+^N \beta_N>$ $(Eq. S12)$

After deriving the resonance conditions, we obtain the magnetic field

$$B = \pm \frac{J_{12} + J_{34} \pm \frac{(J_{15} + J_{25}) - (J_{35} + J_{45}) \mp (J_{13} + J_{14} + J_{23} + J_{24})}{4}}{\gamma_H - \gamma_N} \quad (Eq. S13)$$

The driving force of hyperpolarization transfer derived from the subsets of the state combinations shown above (Eq. S10 and Eq. S12) are $\pm\frac{(J_{13}-J_{14}-J_{23}+J_{24})}{4}$. Using values $J_{12} = -19\,Hz$, $J_{13} = -39\,Hz$, $J_{14} = -19\,Hz$, $J_{15} \approx 0$, $J_{23} \approx -11.5\,Hz$, $J_{24} \approx 0$, $J_{25} \approx 0$, $J_{34} = 7.36\,Hz$, $J_{35} = 0.6\,Hz$, $J_{45} = 14.4\,Hz$, $\gamma_H = 4.2576\frac{kHz}{G}$, $\gamma_N = -0.4316\frac{kHz}{G}$, we obtain the absolute values for the magnetic fields where hyperpolarized ^{15}N magnetization on the ^{15}N (3,4) spin pair are created as ~ 0.6 μT and ~ 0.5 μT (calculated by Eq. S11), ~ 0.04 μT and ~ 0.2 μT (calculated by Eq. S13). The $J_{hydride-15N}$ and $J_{15N-15N}$ coupling constants were obtained from the hydride spectrum (Figure S3) and the hyperpolarized ^{15}N spectrum (Figure S1c), respectively.

B) Creating hyperpolarized ^{15}N magnetization on the ^{15}N (5) spin

Hyperpolarized ^{15}N magnetization on the ^{15}N (5) spin can be created by connecting the hydride singlet state with the ^{15}N Zeeman state, for example, the $|S_0^H T_+^N \alpha_N>$ state can be connected to the $|T_+^H T_+^N \beta_N>$ state,

$$\begin{array}{c} \\ |S_0^H T_+^N \alpha_N> \\ |T_+^H T_+^N \beta_N> \end{array} \begin{array}{c} \begin{array}{cc} |S_0^H T_+^N \alpha_N> & |T_+^H T_+^N \beta_N> \end{array} \\ \begin{bmatrix} \frac{(J_{35} + J_{45})}{2} & \frac{-J_{15} + J_{25}}{2\sqrt{2}} \\ \frac{-J_{15} + J_{25}}{2\sqrt{2}} & \nu_H - \nu_N + J_{12} + \frac{(J_{13} + J_{14} + J_{23} + J_{24}) - (J_{15} + J_{25})}{4} \end{bmatrix} \end{array} \quad (Eq. S14)$$

According to Eq. S14, hyperpolarization is transferred by depleting the hydride singlet and affecting population in the $|\alpha>$ and $|\beta>$ states. The driving force of the hyperpolarization transfer is the off-diagonal element $\frac{-J_{15}+J_{25}}{2\sqrt{2}}$. Since other resonance conditions that deplete the hydride singlet and affect the $|\alpha>$ and $|\beta>$ population also have the potential to create hyperpolarized ^{15}N magnetization on the ^{15}N (5) spin, we identified all such subsets of the state combinations from the Hamiltonian matrix as listed below,

$|S_H^0 S_N^0 \alpha_N>$ and $|T_H^+ S_N^0 \beta_N>$; $|S_H^0 S_N^0 \beta_N>$ and $|T_H^- S_N^0 \alpha_N>$; $|S_H^0 T_N^0 \alpha_N>$ and $|T_H^+ T_N^0 \beta_N>$; $|S_H^0 T_N^0 \beta_N>$ and $|T_H^- T_N^0 \alpha_N>$ $(Eq. S15)$

$|S_H^0 T_N^+ \alpha_N>$ and $|T_H^+ T_N^+ \beta_N>$; $|S_H^0 T_N^+ \beta_N>$ and $|T_H^- T_N^+ \alpha_N>$; $|S_H^0 T_N^- \alpha_N>$ and $|T_H^+ T_N^- \beta_N>$; $|S_H^0 T_N^- \beta_N>$ and $|T_H^- T_N^- \alpha_N>$ $(Eq. S16)$

After deriving the resonance conditions, we obtain the magnetic fields for Eq. S15 and Eq. S16, respectively,

$$B = \pm \frac{J_{12} - \frac{(J_{15} + J_{25})}{4}}{\gamma_H - \gamma_N} \quad (Eq. S17)$$

$$B = \pm \frac{J_{12} \pm \frac{(J_{13} + J_{14} + J_{23} + J_{24})}{4} \mp \frac{(J_{35} + J_{45})}{2} - \frac{(J_{15} + J_{25})}{4}}{\gamma_H - \gamma_N} \quad (Eq. S18)$$

The driving force of hyperpolarization transfer derived from the subsets of the state combinations shown above (Eq. S15 and Eq. S16) are $\pm(\frac{J_{15}-J_{25}}{2\sqrt{2}})$. Using values $J_{12} = -19\ Hz$, $J_{13} = -39\ Hz$, $J_{14} = -19\ Hz$, $J_{15} \approx 0$, $J_{23} \approx -11.5\ Hz$, $J_{24} \approx 0$, $J_{25} \approx 0$, $J_{34} = 7.36\ Hz$, $J_{35} = 0.6\ Hz$, $J_{45} = 14.4\ Hz, \gamma_H = 4.2576 \frac{kHz}{G}, \gamma_N = -0.4316 \frac{kHz}{G}$, we obtain the absolute values for the magnetic fields where hyperpolarized ^{15}N magnetization on the ^{15}N (5) spin are created as ~ 0.4 μT (calculated by Eq. S17), ~ 0.9 μT and ~ 0.1 μT (calculated by Eq. S18).

In conclusion, the resonance condition for creating hyperpolarized ^{15}N magnetization is magnetic field dependent. From the theoretical calculation, the magnetic field is in the range of [-1 μT, 1 μT]. This matches our experimental findings where 0.5 μT was used to achieve hyperpolarized ^{15}N magnetization. Note that, since the *J*-couplings in the system, such as J_{15}, J_{23}, J_{24}, J_{25}, are associated with uncertainty, it is reasonable that the resonance conditions may be relatively broad. The driving force of hyperpolarization transfer from hydride singlet state to the $|\alpha>$ or $|\beta>$ states of the ^{15}N (5) spin is $\pm(\frac{J_{15}-J_{25}}{2\sqrt{2}})$, resulting in less efficient polarization transfer due to the small values of J_{15} and J_{25}. This is consistent with the experimental observation where the obtained polarization level of ^{15}N (5) (^{15}Nα in the main text) is low. Furthermore, it is also possible that hyperpolarized ^{15}N magnetization on ^{15}N (5) can be created by polarization transfer from ^{15}N (3,4) through the *J*-coupling network, as we identified the corresponding subsets of the state combinations from the full Hamiltonian matrix, for example, the connection of the $|T_+^H S_0^N \alpha_N>$ and $|T_+^H T_+^N \beta_N>$ states.

$$\begin{array}{c} \\ |T_+^H S_0^N \alpha_N> \\ |T_+^H T_+^N \beta_N> \end{array} \begin{array}{c} \begin{array}{cc} |T_+^H S_0^N \alpha_N> & |T_+^H T_+^N \beta_N> \end{array} \\ \begin{bmatrix} -4J_{34} + J_{15} + J_{25} & \frac{-J_{35} + J_{45}}{2\sqrt{2}} \\ \frac{-J_{35} + J_{45}}{2\sqrt{2}} & J_{13} + J_{14} + J_{23} + J_{24} - (J_{15} + J_{25}) - (J_{35} + J_{45}) \end{bmatrix} \end{array} \quad (Eq. 19)$$

As shown in Eq. S7, hyperpolarization is transferred from hydride singlets to the ^{15}N (3,4) spin pair by depleting the S_0^H and T_+^N states, resulting in the populated T_+^H and S_0^N states. Then the connection of the $|T_+^H S_0^N \alpha_N >$ and $|T_+^H T_+^N \beta_N >$ states shown in Eq. S19 allows hyperpolarization transfer from the ^{15}N (3,4) spin pair to the ^{15}N (5) spin by depleting the S_0^N state and thus affecting population in the $|\alpha >$ and $|\beta >$ states of the ^{15}N (5) spin. The driving force is the off-diagonal element $\frac{-J_{35}+J_{45}}{2\sqrt{2}}$. The optimal condition for polarization transfer is obtained by setting the diagonal elements equivalent to each other,

$$J_{13} + J_{14} + J_{23} + J_{24} - (J_{15} + J_{25}) - (J_{35} + J_{45}) = -4J_{34} + (J_{15} + J_{25}) \qquad (Eq.S20)$$

The values of $J_{13} + J_{14} + J_{23} + J_{24} - (J_{15} + J_{25}) - (J_{35} + J_{45})(\approx -84.5\, Hz)$ and $-4J_{34} + (J_{15} + J_{25})(\approx -29.4\, Hz)$ are negative, which is the connection between the two states that creates polarization transfer from ^{15}N (3,4) to ^{15}N (5). Since *J*-coupling constants are magnetic field independent, the values calculated on the left side of Eq. S20 are not exactly matched with that on the right side and therefore the resonance condition is not fulfilled exactly. This indicates hyperpolarization transfer from ^{15}N (3,4) to ^{15}N (5) is less efficient which further explains the low polarization level obtained on ^{15}N (5) (^{15}N (α) in the main text).

While the SABRE-SHEATH polarizations are relatively low, the dramatic advantages of this method (including reduced cost and convenience) suggest these are promising targets. In the simplest cases of SABRE polarization (such as ^{15}N-pyridine) level anticrossing conditions are traditionally used to calculate an "optimal" field in the microtesla regime; in this case, the complex coupling network makes such calculations quite problematic. Some ongoing work (unpublished) shown that highly nontuitive field conditions are capable of enhancing these signals.

3. Hyperpolarized ^{15}N-NMR spectra

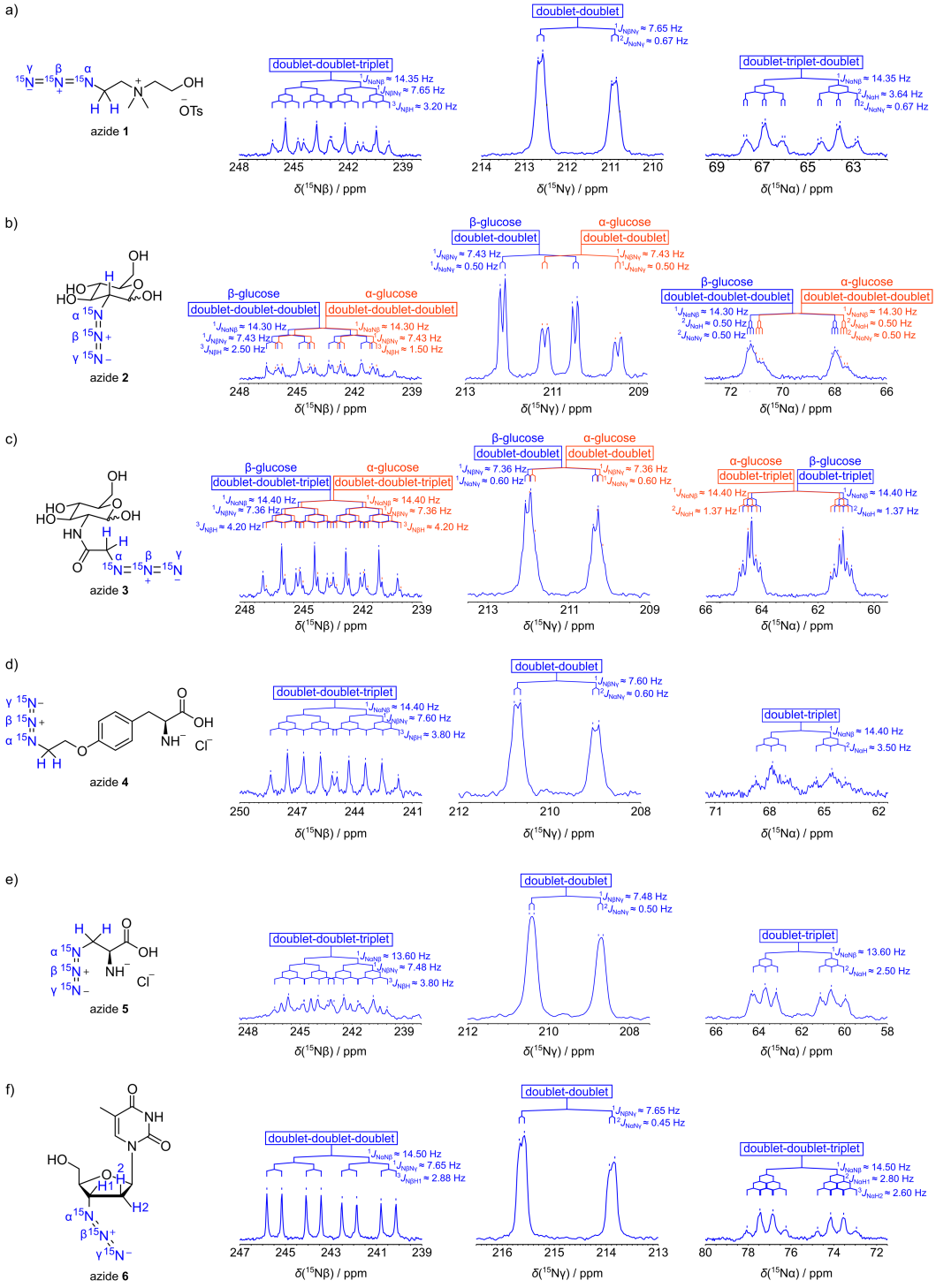

Figure S1. a)-f) Hyperpolarized ^{15}N spectra of $^{15}N_3$-azides (**1–6**) and *J*-coupling analysis. The spectra were measured by d-DNP at magnetic field of 1 T with 10° small flip angle pulses. The spectra acquired at $t = 0$ are shown. Note that line broadening (lb) = 0.1 Hz was applied to spectra shown in a), b), c) and f). lb = 0.2 Hz and 0.4 Hz were applied to spectra shown in d) and e), respectively.

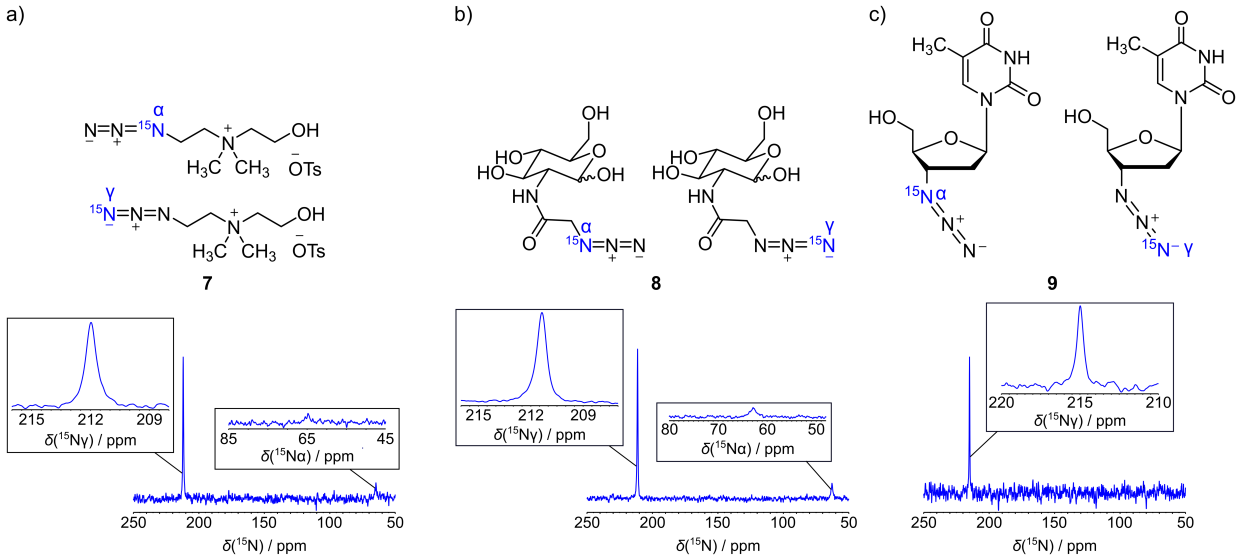

Figure S2. a)-c) Hyperpolarized ^{15}N spectra of (^{15}N)(^{14}N)$_2$-azides (**7–9**), respectively. The spectra were measured by d-DNP at magnetic field of 1 T with 10° small flip angle pulses. The spectra acquired at $t = 0$ are shown for ^{15}Nγ sites. Note that line broadening (lb) = 1 Hz was applied to all spectra. The ^{15}N spectra are T_2-broadened due to the fast quadrupolar relaxation of the directly bonded ^{14}N nuclei. Signal to noise ratio too low for the detection at ^{15}Nα site.

4. ^{1}H Spectrum of the Hydride Region

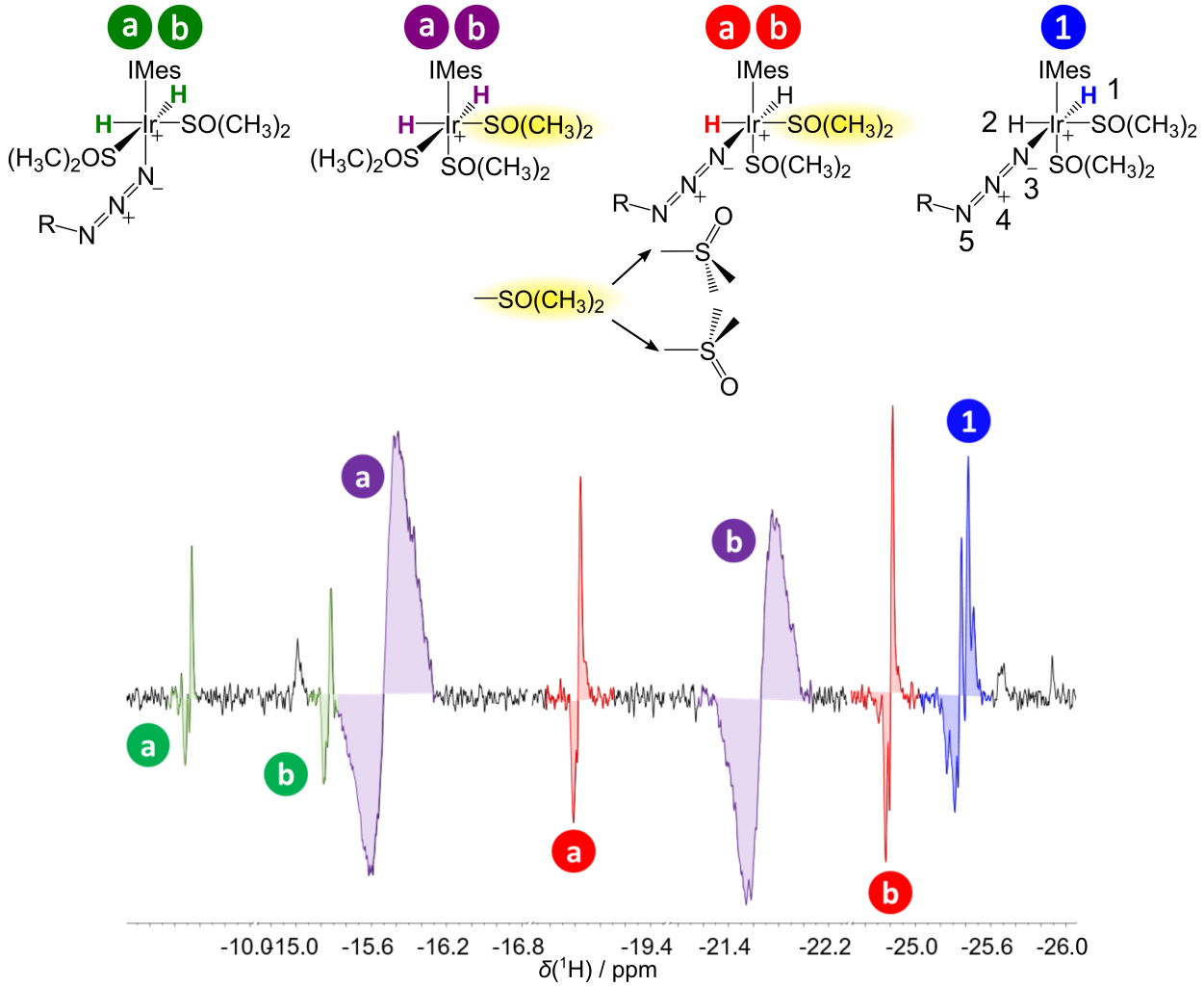

Figure S3. ^{1}H spectrum of the hydride region. The spectrum was measured at magnetic field of 8.45 T while slowly bubbling *para*-H_2 (enrichment ~ 90%) to the sample. The composition of the sample was the same as that for the SABRE-SHEATH experiment. The structures of the hydride resonances are depicted above the spectrum. IMes represents [1,3-bis(2,4,6- trimethylphenyl)-imidazoyl]. The hydride signals arise from the active species corresponding to H1 (blue, δ = -25.4 ppm), Ha (red, δ = -24.8 ppm) and Hb (red, δ = -18.8 ppm) showing J_{12} = -19 Hz, J_{13} = -39 Hz, J_{14} = -19 Hz, $J_{23} \approx$ -11.5 Hz (the resonance numbers are shown in the structure on the right).

5. References

1. Markley, J. L.; Bax, A.; Arata, Y.; Hilbers, C. W.; Kaptein, R.; Sykes, B. D.; Wright, P. E.; Wuthrich, K., Recommendations for the presentation of NMR structures of proteins and nucleic acids. IUPAC-IUBMB-IUPAB Inter-Union Task Group on the Standardization of Data Bases of Protein and Nucleic Acid Structures Determined by NMR Spectroscopy. *J. Biomol. NMR* **1998,** *12*, 1–23.
2. Brauer, G., *Handbook of Preparative Inorganic Chemistry*. 2nd ed.; Academic Press: New York, 1963; Vol. 1.
3. Zaro, B. W.; Batt, A. R.; Chuh, K. N.; Navarro, M. X.; Pratt, M. R., The Small Molecule 2-Azido-2-deoxy-glucose Is a Metabolic Chemical Reporter of O-GlcNAc Modifications in Mammalian Cells, Revealing an Unexpected Promiscuity of O-GlcNAc Transferase. *ACS Chem. Biol.* **2017,** *12*, 787–794.
4. Laughlin, S. T.; Bertozzi, C. R., Metabolic labeling of glycans with azido sugars and subsequent glycan-profiling and visualization via Staudinger ligation. *Nat. Protoc.* **2007,** *2*, 2930–2944.
5. Boibessot, T.; Bénimèlis, D.; Jean, M.; Benfodda, Z.; Meffre, P., Synthesis of a Novel Rhizobitoxine-Like Triazole-Containing Amino Acid. *Synlett* **2016,** *27*, 2685–2688.
6. Link, A. J.; Vink, M. K. S.; Tirrell, D. A., Presentation and Detection of Azide Functionality in Bacterial Cell Surface Proteins. *J. Am. Chem. Soc.* **2004,** *126*, 10598–10602.
7. Czernecki, S.; Valéry, J.-M., An Efficient Synthesis of 3′-Azido-3′-deoxythymidine (AZT). *Synthesis* **1991,** *3*, 239–240.
8. Harris, R. K.; Becker, E. D.; de Menezes, S. M. C.; Granger, P.; Hoffman, R. E.; Zilm, K. W., Further conventions for NMR shielding and chemical shifts (IUPAC Recommendations 2008). *Pure and Applied Chem.* **2008,** *80*, 59.
9. Gajan, D.; Bornet, A.; Vuichoud, B.; Milani, J.; Melzi, R.; van Kalkeren, H. A.; Veyre, L.; Thieuleux, C.; Conley, M. P.; Grüning, W. R.; Schwarzwälder, M.; Lesage, A.; Copéret, C.; Bodenhausen, G.; Emsley, L.; Jannin, S., Hybrid polarizing solids for pure hyperpolarized liquids through dissolution dynamic nuclear polarization. *Proc. Natl. Acad. Sci.* **2014**, *111*, 14693–14697.
10. Barskiy, D. A.; Ke, L. A.; Li, X.; Stevenson, V.; Widarman, N.; Zhang, H.; Truxal, A.; Pines, A. Rapid Catalyst Capture Enables Metal-Free *para*-Hydrogen-Based Hyperpolarized Contrast Agents. *J. Phys. Chem. Lett.* **2018**, *9*, 2721–2724.
11. Kidd, B. E.; Gesiorski, J. L.; Gemeinhardt, M. E.; Shchepin, R. V.; Kovtunov, K. V.; Koptyug, I. V.; Chekmenev, E. Y.; Goodson, B. M. Facile Removal of Homogeneous SABRE Catalysts for Purifying Hyperpolarized Metronidazole, a Potential Hypoxia Sensor. *J. Phys. Chem. C* **2018**, *122*, 16848–16852.
12. Lama, B.; Collins, J. H. P.; Downes, D.; Smith, A. N.; Long, J. R., Expeditious dissolution dynamic nuclear polarization without glassing agents. *NMR Biomed.* **2016**, *29*, 226–231.
13. Miéville, P.; Ahuja, P.; Sarkar, R.; Jannin, S.; Vasos, P. R.; Gerber-Lemaire, S.; Mishkovsky, M.; Comment, A.; Gruetter, R.; Ouari, O.; Tordo, P.; Bodenhausen, G., Scavenging Free

Radicals To Preserve Enhancement and Extend Relaxation Times in NMR using Dynamic Nuclear Polarization. *Angew. Chem. Int. Ed.* **2010**, *49*, 6182–6185.

14. Harris, T.; Szekely, O.; Frydman, L., On the Potential of Hyperpolarized Water in Biomolecular NMR Studies. *J. Phys. Chem. B* **2014**, *118*, 3281–3290.
15. Capozzi, A.; Hyacinthe, J.-N.; Cheng, T.; Eichhorn, T. R.; Boero, G.; Roussel, C.; van der Klink, J. J.; Comment, A., Photoinduced Nonpersistent Radicals as Polarizing Agents for X-Nuclei Dissolution Dynamic Nuclear Polarization. *J. Phys. Chem. C* **2015**, *119*, 22632–22639.
16. Eichhorn, T. R.; Takado, Y.; Salameh, N.; Capozzi, A.; Cheng, T.; Hyacinthe, J. N.; Mishkovsky, M.; Roussel, C.; Comment, A., Hyperpolarization without persistent radicals for in vivo real-time metabolic imaging. *Proc. Natl. Acad. Sci. USA* **2013**, *110*, 18064–18069.
17. Zeng, H.; Lee, Y.; Hilty, C., Quantitative Rate Determination by Dynamic Nuclear Polarization Enhanced NMR of a Diels−Alder Reaction. *Anal. Chem.* **2010,** *82*, 8897–8902.
18. Cho, A.; Eskandari, R.; Miloushev, V. Z.; Keshari, K. R., A non-synthetic approach to extending the lifetime of hyperpolarized molecules using D_2O solvation. *J. Magn. Reson.* **2018**, *295*, 57–62.
19. L. Sudmeier, J.; E. Anderson, S.; S. Frye, J. Calculation of Nuclear Spin Relaxation Times. *Concepts Magn. Reson.* **1990**, *2*, 197–212.
20. Chiavazza, E.; Kubala, E.; Gringeri, C. V.; Düwel, S.; Durst, M.; Schulte, R. F.; Menzel, M. I., Earth's magnetic field enabled scalar coupling relaxation of ^{13}C nuclei bound to fast-relaxing quadrupolar ^{14}N in amide groups. *J. Magn. Reson.* **2013**, *227*, 35-38.
21. Reed, G. D.; Morze, C. V.; Bok, R.; Koelsch, B. L.; Criekinge, M. V.; Smith, K. J.; Shang, H.; Larson, P. E. Z.; Kurhanewicz, J.; Vigneron, D. B., High Resolution ^{13}C MRI With Hyperpolarized Urea: In Vivo T_2 Mapping and ^{15}N Labeling Effects. *IEEE Trans. Med. Imaging* **2014**, *33*, 362–371.

6. NMR spectra

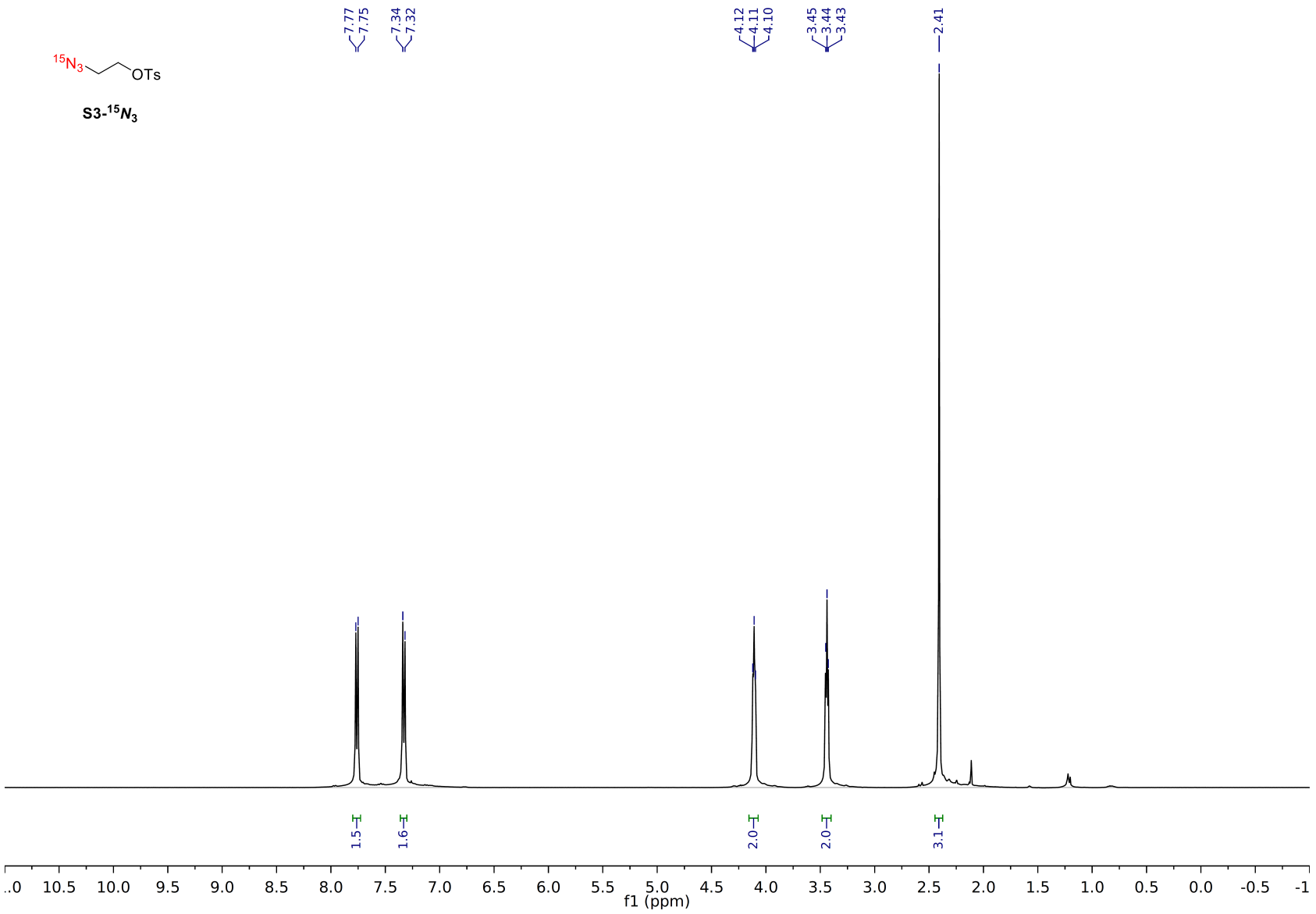

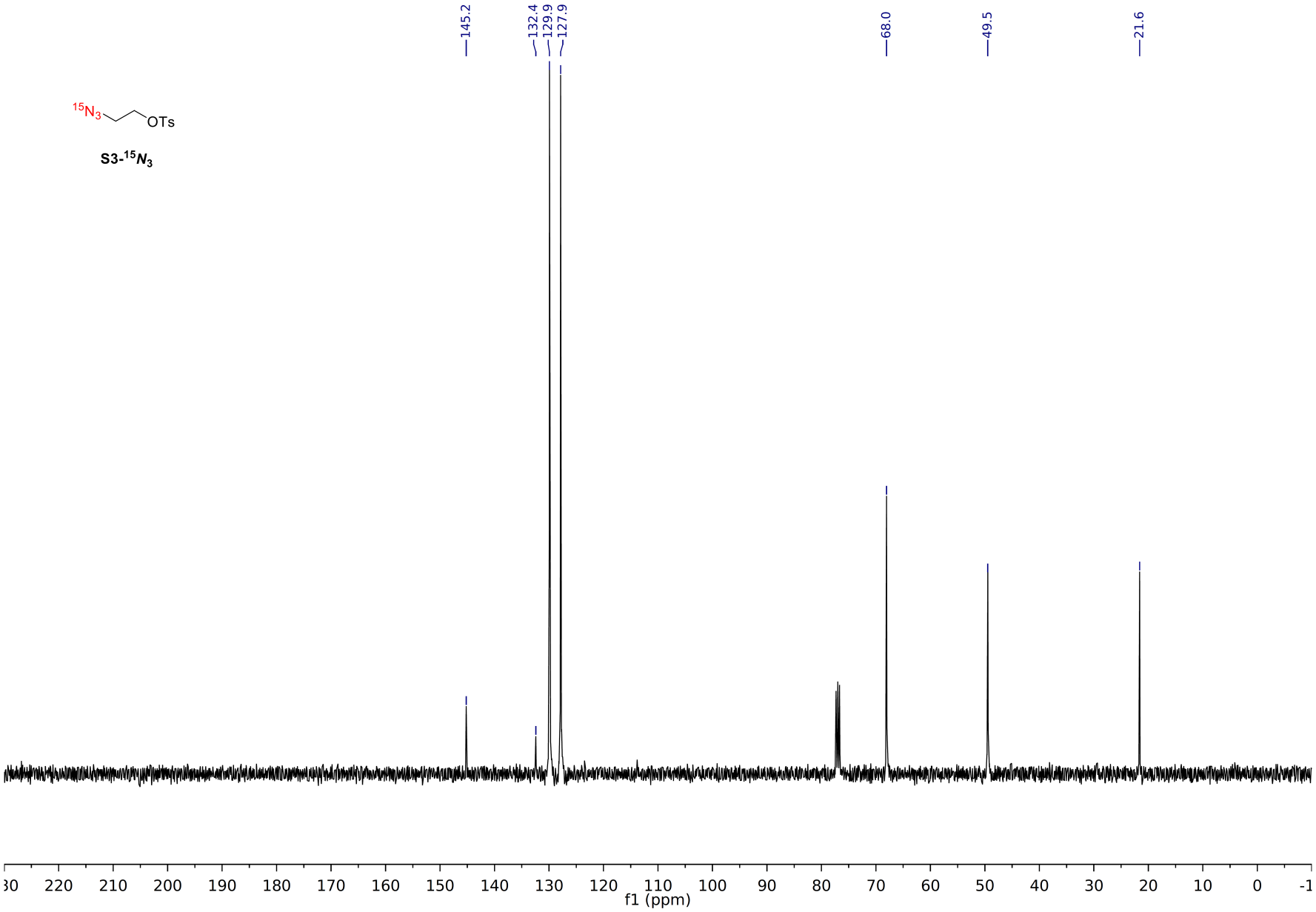
145.2
132.4
129.9
127.9
68.0
49.5
21.6
15N3
OTs
S3-15N3
f1 (ppm)

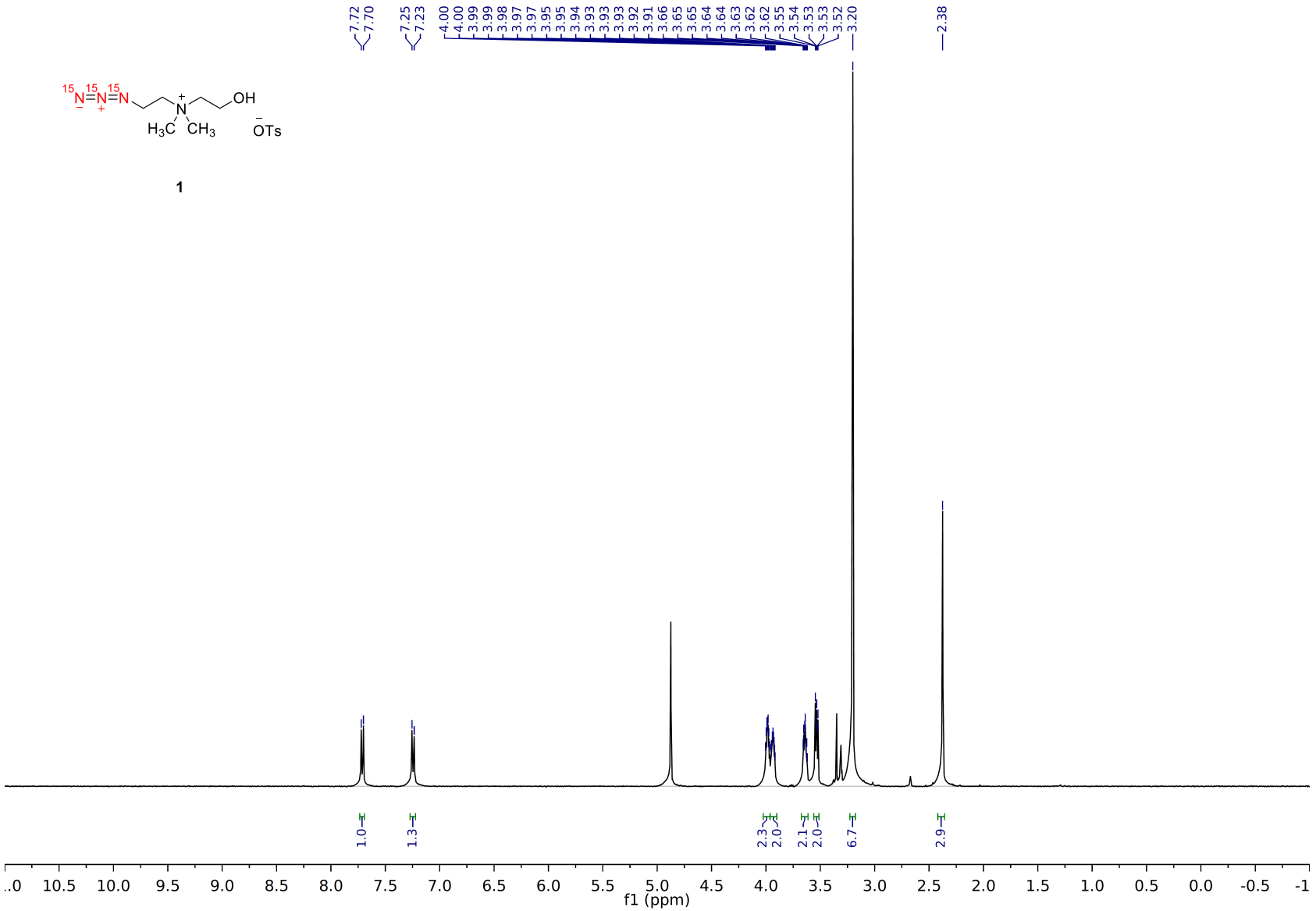
7.72
7.70
7.25
7.23
4.00
4.00
3.99
3.99
3.98
3.97
3.97
3.95
3.95
3.94
3.93
3.93
3.93
3.92
3.91
3.66
3.65
3.65
3.64
3.64
3.63
3.62
3.62
3.55
3.54
3.53
3.53
3.52
3.20
2.38
15N=15N=15N
OH
H3C CH3
OTs
1
1.0
1.3
2.3
2.0
2.1
2.0
6.7
2.9
f1 (ppm)

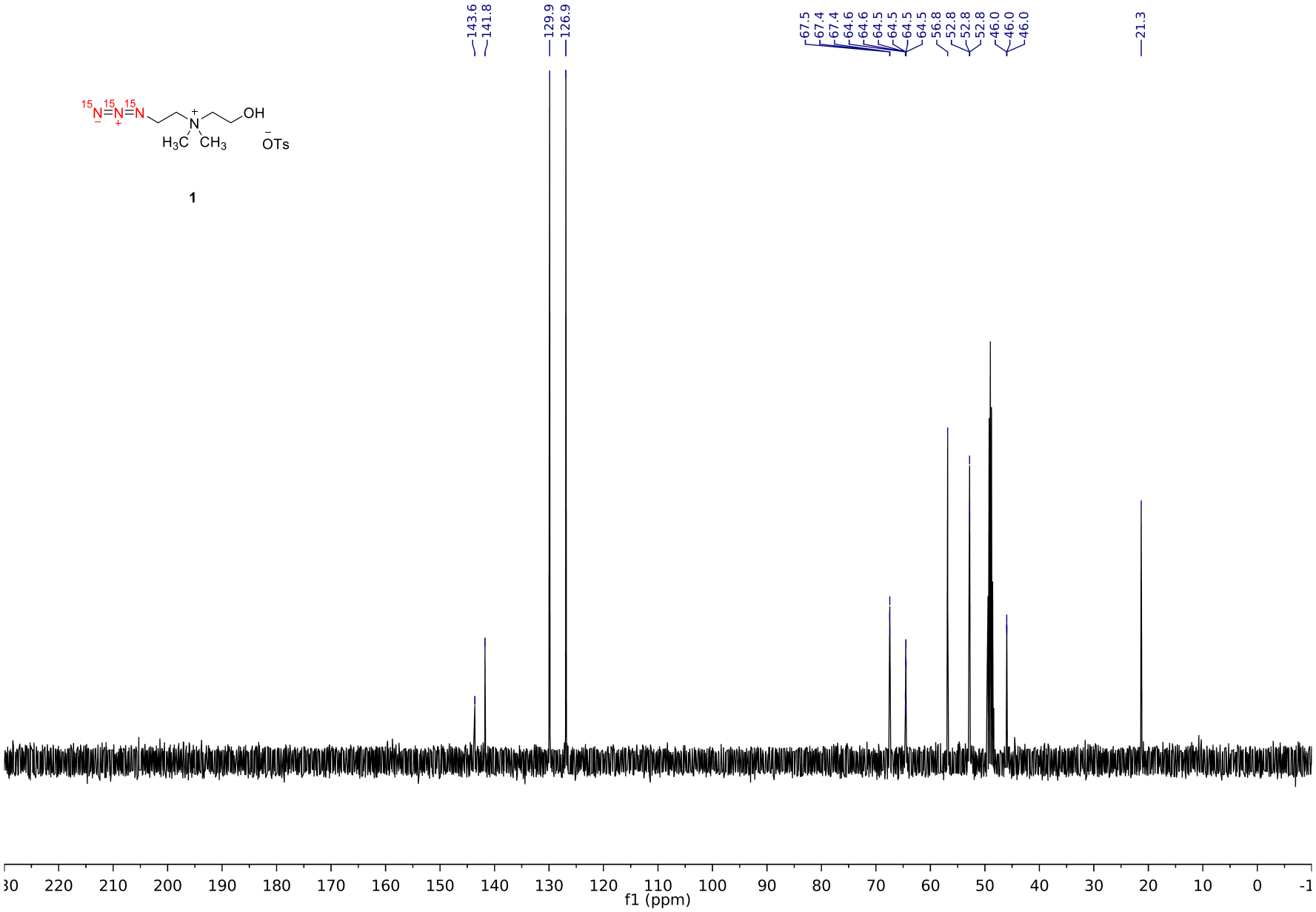
143.6
141.8
129.9
126.9
67.5
67.4
67.4
64.6
64.6
64.5
64.5
64.5
64.5
56.8
52.8
52.8
52.8
46.0
46.0
46.0
21.3
OH
OTs
1
f1 (ppm)

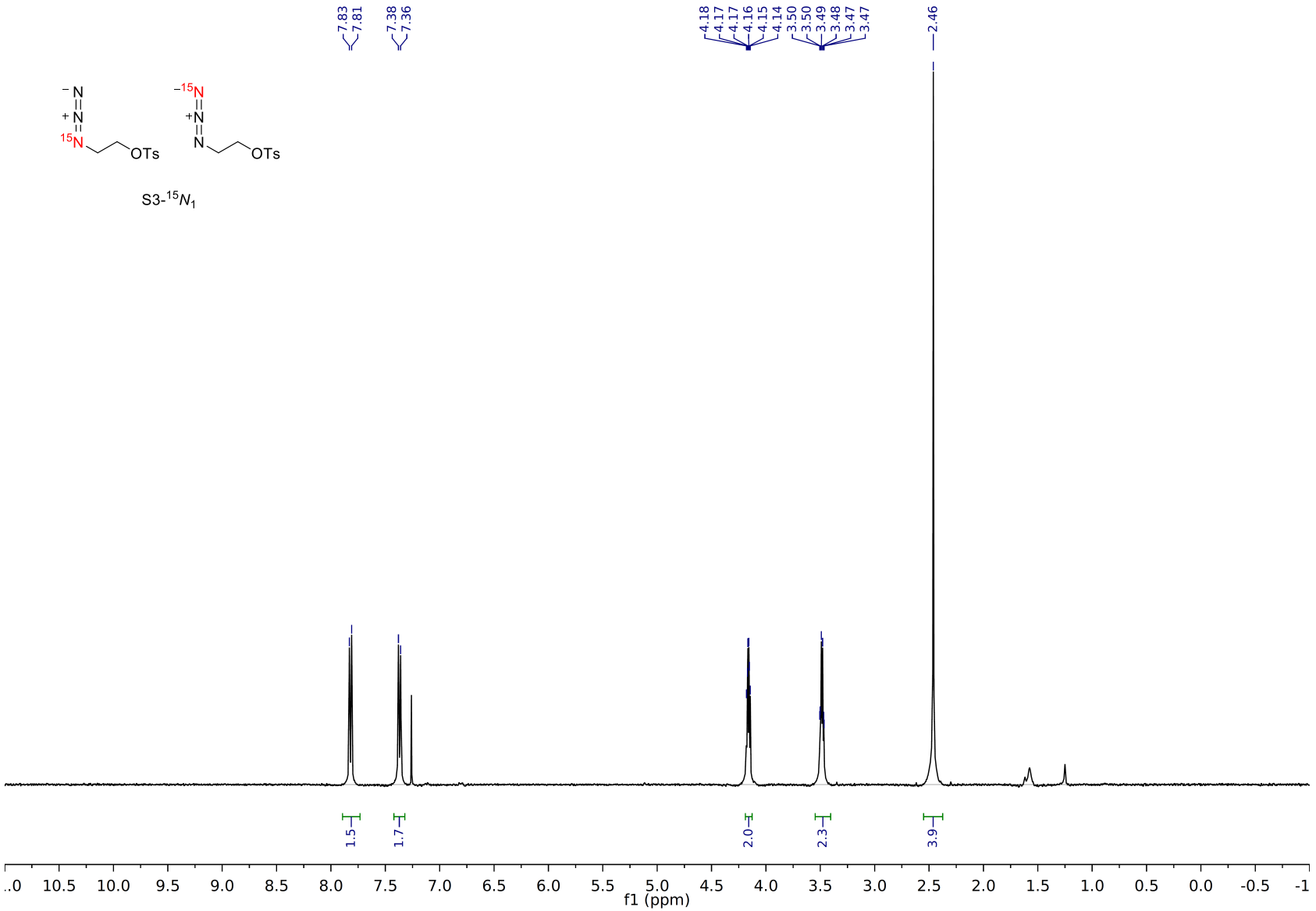
7.83
7.81
7.38
7.36
4.18
4.17
4.17
4.16
4.15
4.14
3.50
3.50
3.49
3.48
3.47
3.47
2.46
1.5
1.7
2.0
2.3
3.9
f1 (ppm)

S3-$^{15}N_1$

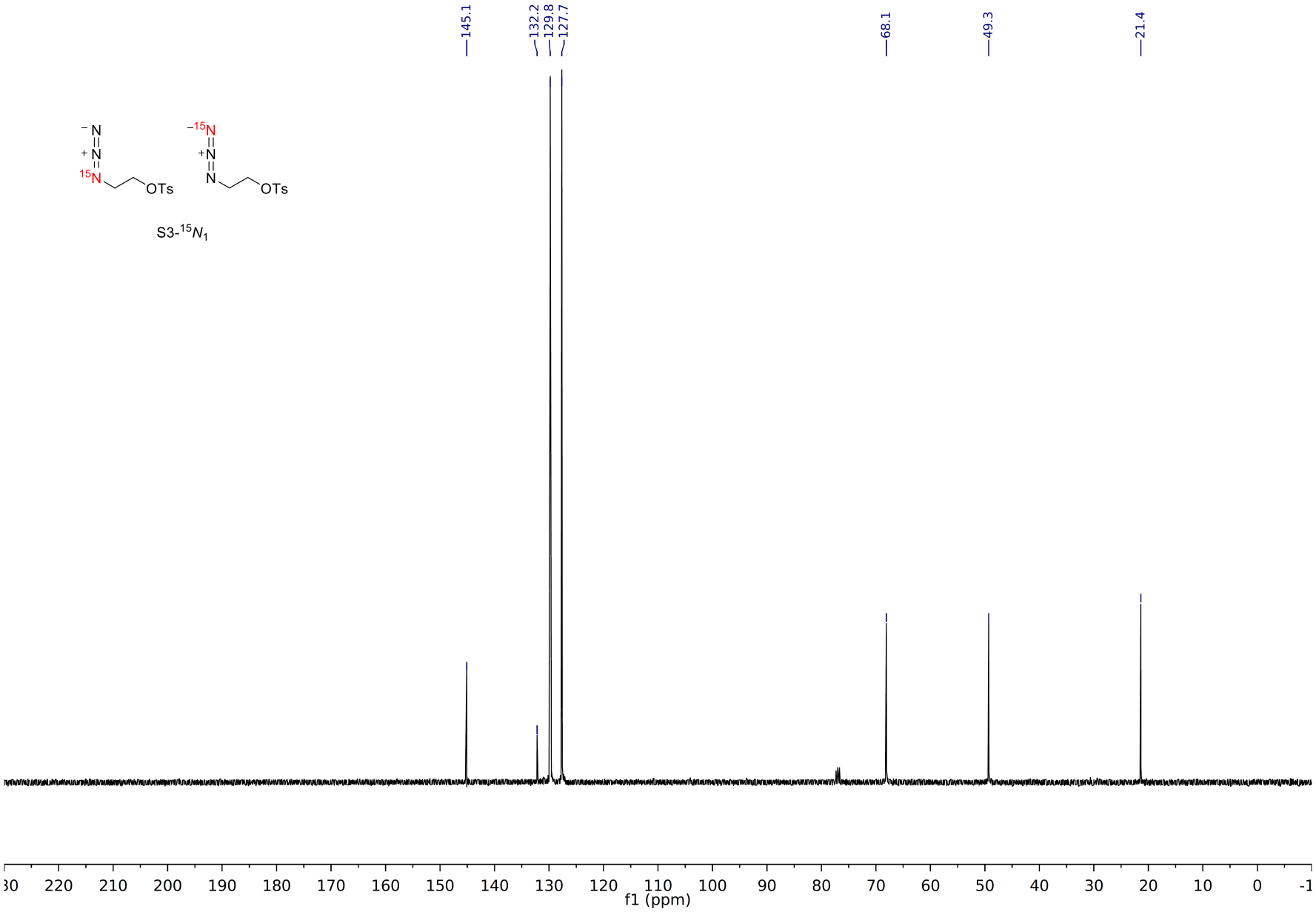
145.1
132.2
129.8
127.7
68.1
49.3
21.4
OTs
OTs
S3-15N1
f1 (ppm)

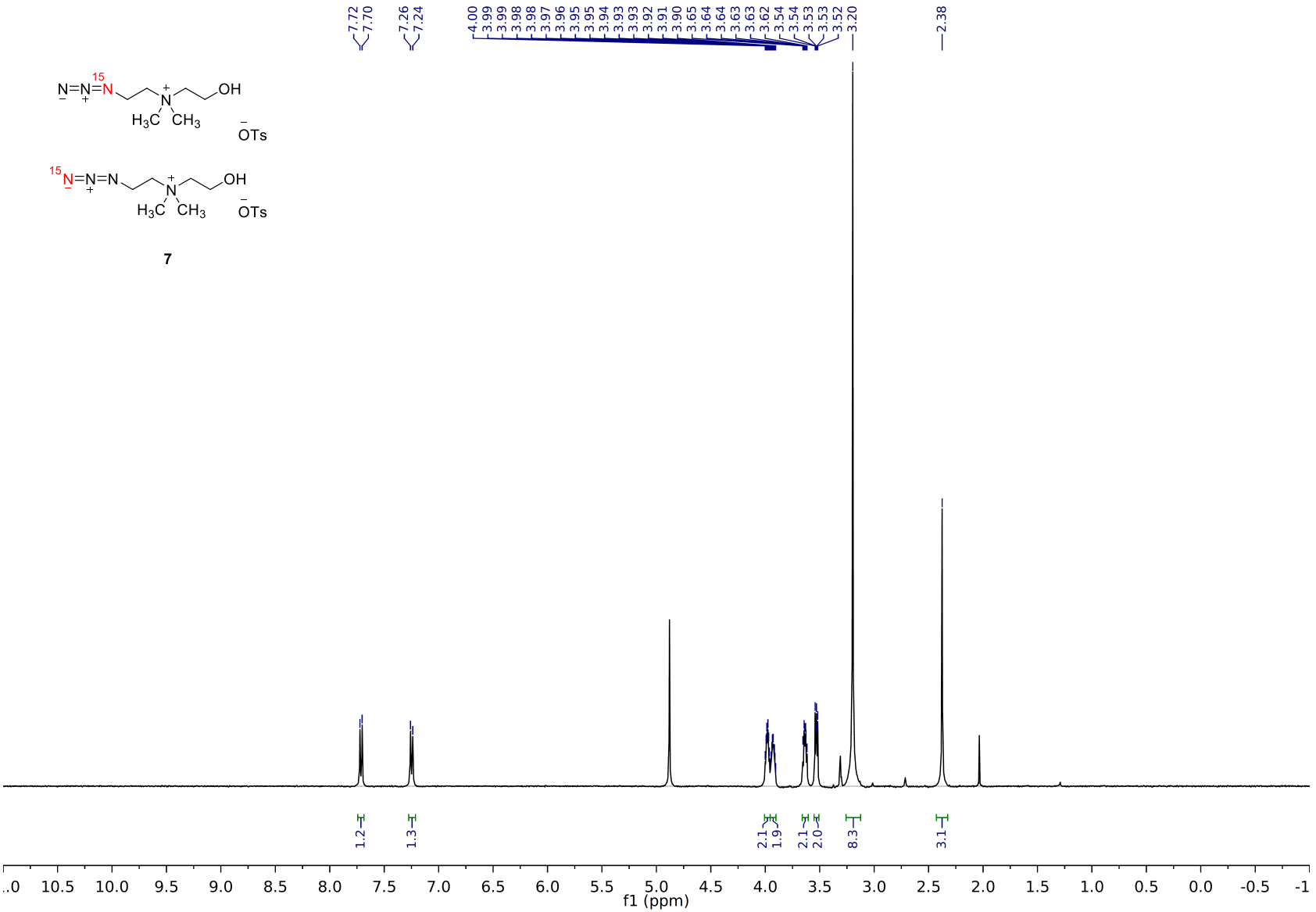
7.72
7.70
7.26
7.24
4.00
3.99
3.99
3.98
3.98
3.97
3.96
3.95
3.95
3.94
3.93
3.93
3.92
3.91
3.90
3.65
3.64
3.64
3.63
3.63
3.62
3.54
3.54
3.53
3.53
3.52
3.20
2.38
1.2
1.3
2.1
1.9
2.1
2.0
8.3
3.1
f1 (ppm)

7

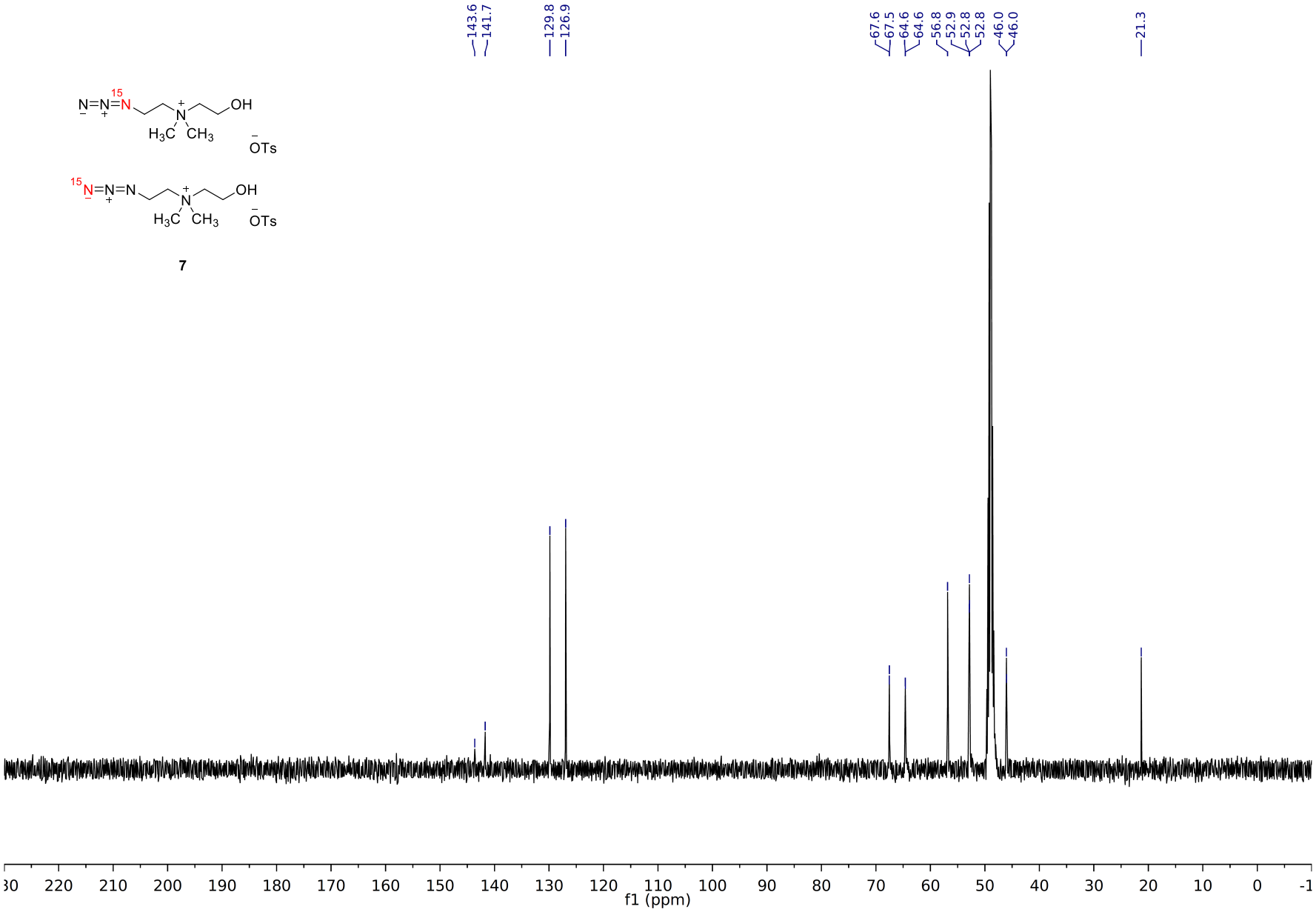
143.6
141.7
129.8
126.9
67.6
67.5
64.6
64.6
56.8
52.9
52.8
52.8
46.0
46.0
21.3
f1 (ppm)

7

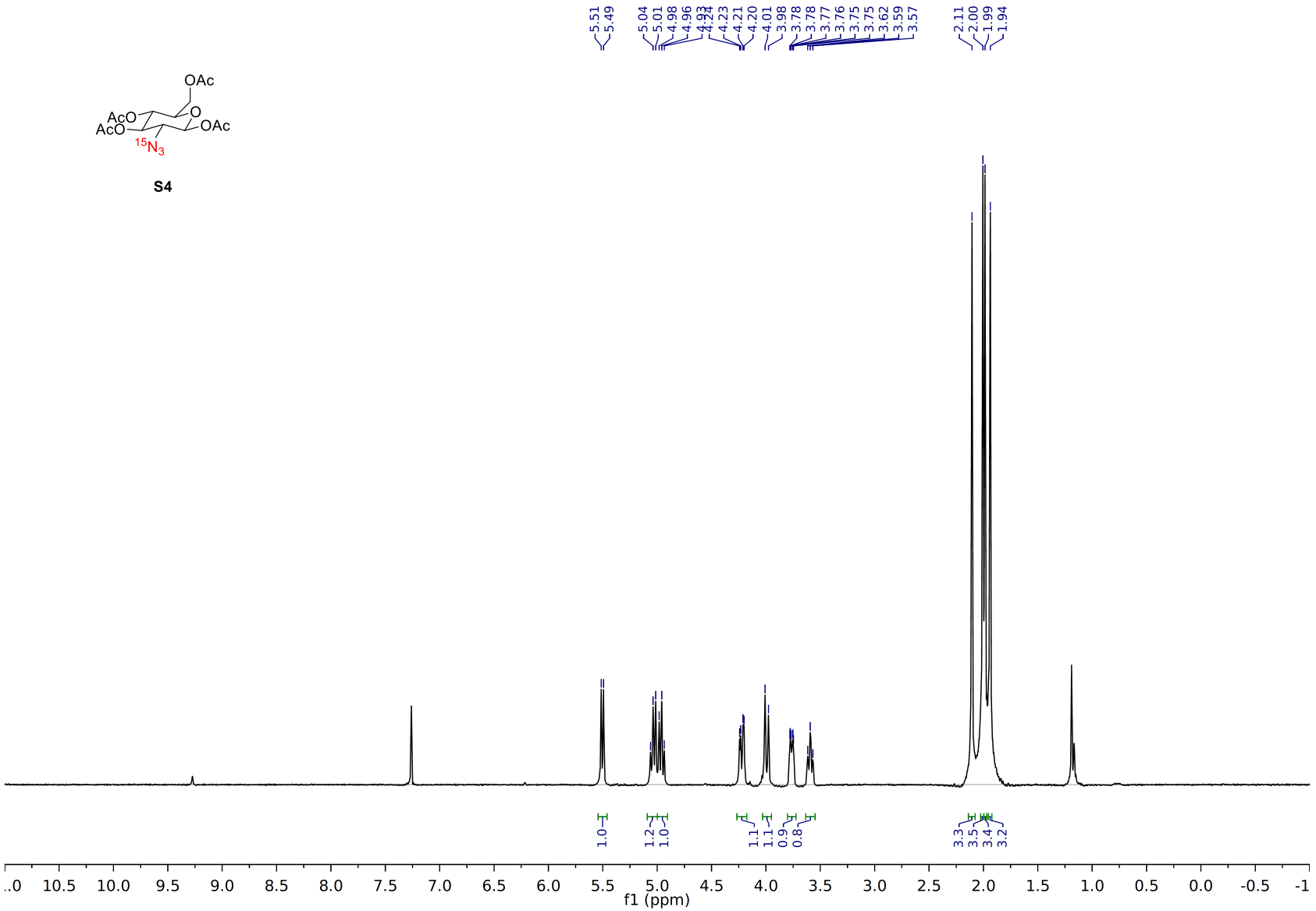
OAc
AcO
AcO
O
OAc
$^{15}N_3$
S4
5.51
5.49
5.04
5.01
4.98
4.96
4.23
4.21
4.20
4.01
3.98
3.78
3.78
3.77
3.76
3.75
3.75
3.62
3.59
3.57
2.11
2.00
1.99
1.94
1.0
1.2
1.0
1.1
1.1
0.9
0.8
3.3
3.5
3.4
3.2
f1 (ppm)

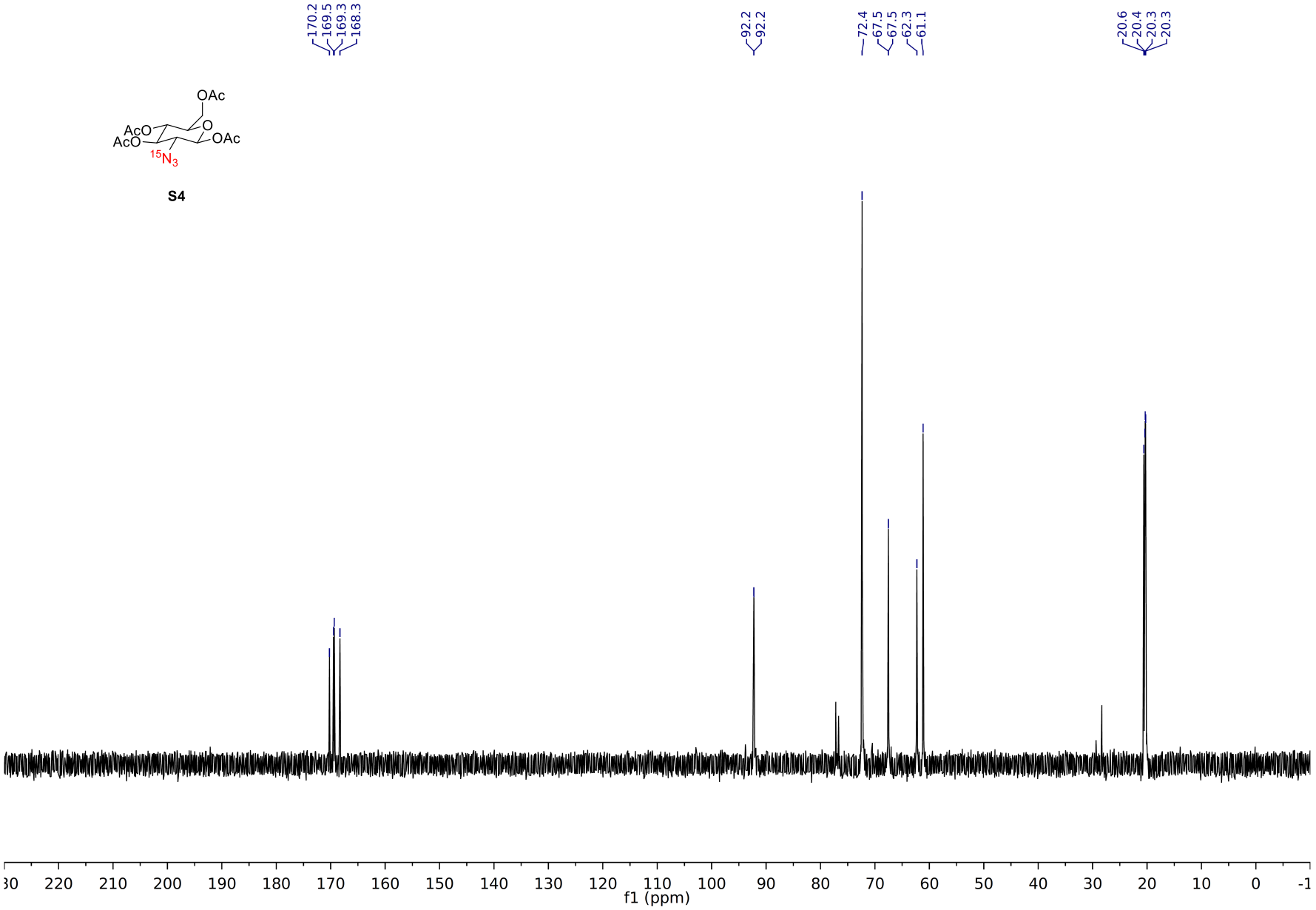
170.2
169.5
169.3
168.3
92.2
92.2
72.4
67.5
67.5
62.3
61.1
20.6
20.4
20.3
20.3
OAc
AcO
AcO
O
OAc
$^{15}N_3$
S4
f1 (ppm)

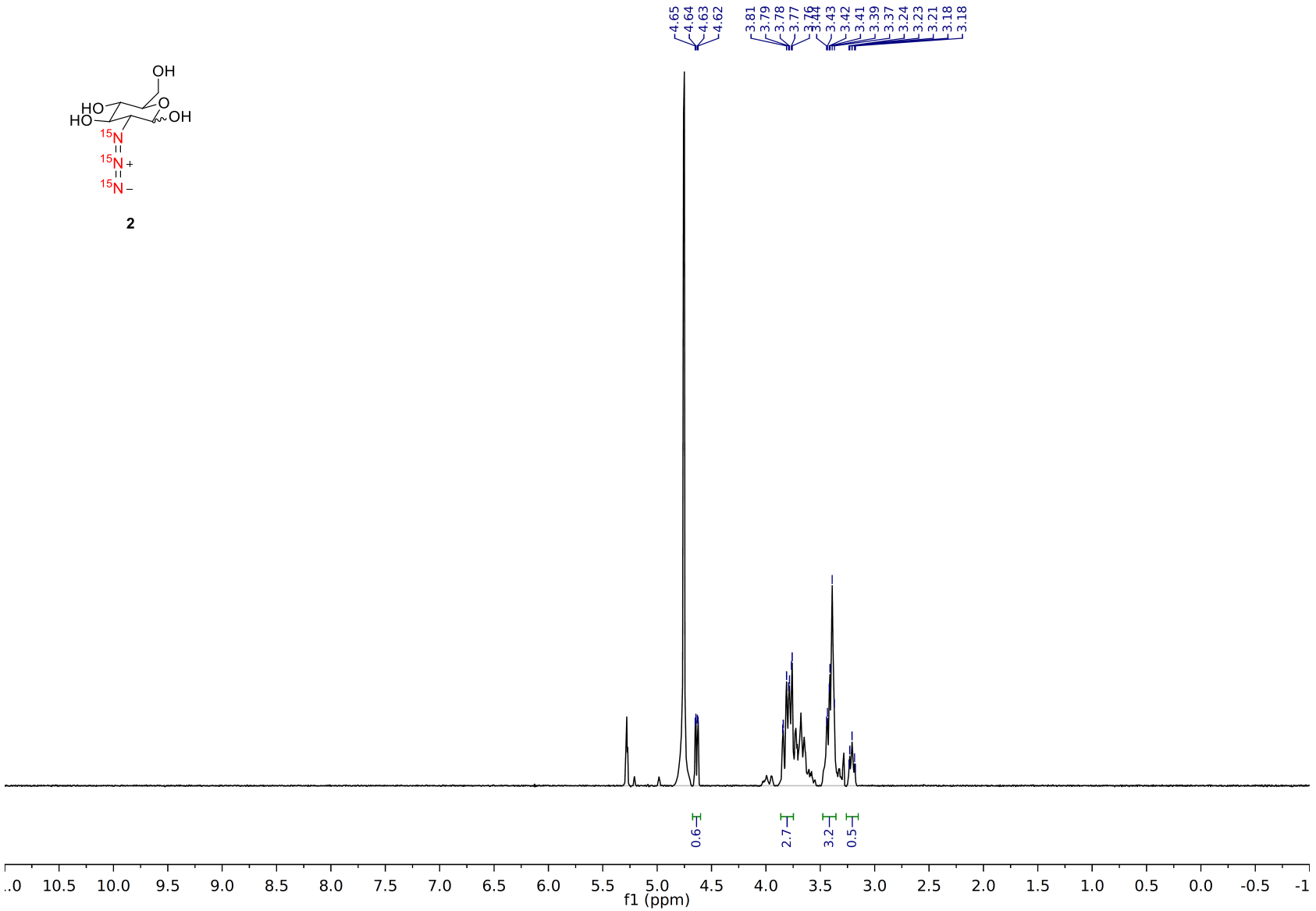
4.65
4.64
4.63
4.62
3.81
3.79
3.78
3.77
3.76
3.44
3.43
3.42
3.41
3.39
3.37
3.24
3.23
3.21
3.18
3.18
OH
HO
HO
O
OH
15N
15N +
15N –
2
0.6
2.7
3.2
0.5
f1 (ppm)

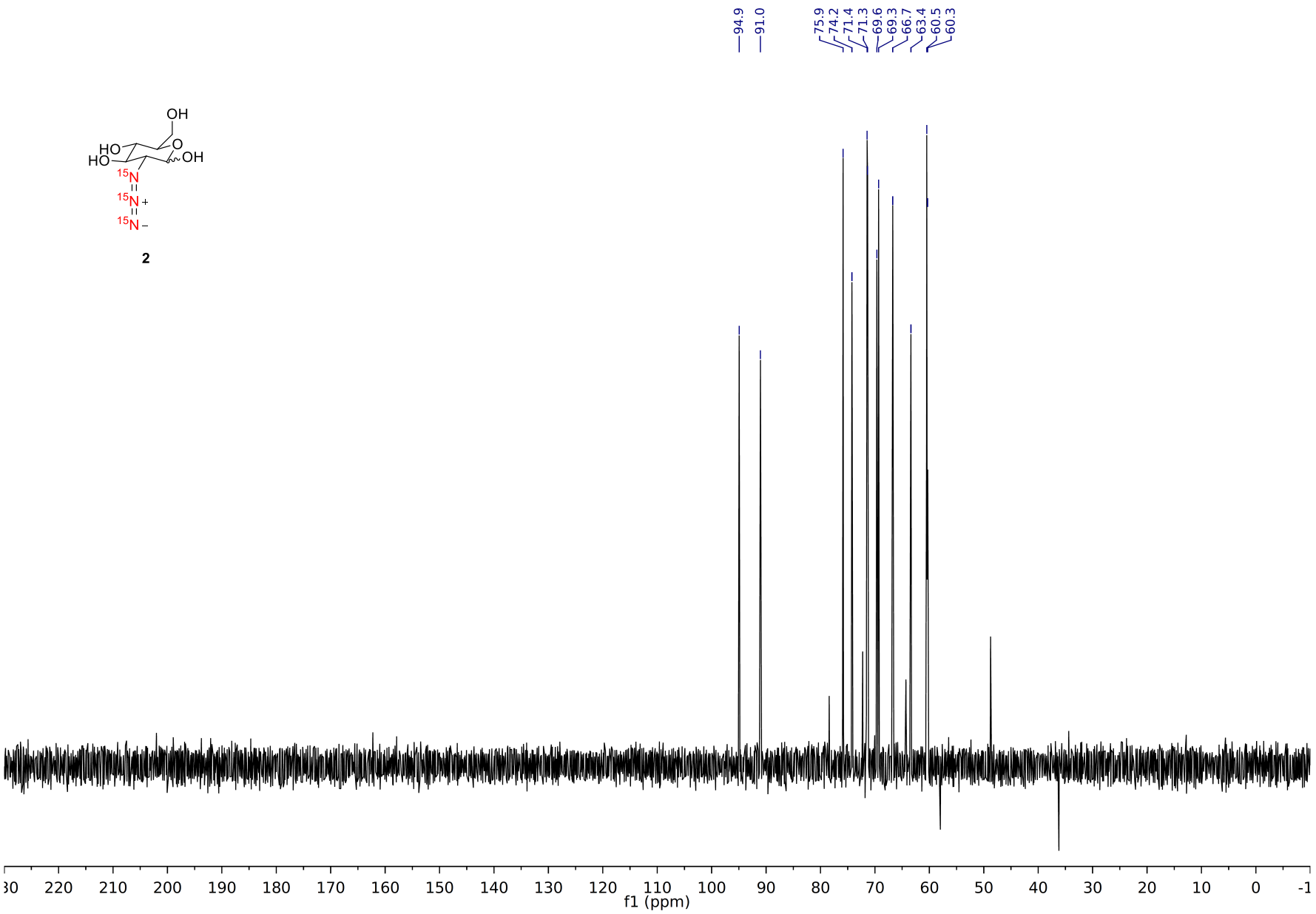
94.9
91.0
75.9
74.2
71.4
71.3
69.6
69.3
66.7
63.4
60.5
60.3
OH
HO
HO
O
OH
15N
15N+
15N−
2
f1 (ppm)

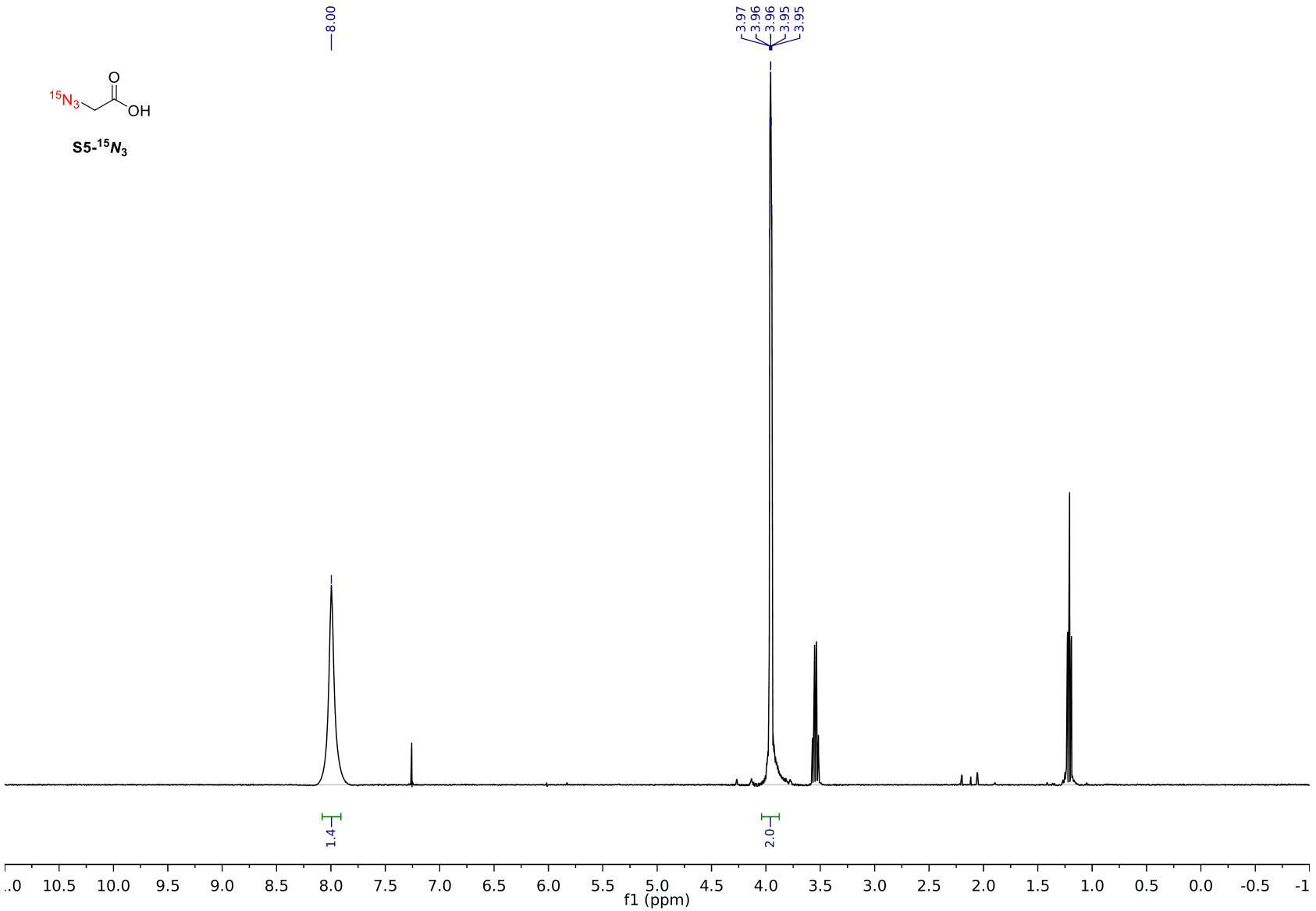
8.00
3.97
3.96
3.96
3.95
3.95
O
$^{15}N_3$
OH
S5-$^{15}N_3$
1.4
2.0
f1 (ppm)

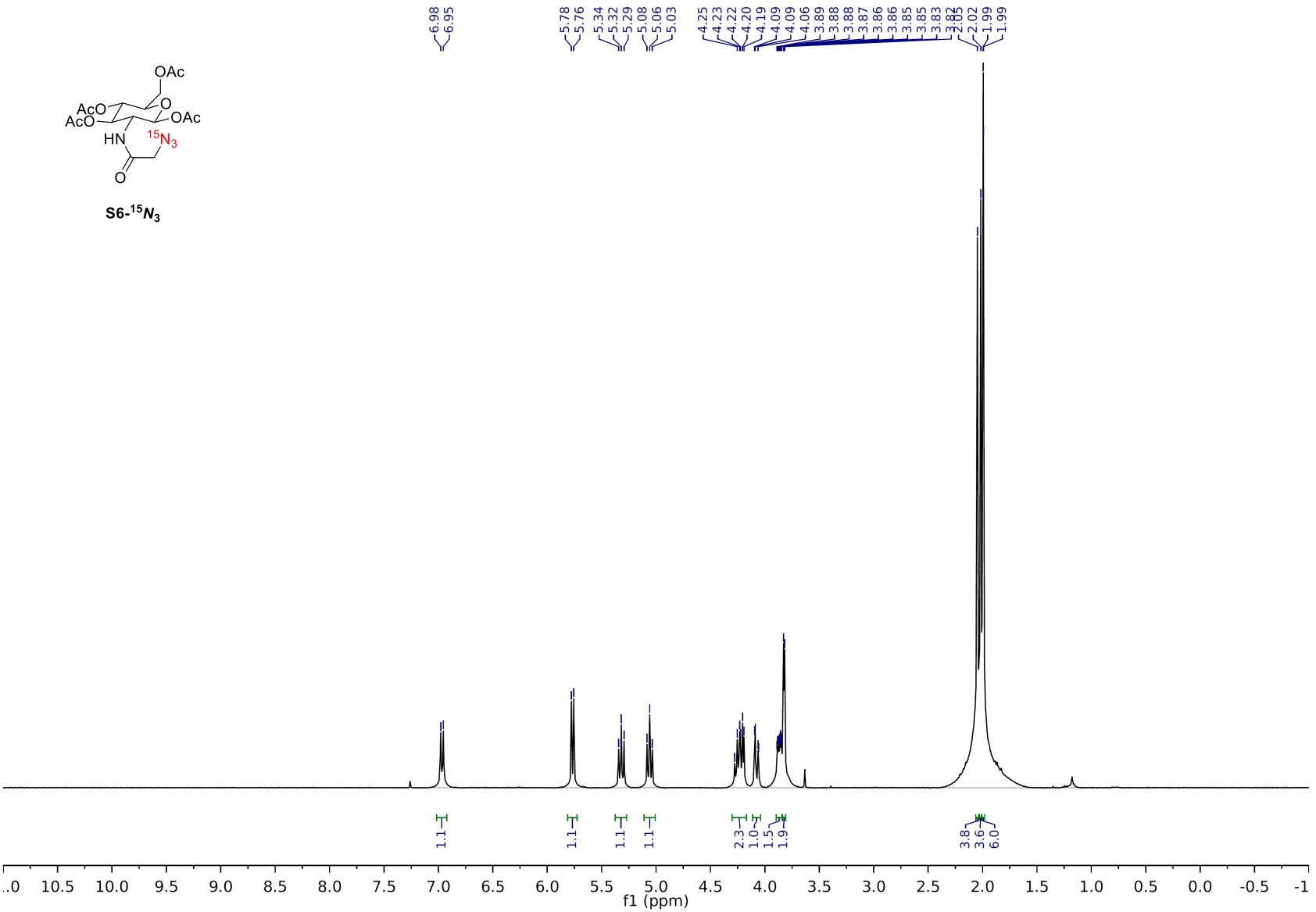
OAc
AcO
AcO
O
OAc
HN
$^{15}N_3$
O
6.98
6.95
5.78
5.76
5.34
5.32
5.29
5.08
5.06
5.03
4.25
4.23
4.22
4.20
4.19
4.09
4.09
4.06
3.89
3.88
3.88
3.87
3.86
3.86
3.85
3.85
3.83
2.02
1.99
1.99
1.1
1.1
1.1
1.1
2.3
1.0
1.5
1.9
3.8
3.6
6.0
f1 (ppm)

S6-$^{15}N_3$

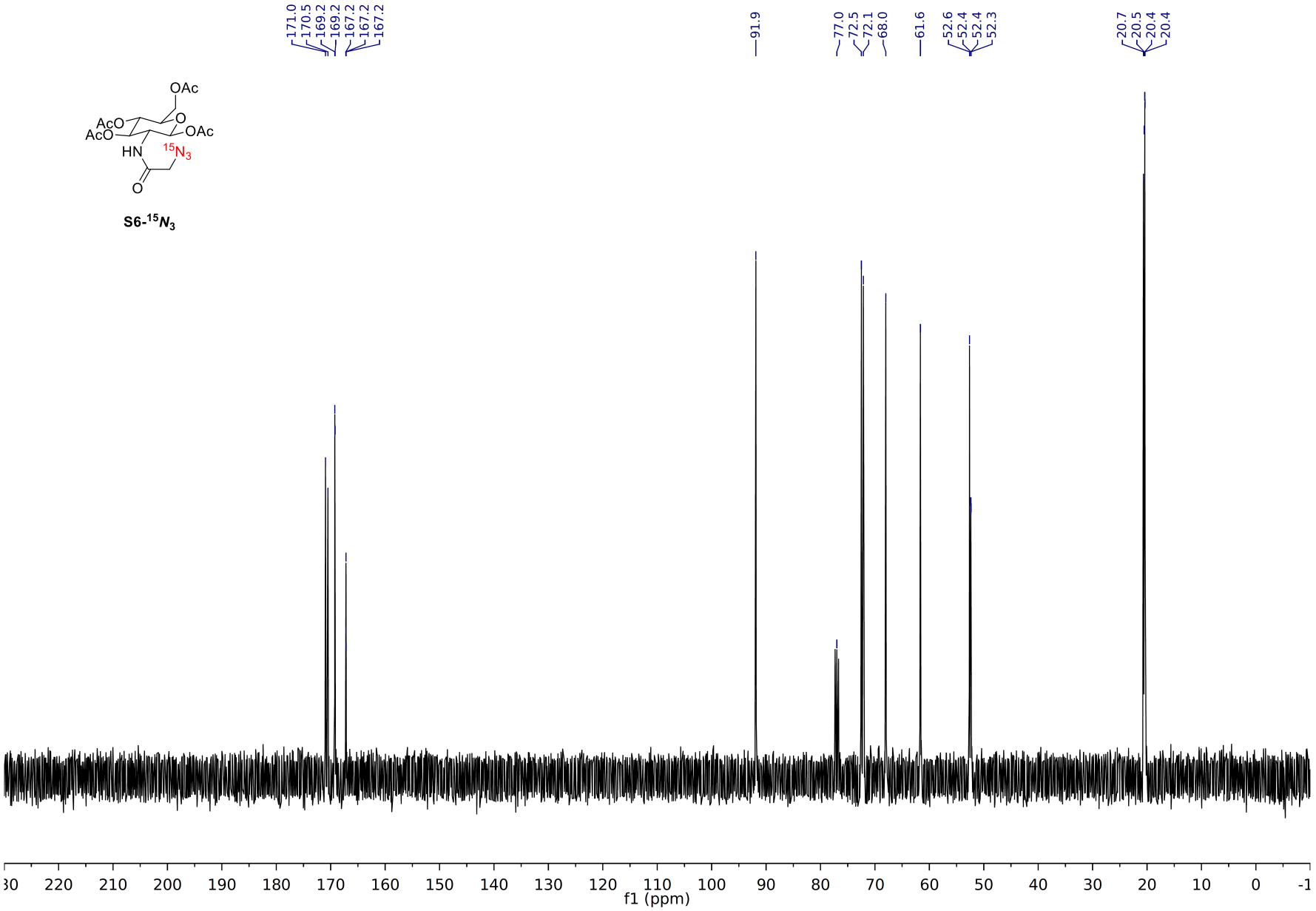
171.0
170.5
169.2
169.2
167.2
167.2
167.2
91.9
77.0
72.5
72.1
68.0
61.6
52.6
52.4
52.4
52.3
20.7
20.5
20.4
20.4
OAc
AcO
AcO
O
OAc
HN
15N3
O
S6-15N3
f1 (ppm)

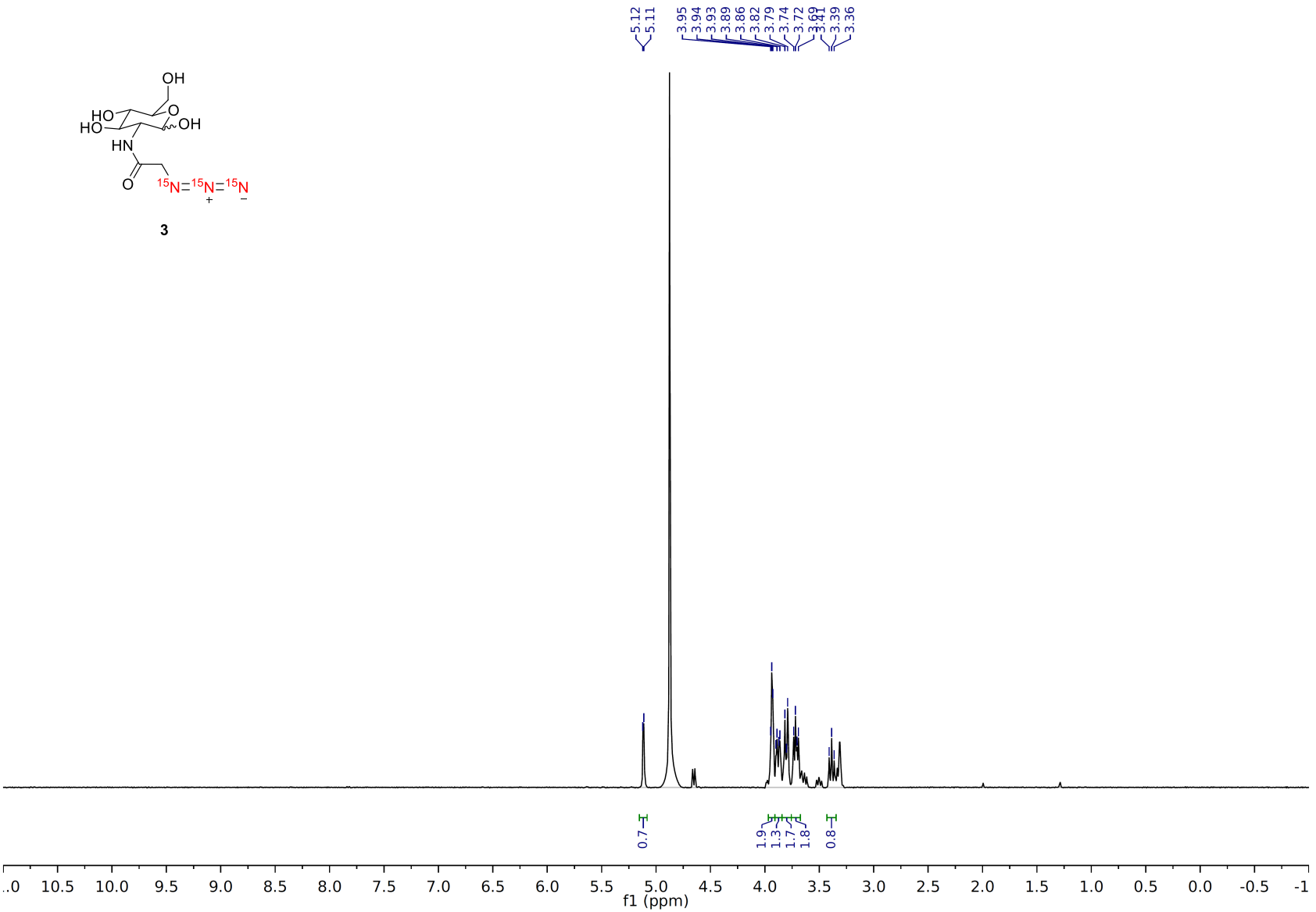
OH
HO
HO
O
OH
HN
O
15N=15N=15N
+
−
3
5.12
5.11
3.95
3.94
3.93
3.89
3.86
3.82
3.79
3.74
3.72
3.69
3.41
3.39
3.36
0.7
1.9
1.3
1.7
1.8
0.8
f1 (ppm)

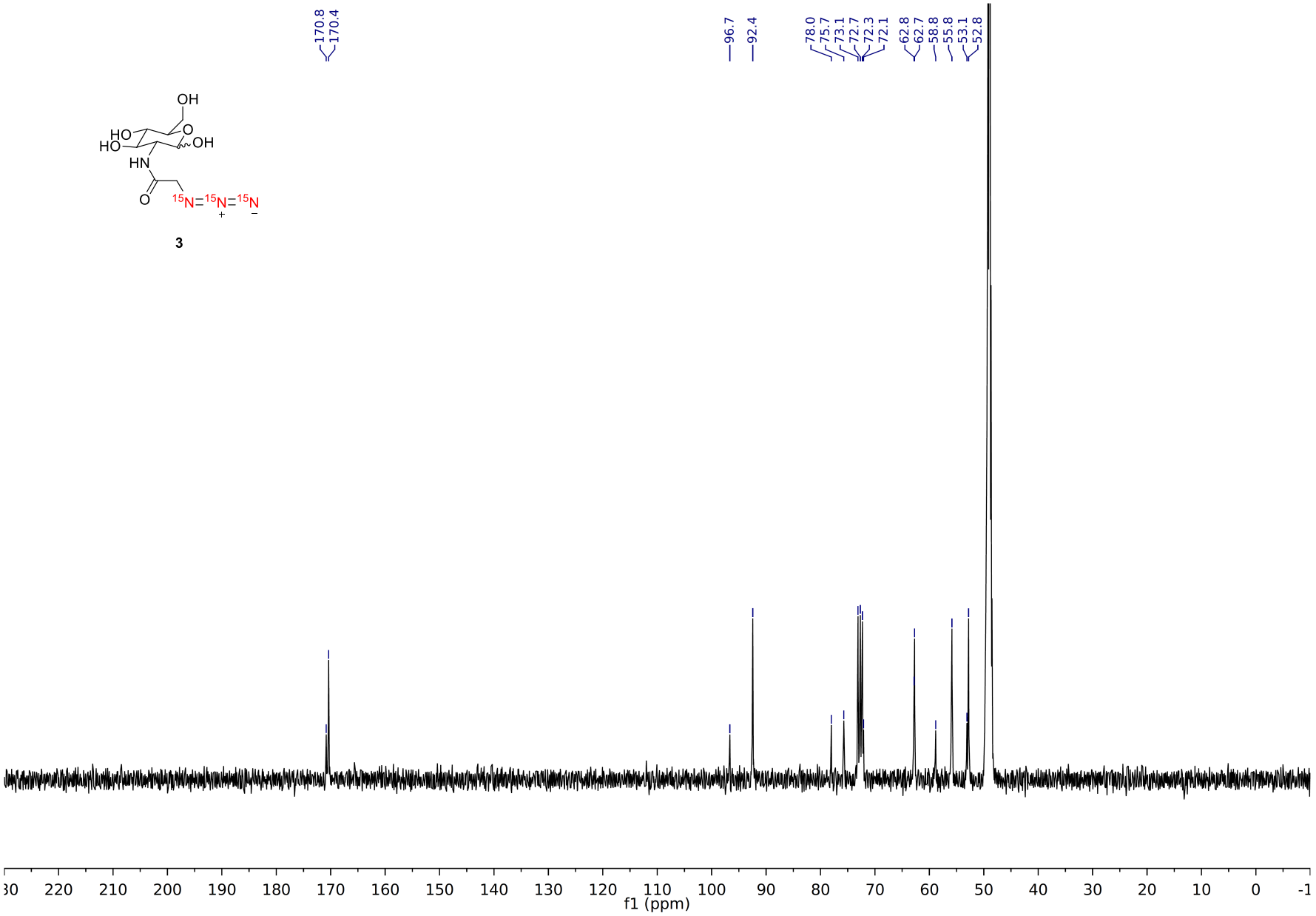
170.8
170.4
96.7
92.4
78.0
75.7
73.1
72.7
72.3
72.1
62.8
62.7
58.8
55.8
53.1
52.8
OH
HO
HO
O
OH
HN
O
15N=15N=15N
3
f1 (ppm)

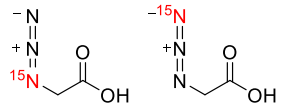

S5-$^{15}N_1$

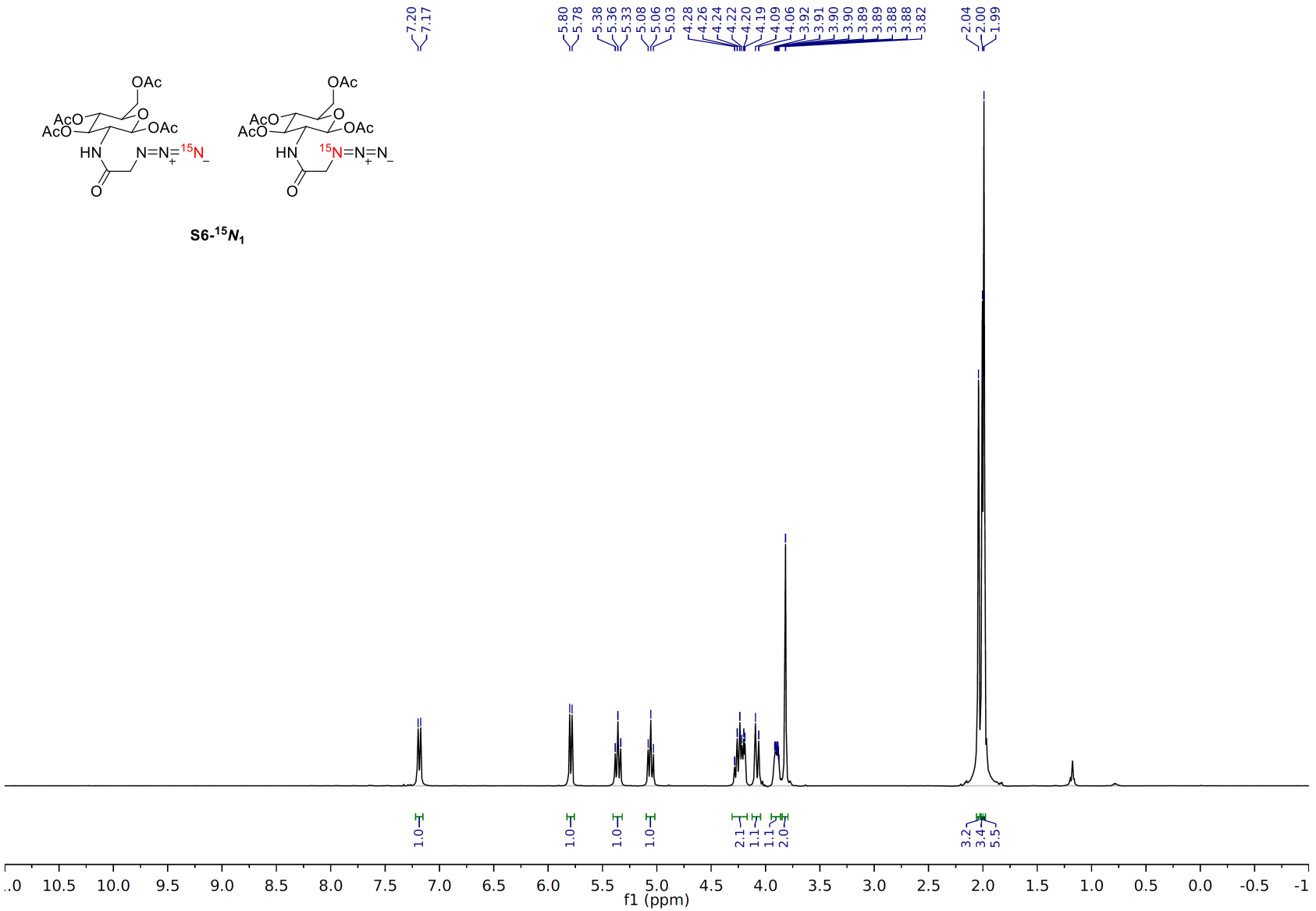
7.20
7.17
5.80
5.78
5.38
5.36
5.33
5.08
5.06
5.03
4.28
4.26
4.24
4.22
4.20
4.19
4.09
4.06
3.92
3.91
3.90
3.90
3.89
3.89
3.88
3.88
3.82
2.04
2.00
1.99
OAc
AcO
AcO
OAc
HN
N=N=15N
O
OAc
AcO
AcO
OAc
HN
15N=N=N
O
1.0
1.0
1.0
1.0
2.1
1.1
1.1
2.0
3.2
3.4
5.5
f1 (ppm)

S6-$^{15}N_1$

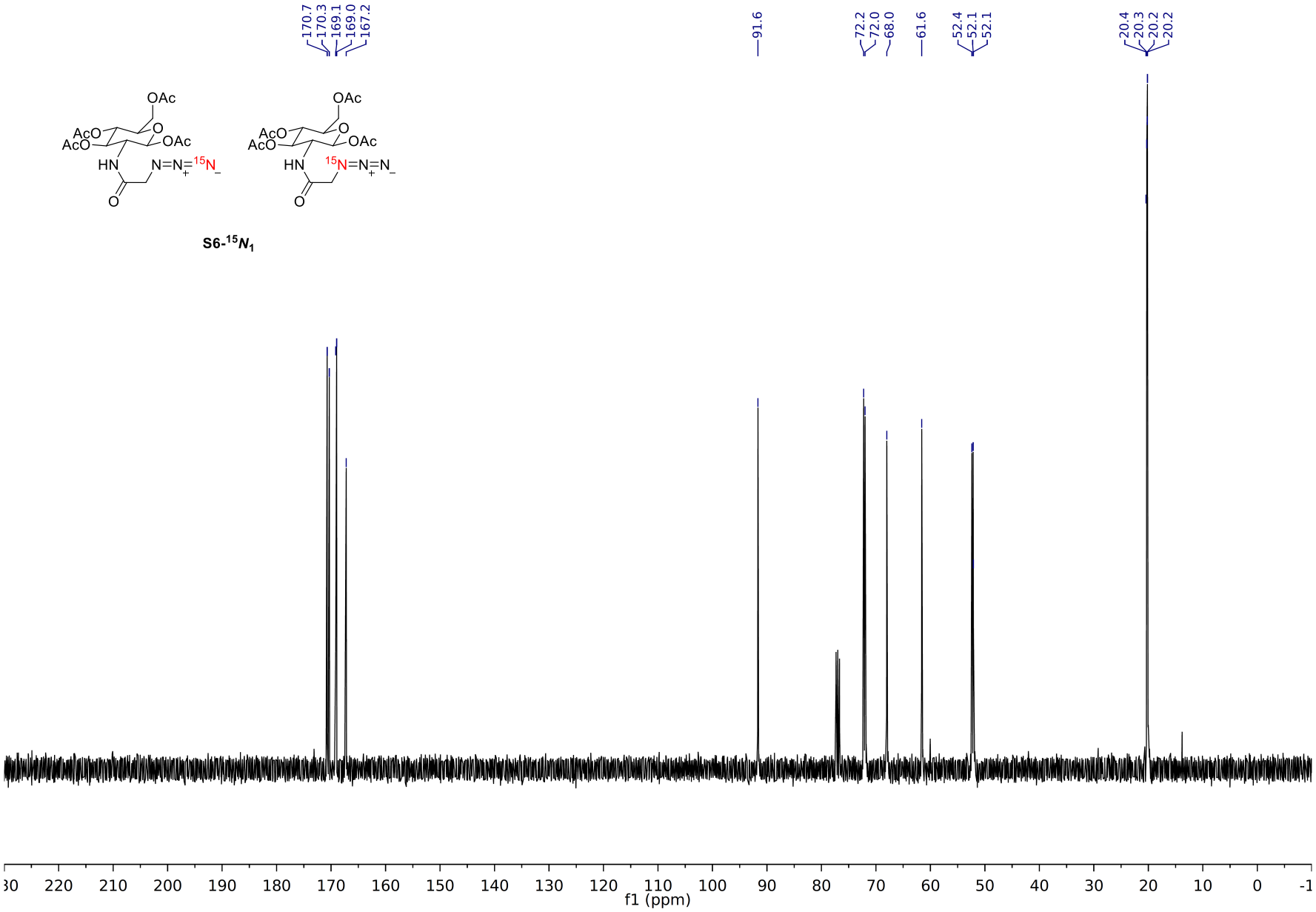
170.7
170.3
169.1
169.0
167.2
91.6
72.2
72.0
68.0
61.6
52.4
52.1
52.1
20.4
20.3
20.2
20.2
OAc
AcO
AcO
OAc
HN
N=N=15N
O
OAc
AcO
AcO
OAc
HN
15N=N=N
O
S6-15N1
f1 (ppm)

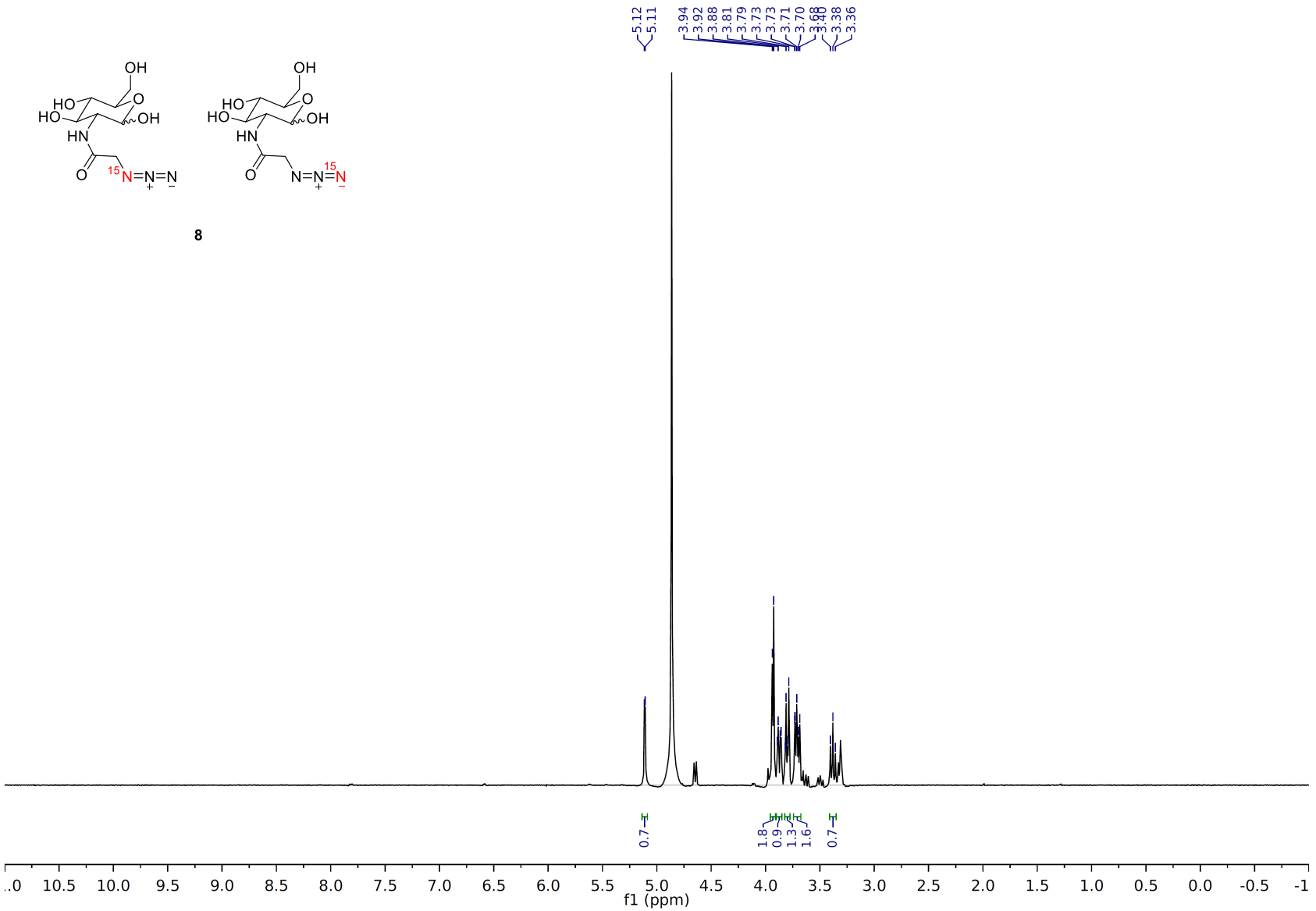
OH
HO
O
HO
OH
HN
O
15N=N=N
OH
HO
O
HO
OH
HN
O
N=N=15N
5.12
5.11
3.94
3.92
3.88
3.81
3.79
3.73
3.73
3.71
3.70
3.38
3.36
0.7
1.8
0.9
1.3
1.6
0.7
f1 (ppm)

8

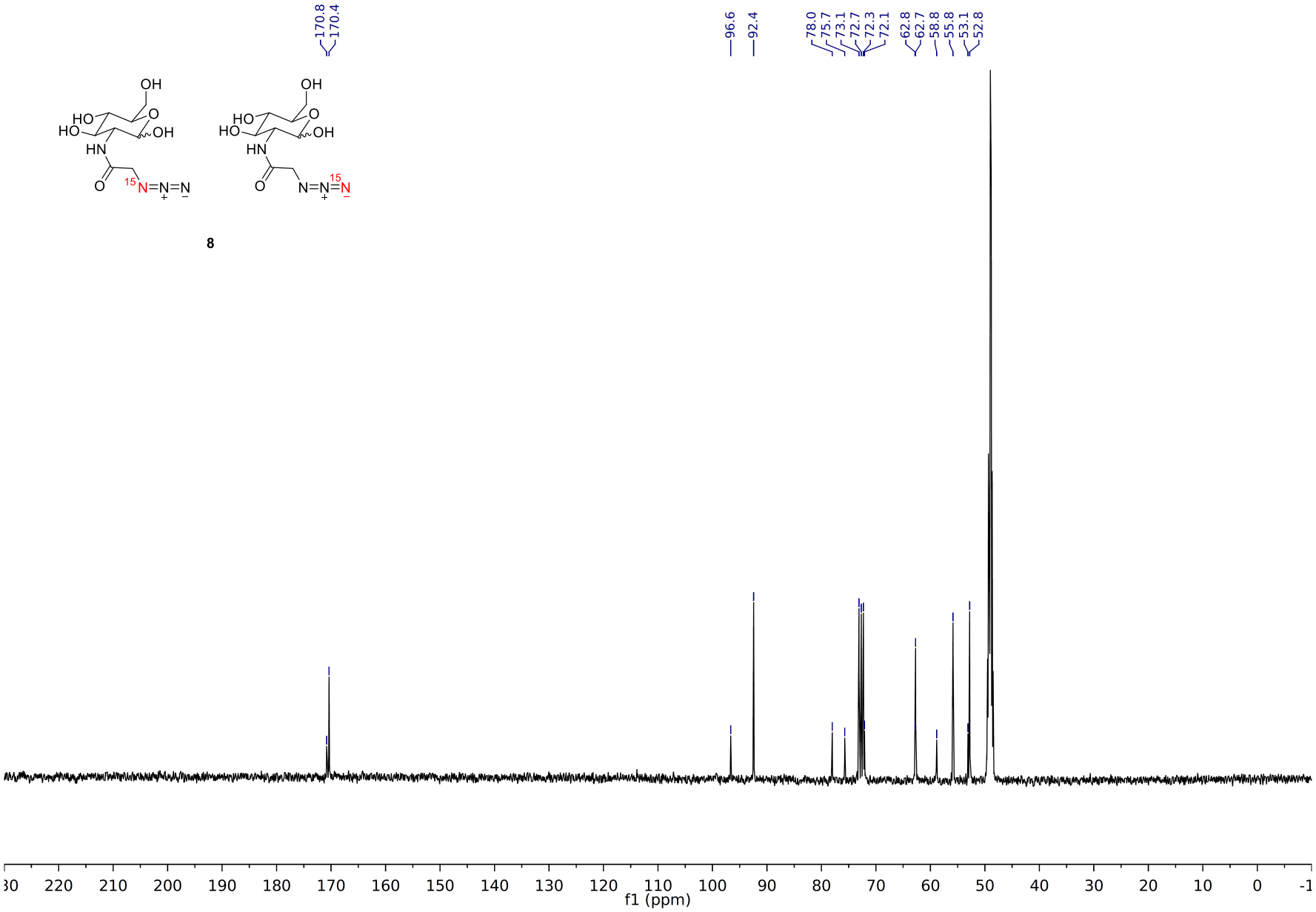
170.8
170.4
96.6
92.4
78.0
75.7
73.1
72.7
72.3
72.1
62.8
62.7
58.8
55.8
53.1
52.8
OH
HO
HO
O
OH
HN
O
15N=N=N
OH
HO
HO
O
OH
HN
O
N=N=15N
8
f1 (ppm)

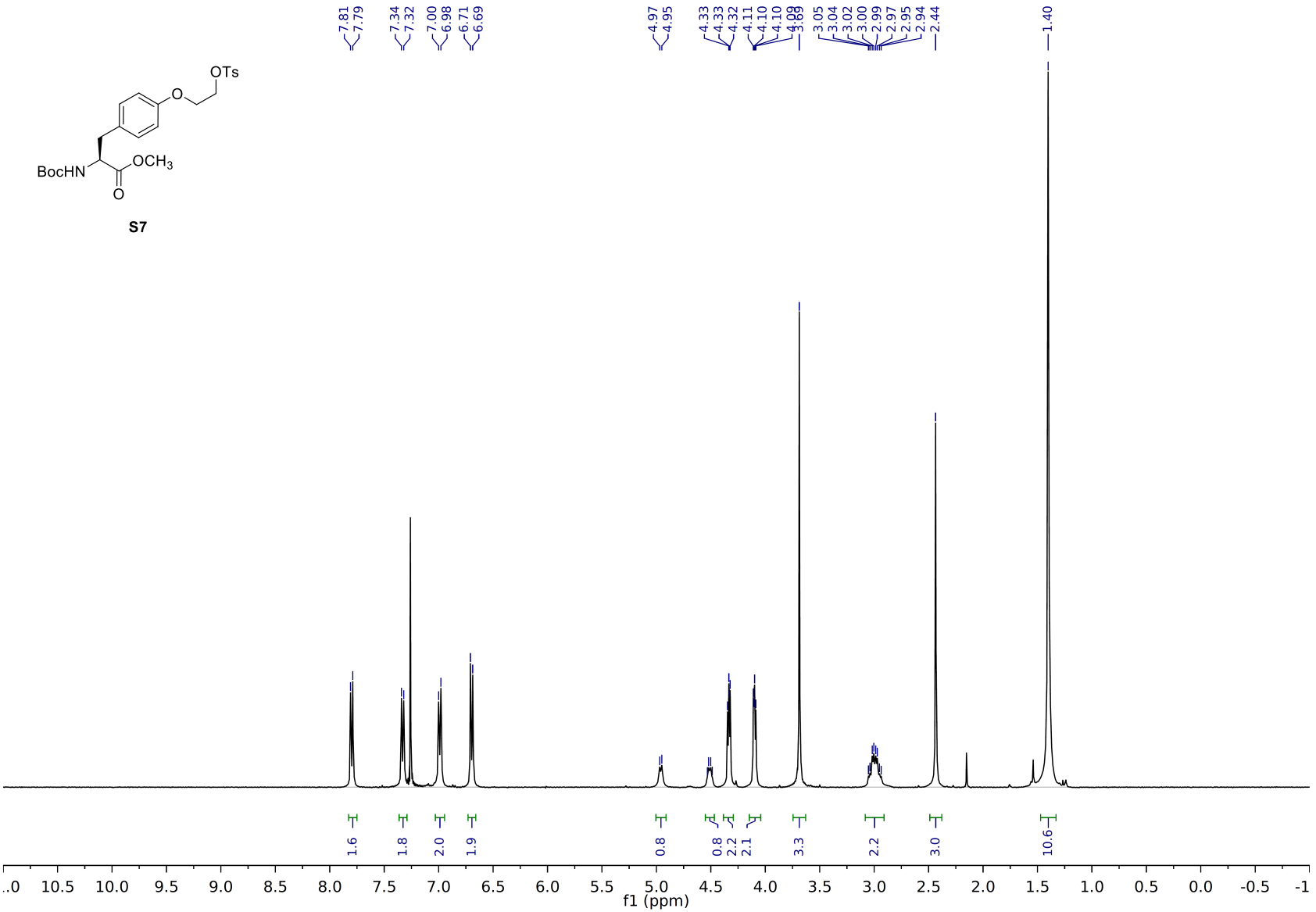
OTs
O
BocHN
OCH3
O
S7
7.81
7.79
7.34
7.32
7.00
6.98
6.71
6.69
4.97
4.95
4.33
4.33
4.32
4.11
4.10
4.10
4.09
3.89
3.05
3.04
3.02
3.00
2.99
2.97
2.95
2.94
2.44
1.40
1.6
1.8
2.0
1.9
0.8
0.8
2.2
2.1
3.3
2.2
3.0
10.6
f1 (ppm)

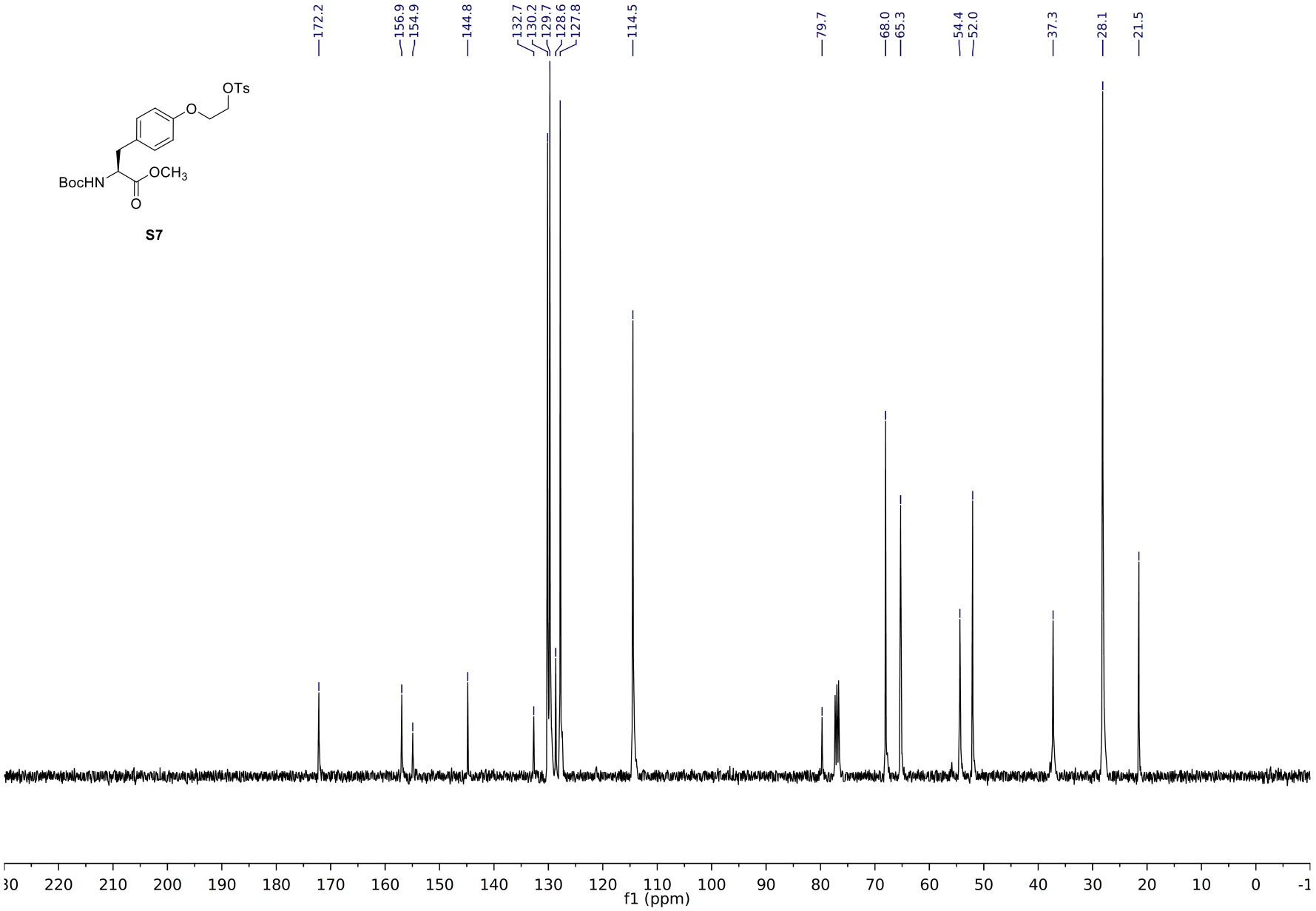
172.2
156.9
154.9
144.8
132.7
130.2
129.7
128.6
127.8
114.5
79.7
68.0
65.3
54.4
52.0
37.3
28.1
21.5
OTs
O
BocHN
OCH3
O
S7
f1 (ppm)

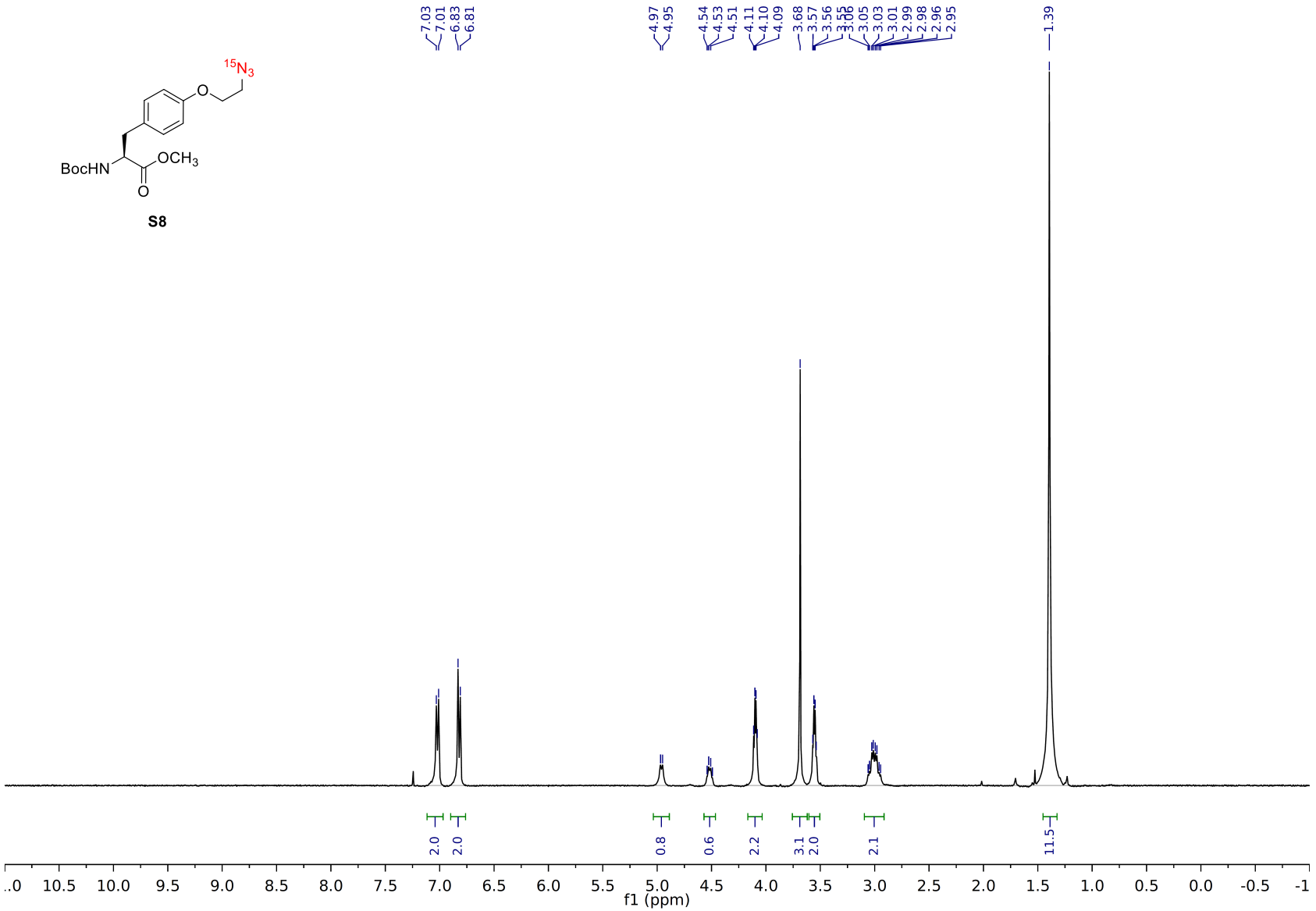
7.03
7.01
6.83
6.81
4.97
4.95
4.54
4.53
4.51
4.11
4.10
4.09
3.68
3.57
3.56
3.05
3.03
3.01
2.99
2.98
2.96
2.95
1.39
2.0
2.0
0.8
0.6
2.2
3.1
2.0
2.1
11.5
f1 (ppm)

S8

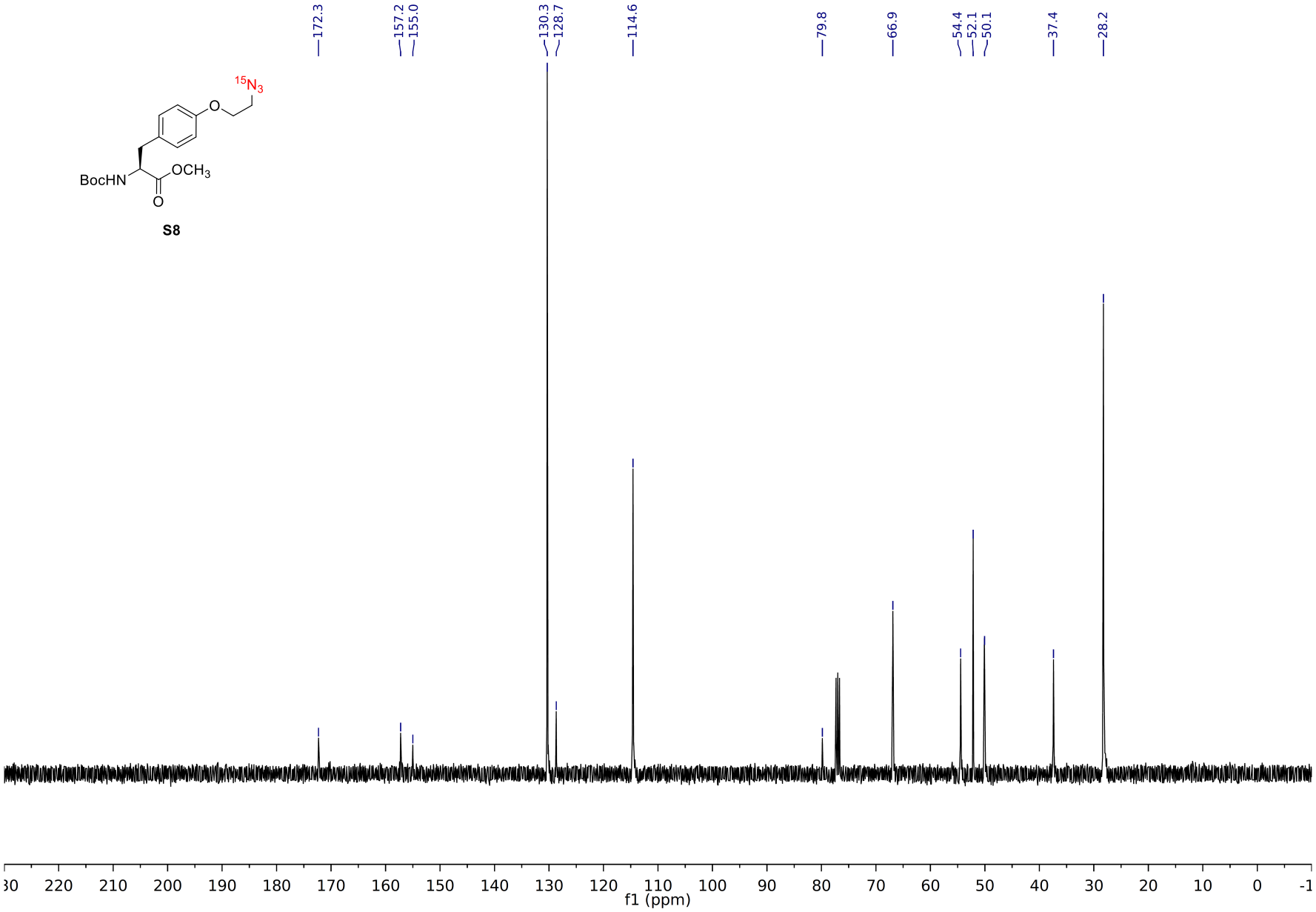
172.3
157.2
155.0
130.3
128.7
114.6
79.8
66.9
54.4
52.1
50.1
37.4
28.2
$^{15}N_3$
O
BocHN
OCH_3
O
S8
f1 (ppm)

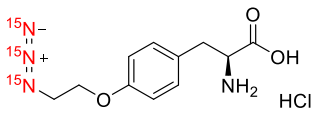
15N
15N
15N
O
OH
NH2
HCl

4

7.24
7.22
7.00
6.98
4.26
4.25
4.23
4.19
4.18
3.65
3.64
3.28
3.27
3.24
3.23
3.16
3.14
3.13
3.11
1.9
1.8
1.2
1.9
1.7
1.0
1.1
f1 (ppm)

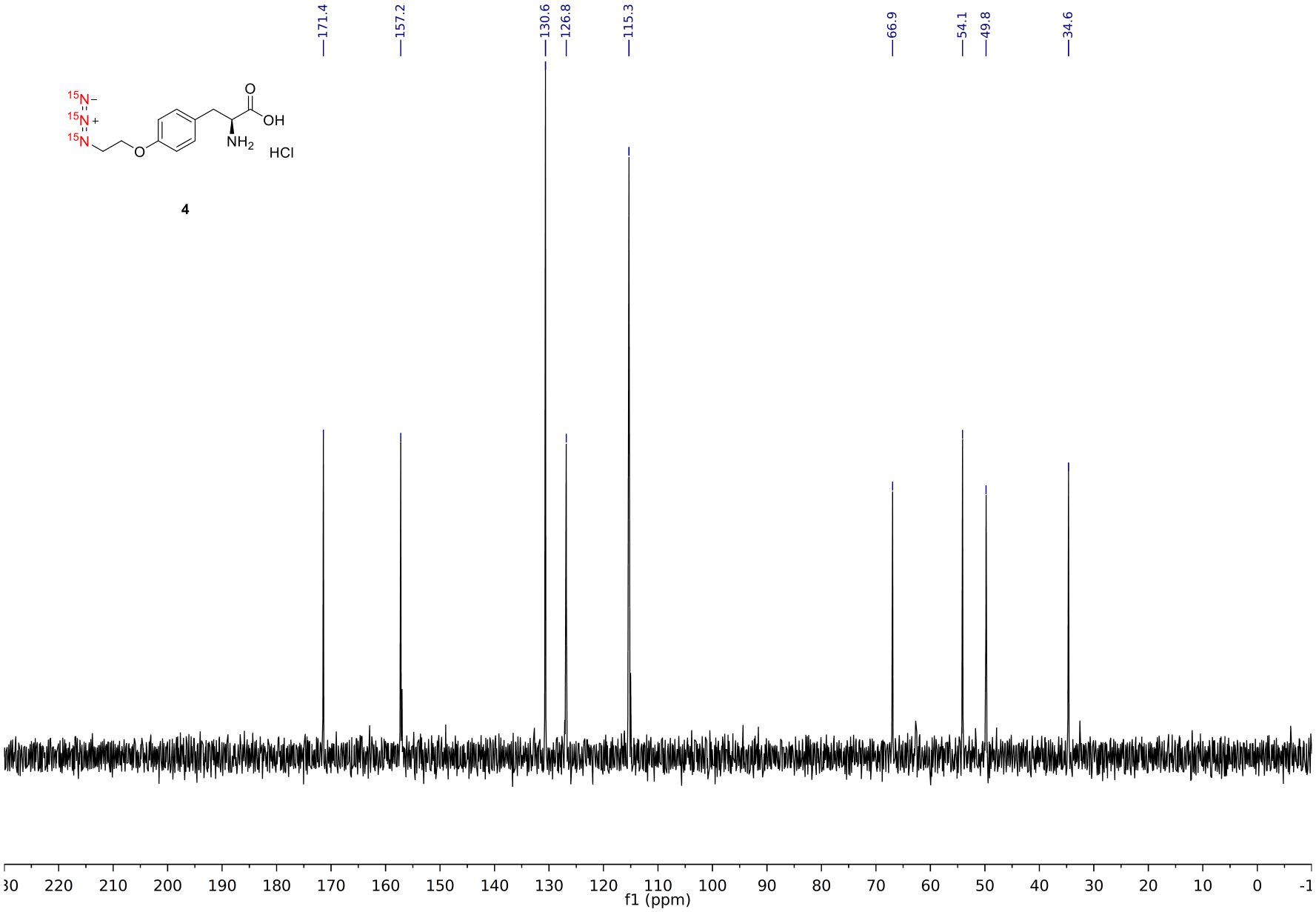

4

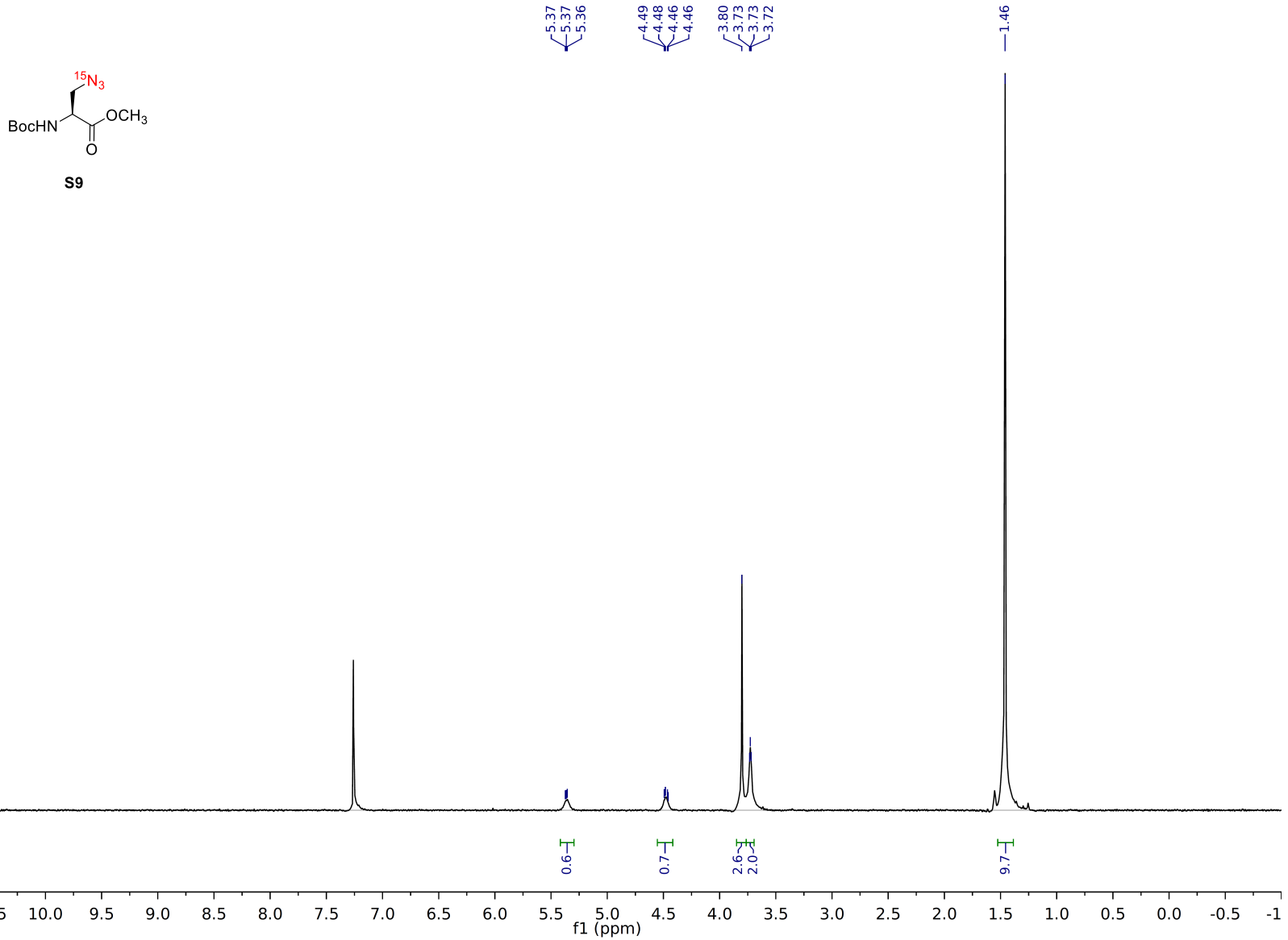
5.37
5.37
5.36
4.49
4.48
4.46
4.46
3.80
3.73
3.73
3.72
1.46
BocHN
OCH3
O
15N3
0.6
0.7
2.6
2.0
9.7
f1 (ppm)

S9

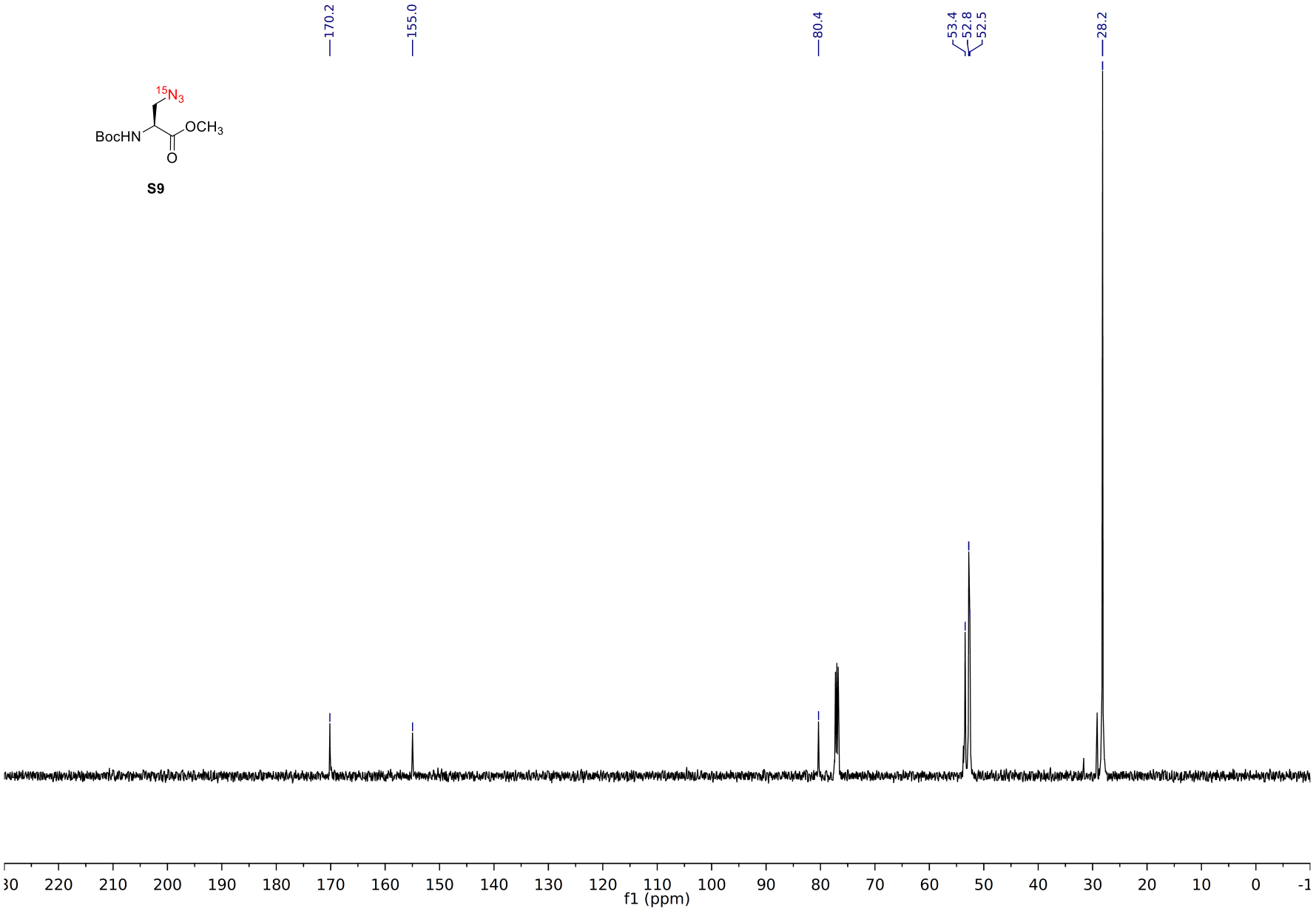
170.2
155.0
80.4
53.4
52.8
52.5
28.2
$^{15}N_3$
BocHN
OCH_3
O
S9
f1 (ppm)

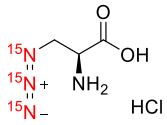
O
OH
^{15}N
^{15}N
^{15}N
NH$_2$
HCl

5

4.26
4.25
4.23
4.23
4.21
4.04
4.02
4.00
3.99
3.98
3.97
3.91
3.90
3.89
3.87
3.86
3.86
1.0
1.0
1.0
..0 10.5 10.0 9.5 9.0 8.5 8.0 7.5 7.0 6.5 6.0 5.5 5.0 4.5 4.0 3.5 3.0 2.5 2.0 1.5 1.0 0.5 0.0 -0.5 -1
f1 (ppm)

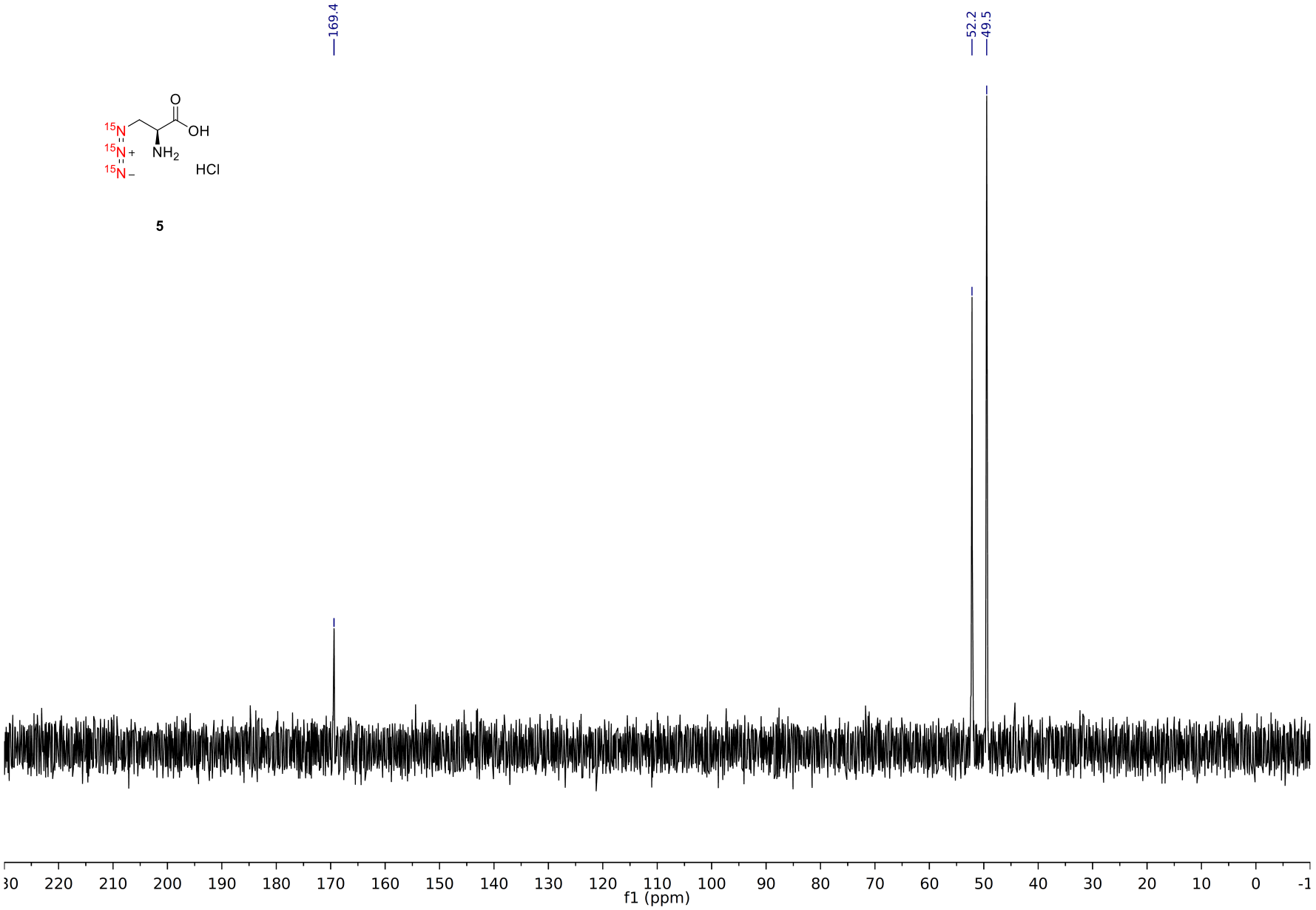
169.4
52.2
49.5
O
OH
^{15}N
^{15}N +
^{15}N –
NH$_2$
HCl
5
f1 (ppm)

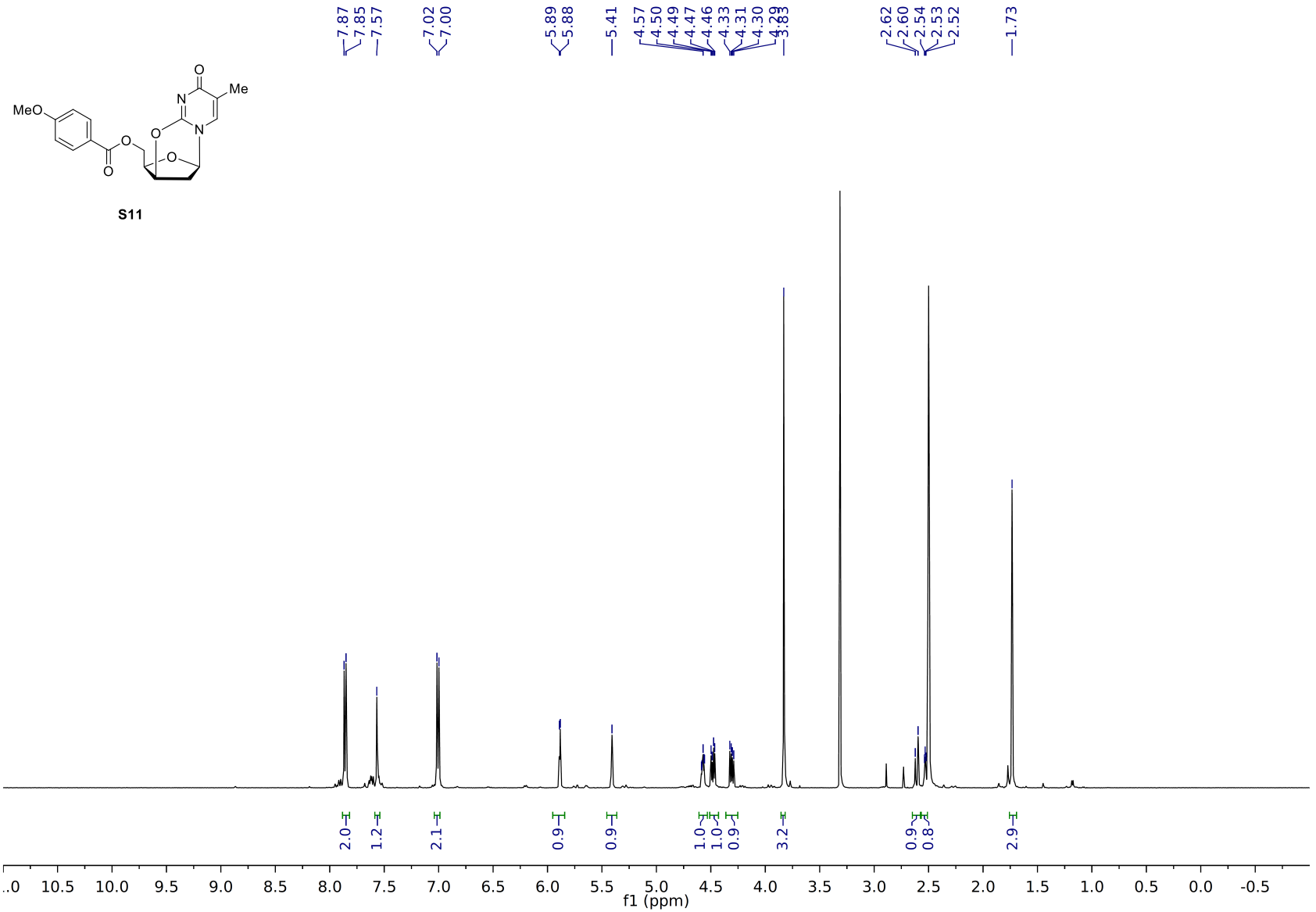
7.87
7.85
7.57
7.02
7.00
5.89
5.88
5.41
4.57
4.50
4.49
4.47
4.46
4.33
4.31
4.30
4.29
3.83
2.62
2.60
2.54
2.53
2.52
1.73
MeO
Me
O
N
O
N
O
O
O
O
2.0
1.2
2.1
0.9
0.9
1.0
1.0
0.9
3.2
0.9
0.8
2.9
f1 (ppm)

S11

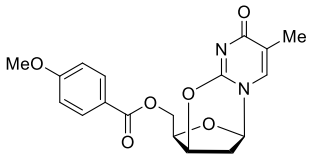
MeO
O
N
Me
O
N
O
O
O

S11

171.3
165.5
163.8
153.8
137.1
131.9
121.7
116.6
114.5
87.4
82.5
77.7
62.8
56.0
33.2
13.5
210
200
190
180
170
160
150
140
130
120
110
100
90
80
70
60
50
40
30
20
10
0
-1
f1 (ppm)

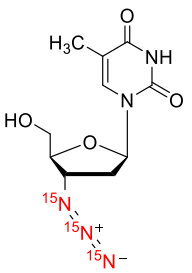
O
H3C
NH
N
O
HO
O
15N
15N+
15N−

6

7.63
6.20
6.18
6.16
4.35
4.35
4.35
4.35
4.34
4.33
4.33
4.02
4.01
3.99
3.87
3.87
3.86
3.84
3.83
3.80
3.79
3.77
3.76
2.50
2.49
2.48
2.48
2.47
2.46
1.87
1.0
0.9
1.0
1.0
1.0
1.1
2.0
3.0
f1 (ppm)

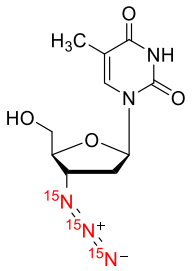
O
H3C
NH
N
O
HO
O
15N
15N+
15N−

6

166.3
151.4
137.3
111.2
84.8
84.0
60.8
59.7
36.0
11.4
f1 (ppm)

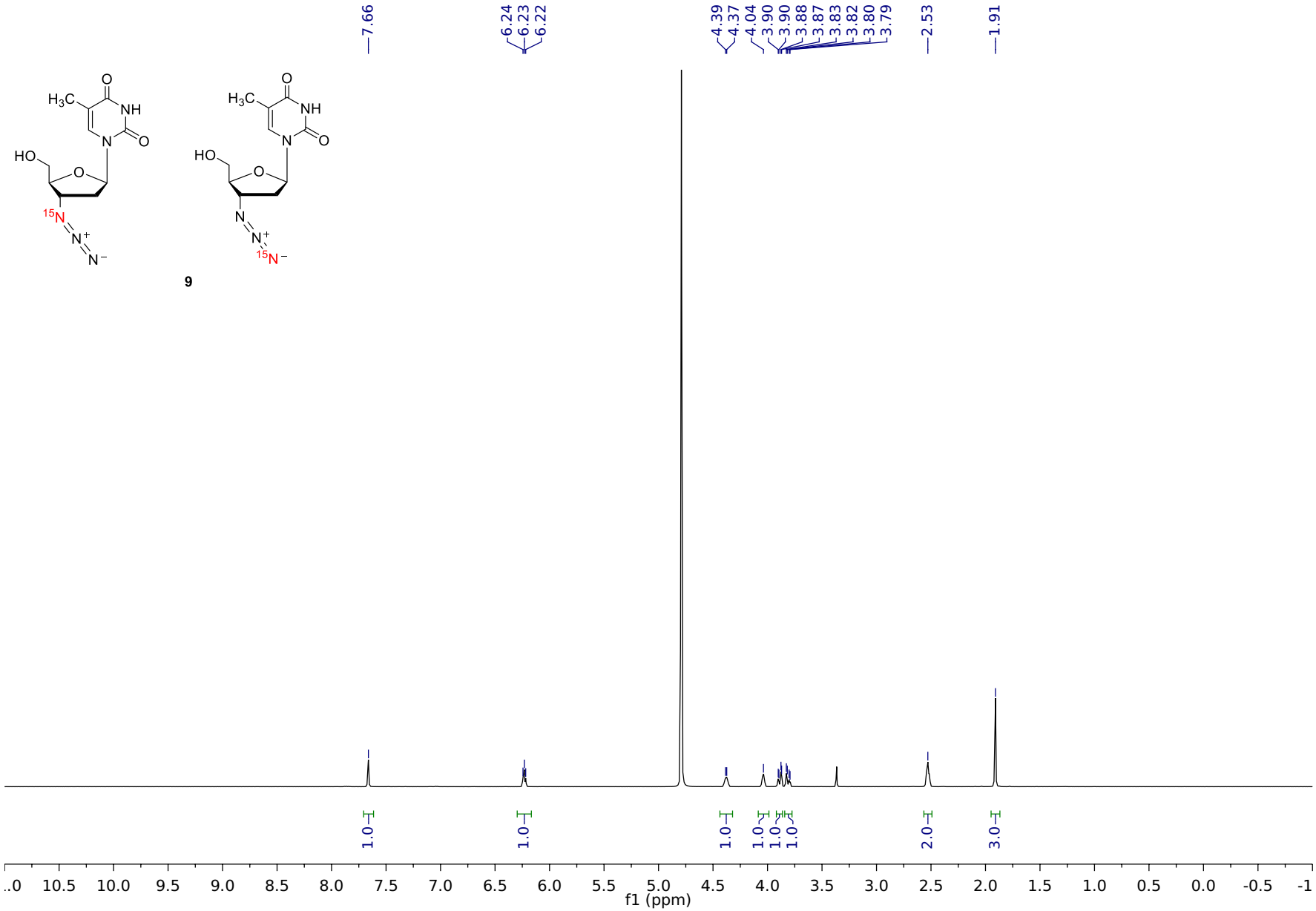
7.66
6.24
6.23
6.22
4.39
4.37
4.04
3.90
3.90
3.88
3.87
3.83
3.82
3.80
3.79
2.53
1.91
1.0
1.0
1.0
1.0
1.0
1.0
2.0
3.0
f1 (ppm)

9